

10713 ETI

NACA TN 4369

0067195



TECH LIBRARY KAFB, NM

NATIONAL ADVISORY COMMITTEE FOR AERONAUTICS

TECHNICAL NOTE 4369

SLIP-FLOW HEAT TRANSFER FROM CYLINDERS IN SUBSONIC AIRSTREAMS

By Lionel V. Baldwin

Lewis Flight Propulsion Laboratory
Cleveland, Ohio



Washington

September 1958

ASME
AFW 6
TECHNICAL LIBRARY
FBI - FBI



0067165

TABLE OF CONTENTS

	Page
SUMMARY	1
INTRODUCTION	2
Review of Previous Investigations	3
Objectives of This Research	5
APPARATUS AND PROCEDURE	5
Apparatus	5
Tunnel and air facility	5
Probe design and tungsten wire	6
Anemometer electrical equipment	8
Procedure	8
DIMENSIONLESS GROUPS OF CORRELATION	9
RESULTS	12
DISCUSSION	13
Preliminary Discussion of Results	13
Effect of Wire Temperature on Heat-Transfer Coefficient	14
Effect of Air Temperature on Heat-Transfer Coefficient	16
Correlation of Slip-Flow Heat-Transfer Data	17
Attempted General Correlation for Nusselt Number in Continuum, Slip, and Free-Molecule Flows	18
Hot-Wire-Anemometer Sensitivity	20
CONCLUDING REMARKS	22
APPENDIXES	
A - SYMBOLS	24
B - CORRECTIONS FOR CONDUCTION TO SUPPORTS	28
Linear Correction	28
Nonlinear Correction	33
C - DERIVATION OF HOT-WIRE-ANEMOMETER SENSITIVITY EQUATIONS . . .	35
REFERENCES	37
TABLE I - RESULTS OF STUDY OF HEAT TRANSFER FROM CYLINDERS IN SUBSONIC SLIP FLOW	40
TABLE II - ORGANIZATION OF RESULTS FOR NOMINAL VALUES OF PARAMETERS	47
FIGURES	48

NATIONAL ADVISORY COMMITTEE FOR AERONAUTICS

TECHNICAL NOTE 4369

SLIP-FLOW HEAT TRANSFER FROM CYLINDERS IN SUBSONIC AIRSTREAMS

By Lionel V. Baldwin

SUMMARY

Over 1000 measured convective heat-transfer coefficients for normal cylinders in subsonic slip flow have been correlated by using Nusselt number as a function of Reynolds and Knudsen (or Mach) numbers. The experimental range corresponds to the following dimensionless groups: Mach number M , 0.05 to 0.80; Reynolds number Re , 1 to 75; Knudsen number Kn , 0.009 to 0.077. Air temperatures between 0° and 280° F and cylinder temperatures between 34° and 620° F were used. At $Kn = 0.009$, the Nusselt number (Nu) correlation extrapolated smoothly into continuum-flow empirical curves, which show Nu as a function of \sqrt{Re} with a small, regular variation in Nu from compressibility or Mach number effects. The data showed increasing sensitivity to Kn as it increased to 0.077. The experimental Nu curves at $Kn = 0.077$ qualitatively verified two characteristics predicted by free-molecular-flow theoretical analysis. These are a shift to first-power dependence on Re and large separation of constant Mach number parametric curves due to rarefied gas-flow phenomena. Therefore, the experimental slip-flow correlation served as a bridge between continuum empirical relations and free-molecular theoretical results, but data between $0.10 < Kn < 2$ are required to complete this general correlation.

A complicated nonlinear dependence of the heat-transfer coefficient to the difference between cylinder and recovery temperature ΔT is reported. The heat-transfer coefficient h increased with increasing ΔT for $Kn < 0.02$; while for $Kn > 0.02$, h decreased with increasing ΔT . The Mach number had a secondary effect on this ΔT phenomenon. For cylinders operated at $\Delta T > 200^{\circ}$ F and over the entire range of this research, an increase in air temperature increased the heat-transfer coefficient. The preceding were second-order effects that caused deviations of up to 20 percent from the general correlation.

Finally, the application of these research results to hot-wire anemometry is discussed.

INTRODUCTION

Fine metal wires, 0.00005 to 0.001 inch in diameter, have been widely used in aerodynamic research as anemometers. The use of hot-wire anemometers for mean flow measurements began with the early work of King (ref. 1), while the investigation of fluctuations in airflows started with the classical research of Dryden and Kuethe (ref. 2). In every application, the sensitivity of the electrically heated anemometer to the flow properties is determined by the heat-transfer characteristics of cylinders in forced convection. Assuming potential flow over the wire, King derived an equation for steady flow that relates the electrical power input to the heat loss by convection:

$$I^2 \Omega_w = (A + B\sqrt{U})(T_w - T_a) \quad (1)$$

where

$$A = alk$$

$$B = bl \sqrt{D_w \rho c_p k}$$

(All symbols are defined in appendix A.) In usual practice, the constants in King's equation, A and B, are obtained experimentally from a calibration curve of $I^2 \Omega_w / (\Omega_w - \Omega_a)$ as a function of \sqrt{U} for each wire used. The sensitivity predicted by King's equation is the basis for hot-wire-anemometer techniques that have become rather elaborate (e.g., ref. 3) in slow subsonic flows.

As aerodynamic research progressed into transonic and supersonic flows, it was natural to investigate the heat-loss characteristics of hot wires and to attempt extension of this research tool. In order to describe the influence of flow parameters over a wide range, recent investigators have used dimensionless groups to generalize heat-loss correlations. Hot-wire heat-loss studies not only supply anemometer sensitivity, but also have furnished the bulk of the heat-transfer measurements for cylinders in slip and near-free-molecule flows. Interest in this phase of aerodynamics has grown greatly as it has become necessary to compute heat transfer to missiles and satellites that fly at high altitudes. Though these objects generally fly at very high speeds, the actual flow over the body is subsonic in many cases, because shock waves occur near forward surfaces. This investigation follows some excellent research in this field during the past eight years; therefore, it is appropriate to outline the problem studied here in terms of what previous workers have established.

Review of Previous Investigations

The Reynolds number (based on cylinder diameter) and Mach number are the usual dimensionless groups chosen to specify the regimes for airflow over normal cylinders. Figure 1 is a convenient summary of recent heat-transfer experiments with normal cylinders. The Mach number of the ordinate is based on free-stream velocity and static temperature; the abscissa is the Reynolds number based on the cylinder diameter and on free-stream density, velocity, and viscosity. The shaded areas indicate the experimental ranges of previous work, and these areas are keyed by numbers to the reference list of this report (refs. 4 to 16). Figure 1 also shows the research region of this paper.

The two constant Knudsen number lines in figure 1 provide a guide to the flow regimes. Though the boundaries of free-molecule, slip, and continuum flows probably are not sharply defined, reference 15 proposed the following definitions for flow over normal cylinders:

- (1) Continuum flow: $\text{Kn} < 0.001$
- (2) Slip flow: $0.001 < \text{Kn} < 2$
- (3) Free-molecule flow: $\text{Kn} > 2$

The Knudsen number Kn is defined as the ratio of the mean free path of the gas λ to the cylinder diameter D_w . Kinetic theory of gases relates the Knudsen number to the ratio of the Mach number to the Reynolds number; for air, this proportionality is as follows:

$$\text{Kn} \equiv \frac{\lambda}{D_w} \approx 1.45 \frac{M}{\text{Re}_t} \sqrt{\frac{T}{T_t}} \quad (2)$$

At atmospheric pressure with anemometer wires 0.0002 inch or smaller in diameter, the flow region for the hot wires in much of the early turbulence work would fall below M of 0.10 and between Re of 3 and 30.

King's equation can be written in terms of nondimensional groups as

$$\text{Nu} = A' + B' \sqrt{\text{Pr}} \sqrt{\text{Re}} \quad (1a)$$

The 0.5-power dependence on Reynolds number is well established in slow subsonic continuum flows (ref. 11). However, Lowell (ref. 10) was the first to point out that the Reynolds number alone does not correlate fine-wire heat-transfer data over an appreciable velocity range. He reported that the Mach number was a parameter at $M = 0.375$ and 0.575 . Then, Laurence and Landes (ref. 9) found that their data correlated if Nu was plotted as a function of $\sqrt{\text{Re}}$, but the Mach number remained a

parameter even in the range of $M = 0.1, 0.2$, and 0.3 . Since the work being reviewed is limited to room-temperature airflows over cylinders (i.e., viscosity is constant), the use of both Re and M simply shows that ρD_w and U are not interchangeable in the product $\rho D_w U$. This has been noted by later investigators (refs. 12, 14, and 16). It is well established that the maximum separation of the constant Mach number lines on a plot of Nu against \sqrt{Re} occurs at the lowest Mach numbers; in fact, by proper choice of fluid properties, this "Mach number effect" can be almost eliminated in supersonic flow (refs. 7, 8, 14, and 15).

The Knudsen number was introduced as a correlating parameter in reference 14. The effect of ρ and D_w in the product ρD_w was found to be fully equivalent over the wide experimental range of reference 14. Since conditions of constant ρD_w are constant Knudsen number flows, the Knudsen and Reynolds numbers were shown to be the governing parameters in the incompressible range. The nonequivalence of ρD_w and U in attempted Reynolds number correlations was most pronounced for very fine wires that exhibited low sensitivity to velocity.

Nearly all the anemometer heat-loss investigators have varied the operating temperature of the wire (refs. 9, 10, 14, and 16). The most extensive research has been reported by reference 14, which found that the Nu varied with wire temperature at a given flow condition, and that this variation depended on both M and ρ . However, no simple correlation was found to cover all of the effects observed when the wire temperature was varied.

Reference 16 reports measurements of the nonlinear variation with wire temperature of the heat-transfer rate from hot wires from $M = 0.5$ to 2.5 and $Re = 18$ to 144. The reference proposed a nonlinear overheat ratio ξ defined as

$$h = h_0(1 - \xi \bar{a}_w) \quad (3)$$

where h_0 is the heat-transfer coefficient extrapolated to $\Delta T = 0$, and $\bar{a}_w = (\dot{Q}_w - \dot{Q}_e)/\dot{Q}_e$. The overheat ratio ξ was found to be a function of Mach and Reynolds numbers. Like reference 14, reference 16 found that the nonlinearity reverses under some flow conditions. That is, for some Reynolds numbers in the subsonic region the heat-transfer coefficient increased with increasing wire temperature; and, depending on M and Re , the heat-transfer coefficient was observed to decrease with increasing wire temperature under other flow conditions.

The work of reference 16 is the nearest approach to formulating clearly the important parameters affecting the nonlinear variation of heat-transfer rate with wire temperature. However, the results are

limited to transonic and supersonic Mach numbers and to three values of Reynolds number. Additional data are required to verify the predicted trends at lower subsonic Mach numbers.

Objectives of This Research

The primary objective of this research was to examine the nonlinear variation of heat transfer with wire and air temperatures. The effect of wire temperature is complicated and not fully clarified by previous work, while there appears to be no systematic variation of air temperature in heat-transfer experiments from fine wires. Besides providing an additional insight into the nonlinearity of heat transfer with ΔT , data taken at various air temperatures are important for some hot-wire-anemometer applications (e.g., appendix E of ref. 17).

Furthermore, sufficient heat-transfer data from normal cylinders have been published in recent years that it should be possible to show clearly the effect of continuum, slip, and free-molecule flows on heat-transfer characteristics. An attempt to find a preliminary general correlation based on the results of this and earlier work is also an objective of this report.

APPARATUS AND PROCEDURE

Apparatus

Tunnel and air facility. - A sketch of the variable-density, low-turbulence tunnel used in this research is shown in figure 2. The incoming air passed through a cone-shaped filter screen covered with filter paper and wool felt. The air then entered the 6-inch-diameter inlet section where a total-pressure probe and heater control thermocouple were located. The tunnel contracted to the 1.50-inch-diameter circular test section in 6 inches; both the inlet and test sections were polished machined steel, "Pentrated" to prevent rust formation. Four static-pressure taps (1/64-in. holes) were located in the plane of the hot-wire probe. Static taps also extended along the length of the contracted area. As shown in the sketch, the hot-wire probe was mounted in a probe actuator that moved the wire out of the airflow into a small dead-air volume for protection when flow conditions were adjusted. A high-pressure valve packing gland acted as the vacuum seal but allowed the in and out motion of the probe. This simple feature was the primary reason for the long test life of the fine tungsten wire probe (number 109) reported here; the design evolved during the breaking of the first 108 wires.

The tunnel was serviced by the central laboratory air facilities. Test-section static pressure could be varied between 3 and 110 inches of mercury absolute. Mass-flow rate was independently adjustable; in this manner, the corresponding test-section Mach number could be varied between 0 and 0.85. For low mass-flow rates, the air mass flow was metered with a calibrated sonic orifice. The measured tunnel total and static pressures were used to calculate the Mach number assuming isentropic relations for all mass flow above 0.014 pound per second. A water U-tube manometer was used for total-static differences less than 2 inches of mercury; all other pressure readings were read from calibrated mercury manometers. Pressures were measured to at least three significant figures on both water and mercury manometers. Some uncontrollable fluctuations occurred in the inlet air supply, which may have resulted in a random error in reading of the third significant figure.

The total temperature of the air could be varied between -10° and 300° F by alternate use of refrigerator coils and electrical heaters. Total temperature was calculated from the measured recovery temperature of a calibrated thermocouple located in the probe test-section plane (see fig. 2). This temperature was read to the nearest half degree on a self-balancing indicator. Although the tunnel and inlet piping were well insulated, it was difficult to control the air total temperature as closely as desired over all the flow conditions. Deviations from the nominal air temperatures in day-to-day operation were $\pm 10^{\circ}$ F. However, the air temperature listed in table I is probably accurate within $\pm 10^{\circ}$ F of the total air temperature for each data point; uncertainty in total air temperature did not contribute significantly to uncertainty of the calculated Nusselt numbers except for wire temperatures only 50° F above recovery temperature. The effect of air-temperature fluctuations during any tunnel flow setting was minimized by making a linear interpolation between the two temperatures measured at the beginning and end of each set of six wire heat-loss measurements.

Probe design and tungsten wire. - A sketch of the probe used throughout this research is shown in figure 3. Several features of this design bear mentioning. One of the prime requirements is that the wire-supporting prongs do not substantially interfere with the airflow over the wire. Evidence that the design used met the requirement has been supplied by reference 12. Several probes of similar design were used in an experimental determination of the effect of yaw angle of attack on fine-wire heat transfer in reference 12, which concluded that no effect of probe interference could be noted in the results. Another important feature is that the four-wire lead design has matched metal junctions; that is, all unlike metal contacts occur symmetrically. Since the probe body was occasionally in a large temperature gradient (e.g., 300° F at fine-wire supports to 80° F at lead connector), it was important that no unbalanced thermocouple electromotive force exist in

the probe, especially when the wire was operated only 50° F above air temperature. Although some of the early probe designs did not satisfy this requirement, the probe reported here did not show any direct-current unbalance at zero power input for all operating temperatures. Finally, the four-lead-wire design and the use of a Kelvin double bridge minimized the electrical resistance of the probe and its influence on the accuracy of the hot-wire heat-loss measurements. This point is clarified further in the discussion of anemometer electrical equipment.

Tungsten wire with a nominal diameter of 0.0002 inch served as the heat-transfer element of the probe. The mounting technique is described in reference 9. Briefly, the wire is copper-plated at the ends for ease in soldering to the Inconel prongs; a high-temperature soft solder (m.p., 650° F) was used. One of the major drawbacks in the use of fine wires as heat-transfer elements is the uncertainty in the wire diameter (e.g., see ref. 9). In an attempt to decrease this uncertainty, electron micrographs were taken of samples from the spool of wire used on probe 109. These photographs are shown in figure 4; each is a different wire sample. An average diameter was calculated from several diameter measurements near the central position of each photograph. The necked-down section of sample C was not included in this average, which was 0.00022 inch. It can only be hoped that any wire sample as irregular as sample C would be eliminated after its room-temperature resistance was measured. That is, annealed tungsten wires of equal lengths have nearly identical resistance if the wire diameter is uniform. Many probes were discarded as a control procedure when their measured resistance deviated ± 5 percent from the average. Though the average diameter obtained from these samples is not necessarily the diameter of the 0.077-inch-long sample used in probe 109, the average is more probable than the manufacturer's nominal diameter, and 0.00022 inch was used in all calculations.

One of the most important physical properties of tungsten for the calculation of heat loss is the relation between temperature and electrical resistance. Early in the research it was apparent that each wire required calibrating if consistent data of the temperature loading effect on heat-transfer coefficient were to be obtained. Therefore, a small calibration heater was constructed, a sketch of which is given in figure 5. Several wires were silver-soldered to probes so the solder junction was unaffected at 650° F. These wires were then annealed by supplying sufficient current to heat the wire to about twice their room-temperature resistance for 30 minutes. The annealing caused the room-temperature resistance to drop several percent, but after 30 minutes no further change was observed. The probes were then inserted into the heater, and a complete calibration curve was obtained from 32° to 600° F. Two sample curves are given in figure 6(a). In all cases, a 1-milliampere detection current was used with the Kelvin bridge; therefore, negligible heating above air temperature resulted from the resistance measurement.

A least-square solution for the best parabola through these points gave the coefficients shown in figure 6(a); the curve was represented by $\Omega_w = \Omega_0[1 + \alpha(T_w - 32) + \beta(T_w - 32)^2]$. From ten such complete resistance-temperature calibration curves, an average value of the second-order coefficient β was calculated to be $3.40 \times 10^{-7} (\text{°F})^{-2}$. Then a partial calibration curve was measured for the soft-soldered wire reported here (probe 109). As shown in figure 6(b), a least-square parabola was determined from the data points assuming $\beta = 3.40 \times 10^{-7} (\text{°F})^{-2}$; the resulting empirical equation was used for all calculations to relate measured wire resistance to wire temperature.

Anemometer electrical equipment. - A sketch of the primary circuit is shown in figure 7. The desired operating wire resistance was set on a Leeds and Northrup Kelvin Double Bridge (Model 4285) to four significant figures. With the switch in "hot" position the constant-average-temperature anemometer circuit varied the power input to the bridge until the wire was heated to the desired resistance and the "error" or galvanometer signal was a minimum. A hand-balanced volt-range potentiometer connected to the potential leads of the double bridge was used to measure the voltage across the hot wire. The power input to the wire element could be reproduced at a given flow setting to at least three significant figures in this manner. To measure the resistance of the unheated wire, the anemometer circuit was switched to "cold" position. This supplied the bridge with about 1-milliampere detection current, and the resistance was found by varying the bridge resistance until a 1.65-microvolt-per-millimeter galvanometer indicated balance.

The use of the Kelvin bridge and four-lead probes made it possible to measure the resistance and voltage drop of only the wire element, solder junction, and support prongs. Since the combined resistance of the junctions and prongs was less than 0.2 ohm, these lead resistances were less than 3 percent of the measured resistances in the worst case.

Procedure

The tunnel was operated at nominal Mach numbers of 0.05, 0.10, 0.20, 0.30, and so on to 0.80. At each Mach number, six static-density settings were used corresponding to nominal wire Knudsen numbers of 0.00916, 0.0143, 0.0256, 0.0416, 0.0555, and 0.0770. Most of these combinations were set at all four nominal total air temperatures of tunnel operation: 0°, 80°, 180°, and 280° F. An important feature of the test procedure was the somewhat random schedule of data taking. The run numbers in tables I and II are chronological. As will be emphasized in the RESULTS section, this procedure decreases the probability of systematic error in the measurements.

After the tunnel had been set at the desired condition and the probe moved into the test section, the manometer readings and test-section total temperature were recorded. The unheated or recovery resistance of the wire was measured next. Then, five or six hot-wire resistances were set and the voltage across the wire was recorded at each setting. About 5 minutes were required for all these heat-loss measurements. Finally, the recovery resistance and manometer-temperature readings were recorded again to complete the procedure.

The measured wire recovery resistance was used as a check of the wire temperature-resistance calibration. At no time during the reported runs did the measured Q_e differ from that predicted by figure 6(b), nor the calculated T_e by more than 1 percent and on the average within 0.5 percent; T_e was calculated from the measured air total temperature in a manner discussed in the next section.

DIMENSIONLESS GROUPS OF CORRELATION

In this section, the dimensionless groups used in correlating the data are related to the physical measurements. An energy balance considering convection, conduction, and radiation for a hot wire in steady operation is

$$Q_p = Q_c + Q_k + Q_r \quad (4)$$

The heat input per unit time is simply

$$Q_p = J^2 I^2 Q_w \quad (5)$$

The convective heat-loss rate defines the heat-transfer coefficient h :

$$Q_c = h \pi D_w l (T_w - T_e) \quad (6)$$

Equation (6) has equilibrium or recovery temperature T_e of an insulated wire in the temperature difference $(T_w - T_e)$. Therefore, as the wire temperature approaches its recovery value, the convective heat-transfer rate goes to zero. Figure 8 (from ref. 10) is the equilibrium temperature ratio used to obtain T_e from the measured air total temperature. It is well established that, for Knudsen numbers less than 0.10, the equilibrium temperature ratio for normal wires in both slip and continuum flow is a function only of Mach number (refs. 10 and 13 to 16).

The conduction loss rate to the supporting prongs Q_k is discussed in detail in appendix B. The radiation rate Q_r was calculated to be

less than 0.1 percent of the power input Q_p , and no correction for radiation was made. However, since the heat loss to the supports was appreciable, an "end-loss" correction was made.

The Nusselt number is defined as

$$Nu = \frac{hD_w}{k} \quad (7)$$

The air thermal conductivity k has been evaluated at various temperatures by previous investigators. Some use static, others equilibrium or recovery, or total temperature; frequently in engineering work an arithmetic average "film" temperature is used (ref. 11). The guiding principle for empirical data fitting is, of course, to obtain the best correlation. The DISCUSSION section shows that the nonlinear temperature effect on heat-transfer coefficient of both air and wire temperature is too complicated in the slip-flow region for any of these choices to eliminate either "Mach number" or temperature effects. Therefore, for convenience, the air conductivity has been evaluated at total air temperature (k_t). Since the tunnel was operated at set values of total temperature, this choice introduces no Mach number variation into the Nusselt number correlation at constant Knudsen number:

$$Nu_t = \frac{hD_w}{k_t} \quad (7a)$$

The Nusselt number can be expressed in terms of heat loss using equation (6):

$$Nu_t = \frac{Q_C}{\pi l k_t (T_w - T_e)} \quad (8)$$

The convective heat loss Q_C is the difference between the measured power input Q_p and a calculated correction for Q_K . A convenient way to make this correction is to define an uncorrected Nusselt number Nu_t'' , which is completely determined from measured quantities:

$$Nu_t'' \equiv \frac{Q_p}{\pi l k_t (T_w - T_e)} = \frac{J' I^2 Q_w}{\pi l k_t (T_w - T_e)} \quad (9)$$

Two published end-loss correction procedures were used, as discussed in appendix B; each gave a correction factor ψ , defined as

$$\psi = \frac{Nu_t}{Nu_t''} \quad (10)$$

Therefore, the tabulated Nusselt numbers were obtained from

$$Nu_t = \psi \frac{J' I^2 Q_w}{\pi l k_t (T_w - T_e)} \quad (11)$$

The wire temperature was obtained from measured Q_w and the resistance-temperature calibration:

$$Q_w = Q_0 [1 + \alpha(T_w - 32) + \beta(T_w - 32)^2] \quad (12)$$

The equilibrium wire temperature was calculated from figure 8 and the measured total air temperature. The air conductivity k_t was taken from reference 18. All calculations were performed with an IBM 653 digital computer.

The Reynolds number Re_t for the wire was defined by the free-stream (or static) density and velocity; the air viscosity was evaluated at total air temperature (ref. 18):

$$Re_t = \frac{\rho U D_w}{\mu_t} \quad (13)$$

The Knudsen number was calculated from free-stream density and the wire diameter using the formula suggested by reference 14:

$$Kn = \frac{\lambda}{D_w} = \frac{1.5870 \times 10^{-8}}{\rho D_w} \quad (14)$$

The constant 1.5870×10^{-8} has the units pounds(mass) \times square feet. Equation (14) assumes that the mean free path for air λ is given by elementary kinetic theory and that $\rho \lambda$ is a constant.

The Mach number was calculated from the velocity measured with a sonic orifice and static temperature:

$$M = \frac{U}{49.02 \sqrt{T}} \quad (15)$$

The measured total-static pressures were used in the isentropic relations ($\gamma = 1.40$) for high-range mass flows to find Mach number.

Finally, the dimensionless turbulent intensity v'/U is known to affect the heat transfer from normal cylinders. However, the excellent work of reference 19 has shown that intensities as high as 20 percent

have negligible effect on heat transfer from fine wires if the scale of turbulence is large compared with cylinder diameter. The intensity of turbulence varied in the test section but was always less than 1 percent. The scale was large compared with D_w . Therefore, turbulence was not a factor in these tests.

RESULTS

Twenty-three plots using all 1100 data points are presented in this section. These figures are intended to show the general consistency and the scope of the data. In the following section, these plots are used to point out some of the complicated effects observed in slip flow. Figure 9 shows the Nusselt number variation with Mach number for specified values of Knudsen number and wire and air temperatures. Figure 9(a) gives results for increasing wire temperatures at a total air temperature of 0° F. Similarly, figures 9(b), (c), and (d) are for air temperatures of 80° , 180° , and 280° F, respectively.

With the exception of the lowest wire temperature at each air temperature, the general consistency of the data is good. There are two experimental checks that can be used as a guide to data reliability. The first has already been discussed in the Procedure section; that is, the recovery resistance of the wire at a given air temperature and Mach number can be checked against the measured air temperature and the resistance-temperature calibration. The fact that these measurements usually checked predicted values within 0.5 percent is evidence that the critical Ω -T calibration did not vary during the course of the experiment. Another check for consistency is reproducibility. To demonstrate this feature, the chronological run numbers are shown with the data points in figure 9(b) for T_w of 583.8° F. The fact that the agreement between check points is good is evidence that the heat-transfer characteristics of the wire were unaffected by dirt accumulation, oxidation, or other uncontrollable factors during the experiment.

The data scatter at the lowest wire temperature for each air temperature is reasonable, because in equation (11) it is clear that constant percentage errors in T_w or T_e are magnified when the difference ($T_w - T_e$) is small. However, the scatter at $Kn = 0.0770$ and also at $M > 0.50$ is puzzling. No satisfactory explanation for this scatter has been found. The high Knudsen number suggests that the poor correlation may be associated with the rarefied gas flow. For example, reference 20 calculated a "correction" for the temperature-jump phenomenon of slip flow. Accepted slip theory (ref. 21) was used to calculate the temperature jump. Then, by redefining the heat-transfer coefficient in terms of the difference between jump temperature and recovery temperature, a Nusselt number "correction" that depends only Knudsen number was obtained.

The jump phenomenon does not account for the data scatter observed here at low wire temperatures, because the temperature jump is assumed proportional to $(T_w - T_e)$, going to zero as ΔT vanishes. Furthermore, the correction procedure has dubious value when the slip-flow region is approached from free-molecule flow predictions, because the procedure attempts to force data taken in slip flow to fit the form of continuum-flow observations. In this sense, the correction only confuses the over-all correlation and postpones the inevitable deviation from continuum Reynolds number correlations.

DISCUSSION

In this section some of the non-Reynolds-number effects evident in figure 9 are discussed. Then, the dependence of the Nusselt number on both wire and air temperature is considered. These complicated effects fortunately are relatively small compared with the dependence of Nusselt number on the aerodynamic environment. Therefore, the few generalizations that can be inferred from the data concerning these second-order temperature effects are discussed first. Then, a graphical Nusselt number correlation as a function of Reynolds and Knudsen (or Mach) numbers is presented for the slip-flow data of this research. An attempted general Nusselt number correlation for continuum, slip, and free-molecule flows follows, based on these and earlier data together with free-molecule flow theory. Finally, a fluctuation sensitivity equation for hot-wire anemometers is presented that applies to fine wires in subsonic slip flow.

Preliminary Discussion of Results

The following discussion of figure 9 attempts to point out the deviations from simple \sqrt{Re} dependence of continuum flow that are evident in these slip-flow data. Later in this section, the heat-transfer characteristics of cylinders in continuum, slip, and free-molecule flows are considered. The discussion is limited to air at constant temperature where viscosity is constant. If the Nusselt number were a function only of \sqrt{Re} , lines of constant ρD_w on a logarithmic plot of Nu against U would form a family of parallel straight lines with a common slope of 0.50. The argument changes little if a family of constant Knudsen number lines on a log-log plot of Nusselt number against Mach number is considered. Two important deviations from this behavior should be noted in figure 9. The constant Knudsen number lines are linear only for Mach numbers less than 0.4. The decrease in slope and curvature that occurs around $M = 0.4$ is most pronounced at high Knudsen number where the sensitivity of heat-transfer coefficient to changes in Mach number almost disappears. Secondly, even the straight portions of these

constant Kn curves exhibit slopes other than 0.50. For example, the slopes $(\Delta \log Nu_t) / (\Delta \log M)$ in figure 9(b) for $T_w = 583.8^\circ F$ from $M = 0.05$ to 0.4 increase with increasing Kn from 0.25 to 0.35.

Therefore, it is clear that no simple power dependence of Nu_t against Re_t should be expected to apply to these data over any appreciable range of variables. Furthermore, the wire and air temperatures can be expected to have only secondary influence on any correlation of the data, because the characteristics just discussed appear in all 23 parts of figure 9.

TITLE

Effect of Wire Temperature on Heat-Transfer Coefficient

Many cross plots are necessary in order to show clearly what effect varying the wire temperature has on the heat-transfer coefficient at a given flow condition. Figure 10(a), which presents cross plots of figure 9(a), is a plot of Nusselt number as a function of $(T_w - T_e)$ with Knudsen number as a parameter. All plots are for total air temperature of $0^\circ F$, and each plot is for a particular Mach number. Similarly, figures 10(b), (c), and (d), which are for total air temperatures of 80° , 180° , and $280^\circ F$, respectively, are cross plots of figures 9(b) to (d).

Consider figure 10(b) for $T_t = 80^\circ F$ and $M = 0.10$. The interesting feature is that the Nusselt number increases for the two lowest values of Knudsen number as the wire temperature is increased. For $Kn = 0.0256$ and 0.0416 , Nu_t does not vary appreciably with ΔT , but at the two highest values of Kn , the heat-transfer coefficient decreases as the wire temperature increases. Furthermore, whether Nu_t increases or decreases, the dependence on wire temperature is greatest for ΔT less than $200^\circ F$ and tends to vanish for ΔT greater than $200^\circ F$. This general picture is repeated for all the subsonic Mach numbers at $T_t = 80^\circ$ (fig. 10(b)). The two anomalous points at $M = 0.05$ are probably experimental errors. The percentage change in Nu_t from $\Delta T = 50^\circ F$ to the asymptotic value at $\Delta T > 200^\circ F$ is roughly 20 percent at all Mach numbers for both $Kn = 0.00916$ and $Kn = 0.0770$. There does appear to be a secondary Mach number effect that causes the reversal value of Kn (where the sign of the temperature dependence changes) to increase as M increases. For example, at $M = 0.10$, Nu_t is insensitive to ΔT at $Kn = 0.0256$ and 0.0416 ; but at $M = 0.60$ Nu_t is relatively insensitive to ΔT at higher Kn values (0.0416 and 0.0555).

Therefore, from figure 10(b), the wire temperature appears to affect the heat transfer in a manner primarily dependent on Kn and to a lesser extent on M , over the range of this experiment.

Figures 10(a), (c), and (d) essentially confirm what was observed at $T_t = 80^\circ F$ in figure 10(b). The temperature difference ($T_w - T_e$) again appears to correlate the data into families of curves similar to figure 10(b). It is important to note that between $\Delta T = 50^\circ$ and $200^\circ F$ at all air temperatures the maximum wire-temperature loading effect is evident, and at $\Delta T > 200^\circ F$, Nu_t approaches an asymptote.

Had a nondimensional temperature ratio like $\tau \left(\equiv \frac{T_w - T_e}{T_t} \right)$ been used, this regular feature would not have been observed. In figures 10(c) and (d), the increased air temperature tends to decrease the value of the Knudsen number where the sign of the wire-temperature loading effect reverses. That is, the $Kn = 0.0416$ and 0.0555 lines of both figures 10(c) and (d) show Nu_t increasing with increasing ΔT , while at $T_t = 80^\circ F$ these data were either unaffected or decreased as ΔT increased. This same effect of air temperature on the wire-temperature loading may also be seen in figure 10(a) for $T_t = 0^\circ F$. Disregarding for the moment the $Kn = 0.00916$ and 0.0143 lines in figure 10(a), it is apparent that the insensitivity to ΔT at $M = 0.40$ to 0.80 persists at lower values of Kn in figure 10(a) than in figure 10(b). No explanation for the apparently anomalous behavior of the $Kn = 0.00916$ and 0.0143 curves in figure 10(a) has been discovered.

However, though the air temperature seems to have a secondary role in the wire-temperature loading phenomenon, it should not confuse the primary observation. That is, for $Kn < 0.02$, the heat-transfer coefficient increases with increasing ΔT up to $\Delta T \approx 200^\circ F$, where it assumes an asymptotic value. On the other hand, for $Kn > 0.02$, the heat-transfer coefficient is unaffected or decreases with increasing ΔT to $\Delta T \approx 200^\circ F$, where it again assumes an asymptotic value. The Mach number has a secondary role in this wire-temperature loading effect, generally causing the reversal Knudsen number to assume higher values (> 0.02) as the Mach number increases in the subsonic range.

The trends reported here have been noted by previous investigators. The work of reference 16 was mentioned in the INTRODUCTION. The non-linear overheat coefficient ξ defined by equation (3) is given as a function of Reynolds and Mach number by figure 8 of reference 16. For convenience, this figure is included herein as figure 11, and lines of constant Kn are superimposed. Now, it is clear from figure 10 that the heat-transfer coefficient observed in this research is not a linear function of ΔT (or related \bar{a}_w or τ). However, the sign of the overheat coefficient ξ and its dependence on Kn and M is the important feature of figure 11. In general, in subsonic flow for low Kn , figure 11 predicts an increase in Nu_t with ΔT ; a reversal of sign occurs

between $\text{Kn} = 0.015$ and 0.020 ; while for Kn greater than these latter values, ξ predicts Nu_t will decrease with increasing ΔT . Furthermore, the Mach number has a secondary role causing the reversal value of Kn to increase. With the exception of the asymptotic behavior at large ΔT observed in this research, the work of reference 16 generally substantiates the results reported here. Since similar effects were noted in reference 14, there can be no doubt that these complicated wire-temperature effects are real, even though of second-order magnitude. Appendix B discusses the sole correction to the primary data (conduction loss) at some length to emphasize the fact that the wire-temperature loading effect cannot be traced to improper handling of the primary data.

Effect of Air Temperature on Heat-Transfer Coefficient

In order to isolate the effect of air temperature on the heat-transfer coefficient, it is of course necessary to eliminate the influence of wire-temperature loading. A logical way to accomplish this distinction would be to extrapolate the Nusselt number curves of figure 10 to $\Delta T = 0$. However, this is the region of maximum curvature, and extrapolation to zero overheat would be very uncertain. The asymptotic value of Nu_t for $\Delta T > 200^\circ \text{ F}$ is a more direct Nu_t value that is independent of wire-temperature loading. Therefore, plots of the asymptotic Nu_t ($\Delta T > 200^\circ \text{ F}$) are presented in figure 12 as a function of total air temperature at various Mach numbers. Over the entire range of this experiment, the Nu_t decreases with increasing air temperature. The magnitude of this general trend in figure 12 appears to depend primarily on the value of the Nusselt number, being the order of 5 to 10 percent per 100° F for Nu_t between 3.0 and 4.0 but decreasing to 1 to 2 percent per 100° F near $Nu_t = 1.0$. No clear dependence of the air-temperature loading of Nu_t on either Mach or Knudsen number is discernible in this experimental range.

In figure 12, the Nusselt number decreases with increasing temperature, but it is not clear what dependence the heat-transfer coefficient h has on air temperature. Figure 13, which clarifies this point, is a copy of figure 12(b) for $M = 0.50$ with lines of constant heat-transfer coefficient superimposed. If the heat-transfer coefficient were constant and equal to the value observed in 80° F air, then Nu_t would vary with air temperature as shown by the dashed lines in figure 13. That is, the variation in air thermal conductivity k , which causes the T_t dashed-line dependence, is counterbalanced by an increase in heat-transfer coefficient h as the air temperature is increased. However, since h

is not as temperature-dependent as k in this experimental range, the result is a net decrease in Nu_t with rising T_t .

Reference 6 reports good agreement of data taken at $1540^\circ < T_t < 3000^\circ$ F with the room-temperature correlation of reference 13. Thus, in the range of this work ($450 < Re < 3000$, $0.3 < M < 0.8$), air temperature had little effect on the Nusselt number, though there is a possibility that the high-temperature correlation is slightly lower than the room-temperature results. Therefore, it appears well established that increasing air temperature causes an increase in heat-transfer coefficient for all subsonic conditions where $Re > 1.0$.

The Prandtl number $c_p \mu / k$ varies from about 0.72 at 0° F to 0.68 at 280° F (ref. 18). Several correlations of Nu_t with Pr were attempted in order to eliminate the air-temperature effect shown in figure 13. However, none of these was successful, although plots of Nu_t / Pr_t^2 or Nu_t / Pr_t^3 did generally reduce the air-temperature dependence. The air-temperature range of this research is too small for any valid conclusions concerning Prandtl number correlations to be inferred.

Correlation of Slip-Flow Heat-Transfer Data

The heat-transfer characteristics of cylinders in slip flow are complicated by second-order dependence on body and air temperature. Nevertheless, a correlation of Nusselt number with the flow parameters is desirable as a first approximation in engineering work even though it does not account for the temperature phenomena. The Preliminary Discussion of Results pointed out what deviations from simple \sqrt{Re} dependence are evident in the data, but figure 9 is not a satisfactory substitute for the conventional correlation of Nu and \sqrt{Re} . Figure 14 is an attempt to find a useful correlation. It shows the logarithmic variation of Nu_t with Re_t ; constant M and Kn parametric lines are shown solid and dashed, respectively. Data for $T_t = 80^\circ$ F and $T_w = 584^\circ$ F are plotted in this slip-flow correlation.

The increasing necessity for an additional parameter other than the Reynolds number to correlate these experimental heat-transfer data shows clearly on this plot as Re decreases. This additional parameter is either the Mach number or the Knudsen number. The graphical correlation (fig. 14) makes no distinction between $Nu = f(Re, M)$ or $Nu = f(Re, Kn)$, because both forms are shown. However, only one additional parameter (M or Kn) is independent (eq. (2)). The remainder of this section is devoted to showing that the use of Knudsen number as the additional parameter is preferable. Note that the Kn lines decrease in slope as

Kn increases. However, these constant Kn curves are approaching the slope of the constant Mach number lines at $\text{Kn} = 0.00916$. That is, ρD_w is approaching equivalence to U as required for simple Re correlation as Kn decreases; but the decreasing slopes of the Kn curves as $\text{Kn} \rightarrow 0.0770$ cause a wide divergence of the constant Mach number lines that is most pronounced at low subsonic M (and low Re).

The preceding discussion of figure 14 emphasizes the fact that the failure of the Reynolds number alone to correlate the data, which has been termed a "Mach number effect" (e.g., p. 34 of ref. 22) and associated with compressibility, is, in fact, a rarefied-gas phenomenon and should be termed a "Knudsen number effect." This distinction is important and not just an arbitrary matter of viewpoint, even though equation (2) may make it so appear. When viewed as a rarefied-gas effect, the large separation of subsonic Mach number lines on a plot of Nu_t against Re_t loses its anomalous features and becomes theoretically predictable. Figure 15 was taken from an approximate slip-flow analysis published in 1953 (ref. 23). The qualitative agreement with the data in figure 14 is excellent, considering the approximations made in the theoretical analysis.

Attempted General Correlation for Nusselt Number in Continuum, Slip, and Free-Molecule Flows

Figure 16 combines the correlation of the slip-flow data of this research (fig. 14) with the continuum experimental results of reference 13 and the free-molecular-flow theoretical predictions of references 15 and 24. A brief review of these latter reports is followed by a discussion of figure 16 as a whole.

The experimental range of reference 13 is shown in figure 1. The transient response of thermocouples in air was measured, and the results were correlated within 7.4-percent average deviation of a single observation by the following equation:

$$\text{Nu}_t = 0.431 \sqrt{\text{Re}_t^*} \quad (16)$$

where Re_t^* is a Reynolds number defined by free-stream velocity, total-temperature viscosity, wire diameter, and a density based on static pressure and total temperature. In terms of the Reynolds number defined by equation (13), the Nusselt number correlation of reference 13 is

$$\text{Nu}_t = 0.431 \sqrt{\text{Re}_t} \left(\frac{T}{T_t} \right)^{1/2} \quad (16a)$$

where

$$\frac{T}{T_t} = \left(1 + \frac{\gamma - 1}{2} M^2\right)^{-1}$$

The equation applies in range of the experiment: $250 < Re < 30,000$ and $0.1 < M < 0.9$. A partial plot of equation (16a) is shown in figure 17. The important feature is the small effect that changing the subsonic Mach number has on heat transfer at constant Reynolds number. This Mach number effect increases with increasing M and is practically zero below $M = 0.3$. It is reasonable to expect that a compressibility phenomenon would behave in this manner.

An equation for the free-molecular-flow heat transfer from an infinite cylinder in a diatomic gas stream was derived in reference 24. Evaluating all air properties at $80^\circ F$ and assuming an accommodation coefficient of 0.90, this equation may be written as

$$Nu_t = 0.0297 \frac{g(s)}{Kn} \left(\frac{T}{T_t}\right)^{1/2} \quad (17)$$

where $g(s)$ is a defined function of Mach number plotted in figure 18. Equation (17) applies to all $Kn > 2$. Figure 19 is a plot of equation (17) for $Kn > 2$; it also gives the predictions of slip theory for $Kn < 2$. Although several of the essential features of this free-molecule analysis have been confirmed experimentally, equation (17) has not been tested over an appreciable range of variables. However, free-molecule-analysis theoretical predictions are generally believed reliable. The two essential features of figure 19 for $Kn > 2$ are the first-power dependence on Re and the large separation of subsonic M lines.

Returning to figure 16, the slip-flow experimental data extrapolate smoothly into the continuum-flow empirical curve. However, the slip-flow correlation at $Kn = 0.0770$ cannot be extrapolated to the free-molecule-flow correlation at $Kn = 2$. Nevertheless, several of the trends required by the rarefied-gas analysis are evident in the data. The slip-flow data constant M lines increase in slope and may be approaching first-power Re_t dependence at $Kn = 0.0770$. Furthermore, the increasing Kn dependence causes a spread of the constant M lines at $Kn = 0.0770$ that is most pronounced at low subsonic M . Before the attempted correlation in figure 16 can be reliably extended below $Re = 1.0$, it will be necessary to obtain experimental data between Kn of 0.10 and 10.0. Until these data are published, the theoretical curves from the approximate slip-flow analysis of reference 23 between Kn of 0.04 and 2 shown in figure 19 may be used as a first approximation together with the free-molecule-flow prediction for $Kn > 2$.

Finally, the suggested curve of reference 11 is shown in figure 16 for easy comparison. The low Reynolds number data used to obtain this curve were for very low velocities ($Kn < 0.01$). Furthermore, the attempted general correlation and the reference 11 correlation are not comparable, strictly speaking, because total air temperature was used for calculating conductivity and viscosity in the proposed correlation, while an average "film" temperature was used in reference 11.

Hot-Wire-Anemometer Sensitivity

One application of the heat-transfer correlations presented in the preceding section is for hot-wire-anemometer sensitivity. King's equation (1) sensitivity for wire $Re < 250$ is a crude approximation because the Knudsen number effect complicates the Reynolds number correlation. In the following paragraphs, a sensitivity equation based on dimensionless group correlations is proposed. However, as in the past, the only reliable hot-wire sensitivity is a direct calibration of the particular wire over the flow range of operation. The sensitivity equation serves as a guide to performing this calibration.

The Nusselt number correlation given in figure 14 may be expressed in a general manner as

$$Nu_t = f(M, Kn, \Delta T, T_t) \quad (18)$$

The dependence on ΔT and T_t causes up to 20-percent deviations from figure 14 in a complicated manner. The following derivation assumes that the anemometer wire operates at constant temperature (e.g., see ref. 9). This eliminates the functional dependence of Nu_t on ΔT . It is convenient to express the remaining T_t dependence in equation (18) with a dimensionless temperature ratio τ :

$$\tau = \frac{T_w - \eta T_t}{T_t} = \frac{\Delta T}{T_t} \quad (19)$$

The recovery temperature ratio η (fig. 8) will be assumed a function only of Mach number; this is true for $Kn < 0.10$.

The general sensitivity for a constant-temperature anemometer wire to fluctuating flow velocity, density, and total temperature may be written as

$$2I\Omega_w dI = \frac{\partial}{\partial U} \left[\frac{\pi}{J} \eta k_t Nu_t (T_w - \eta T_t) \right] dU + \frac{\partial}{\partial \rho} \left[\frac{\pi}{J} \eta k_t Nu_t (T_w - \eta T_t) \right] d\rho + \frac{\partial}{\partial T_t} \left[\frac{\pi}{J} \eta k_t Nu_t (T_w - \eta T_t) \right] dT_t \quad (20)$$

Recalling that it is assumed that the wire temperature is maintained constant by a fluctuating feedback current, denoted by i ($=dI$), then equation (20) becomes

$$\begin{aligned} i = & \frac{I}{200} \left[-\left(1 + \frac{\gamma - 1}{2} M^2\right) \frac{M}{\tau} \frac{\partial \eta}{\partial M} - \frac{\eta}{\tau} (\gamma - 1) M^2 + \left(1 + \frac{\gamma - 1}{2} M^2\right) \frac{\partial \log \text{Nu}}{\partial \log M} \right] \\ & \times \frac{100 \delta U}{U} + \frac{I}{200} \left(-\frac{\partial \log \text{Nu}}{\partial \log \text{Kn}} \frac{100 \delta \rho}{\rho} + \frac{I}{200} \left(\frac{\partial \log k}{\partial \log T_t} - \frac{\eta}{\tau} - \frac{\tau + \eta}{\text{Nu}} \frac{\partial \text{Nu}}{\partial \tau} \right) \frac{100 \delta T}{T_t} \right) \end{aligned} \quad (21)$$

Appendix C gives the derivation of equation (21), which relates the fluctuating current i of a constant-temperature anemometer wire to the fluctuating flow variables velocity fluctuation δU , density fluctuation $\delta \rho$, and total-air-temperature fluctuation δT . The average wire current I refers to an infinitely long wire if the sensitivity slopes are taken from Nu_t rather than Nu_t'' plots. The second-order dependence of the general correlation (fig. 14) on air and wire temperatures complicates generalizations concerning the major sensitivity slopes:

$\frac{\partial \log \text{Nu}}{\partial \log M}$, $\frac{\partial \log \text{Nu}}{\partial \log \text{Kn}}$, and $\frac{\partial \text{Nu}}{\partial \tau}$. However, since over a small range of variables each of the logarithmic slopes is linear and approximately independent of the magnitude of the independent variable, it is possible to make two limited generalizations. Figure 20 gives the measured slopes from figure 9(b) for T_w of 583.8° F and its cross plot; these terms are applicable at $T_t \approx 80^\circ \text{ F}$ and $\Delta T > 200^\circ \text{ F}$.

The utility of equation (21) is limited by the lack of a precise universal correlation. However, if the turbulent velocity intensity is the quantity of interest in airflows of $M < 0.4$, equation (21) simplifies considerably. Under these circumstances, density fluctuations are frequently negligible; and, unless heat is added to or taken from the airstream, the total-air-temperature fluctuations are also negligible. The predominant term in the velocity sensitivity is $(\partial \log \text{Nu})/(\partial \log M)$, and this term is as easily obtained experimentally as the usual King's equation calibration curve, perhaps requiring only a larger range of velocity variation.

Finally, it should be pointed out that reference 22 presents sensitivity equations similar to equation (21) for constant-current anemometry, with special emphasis on supersonic-flow applications. In subsonic and transonic applications, equation (21) has the advantage that the Reynolds number was not chosen as an independent variable (M and Kn , rather than M and Re). The use of Reynolds number introduces additional terms in the velocity sensitivity.

CONCLUDING REMARKS

The following conclusions can be drawn from the heat-transfer measurements for cylinders in slip flow presented in this report:

1. An attempted Nusselt number correlation for heat transfer from normal cylinders in subsonic continuum, slip, and free-molecule air-flows is given as figure 16. Slip-flow experimental data of this paper extrapolate into existing continuum-flow experimental data for low values of Knudsen number ($\text{Kn} < 0.01$). The slip-flow data qualitatively verify trends predicted by free-molecule-flow theory ($\text{Kn} > 2$) at Kn approaching 0.10; but extrapolation does not give quantitative agreement. Further experiments in the transition region between slip and free-molecule flows are necessary to complete the general correlation.
2. Empirical equations that give the Nusselt number as a constant power of Reynolds number, familiar in continuum flow, are progressively in error for $\text{Re} < 250$ because of increasing Kn dependence in the slip-flow region. The correlation of Nusselt number for this slip-flow experiment is shown graphically in figure 14 as a function of Reynolds and Knudsen or Mach numbers. This dependence is too complicated for an empirical equation with engineering utility, although simple equations have previously been proposed in both continuum and free-molecule flows.
3. The approximate slip-flow analysis of reference 23 correctly predicts the trends observed but fails to fit the data quantitatively.
4. For air temperatures between 80° and 280° F, the heat-transfer coefficient h increases with increasing temperature difference ΔT at low $\text{Kn} (< 0.02)$. This nonlinearity in h with ΔT has commonly been observed in continuum-flow experiments. However, with air temperatures between 0° and 280° F, at high $\text{Kn} (> 0.02)$ the heat-transfer coefficient decreases with increasing ΔT . In both cases, the effect of ΔT was greatest for ΔT below 200° F, tending to disappear at ΔT greater than 200° F. A secondary Mach number effect causes the reversal Knudsen number of about 0.02 to shift to larger values as M increases. The major trends are corroborated by the work of reference 16.
5. For wires operated at ΔT greater than 200° F, an increase of air temperature causes the heat-transfer coefficient h to increase. This occurs for all flow conditions of this research. The increase in air thermal conductivity with total air temperature tends to cancel the variation of Nusselt number $Nu_t (= hD_w/k_t)$ with air temperature. However, Nu_t decreases slightly with increasing air temperature because the thermal conductivity has a greater temperature-dependence than the heat-transfer coefficient in the range of this research.

6. Constant-temperature hot-wire-anemometer sensitivity to velocity, density, and total-air-temperature fluctuations is extremely complicated with the probe in subsonic slip flow. General sensitivity equations together with a few generalizations observed in this research have been presented. However, individual calibration of wires in the flow range of interest is the only reliable technique for subsonic applications because (a) King's law is a very special case of hot-wire sensitivity ($Kn < 0.001$, $M < 0.3$), and (b) complicated nonlinearity of heat transfer with wire and air temperature prevents accurate generalizations using dimensionless groups.

Lewis Flight Propulsion Laboratory
National Advisory Committee for Aeronautics
Cleveland, Ohio, August 28, 1958

APPENDIX A

SYMBOLS

- A King's equation intercept (eq. (1)), $A = alk$
- A' dimensionless King's equation intercept (eq. (1a)), $A' = a/\pi\Omega_0\alpha$
- A_w cross-sectional area of wire, sq ft
- a, b dimensionless empirical constants (eq. (1))
- a^* dimensionless term in eq. (B24)
- a_s speed of sound
- \bar{a}_w resistance ratio, $(\Omega_w - \Omega_e)/\Omega_e$
- B King's equation slope (eq. (1)), $B = bl\sqrt{D_w\rho c_p k}$
- B_1, B_2 empirical constants (eq. (B16))
- B' dimensionless King's equation slope (eq. (1a)), $B' = b/\pi\Omega_0\alpha$
- B^* dimensionless term defined by eq. (B18)
- C ratio of heat lost by conduction to supports to heat lost to air by convection (eq. (B13))
- c_p isobaric specific heat
- D_s support diameter, ft or in.
- D_w wire diameter, ft or in.
- e, G dimensionless terms defined by eq. (B20)
- g_c conversion factor to engineering units, $(lb(M))(ft)/lb(F)-sec^2$
- h convective heat-transfer coefficient (eq. (6))
- h_0 heat-transfer coefficient extrapolated to $\Delta T = 0$
- I wire current, amp
- J conversion of Btu to ft-lb(F)

J'	conversion of watts to Btu/sec, 9.484×10^{-4}
K _s	thermal conductivity of Inconel support, Btu/(sec)(ft)(°F)
K _w	thermal conductivity of tungsten wire, Btu/(sec)(ft)(°F)
Kn	Knudsen number, λ/D_w
k	thermal conductivity of air, Btu/(sec)(ft)(°F)
l	length of wire, ft
M	Mach number
Nu	Nusselt number, hD_w/k
Nu"	Nusselt number uncorrected for heat loss to supports (eq. (9))
Pr	Prandtl number, $c_p\mu/k$
Q	length-average heating rate, Btu/sec
q	heating rate per unit length, Btu/(ft)(sec)
Re	Reynolds number, $\rho D_w U / \mu$
Re _{f,s}	Reynolds number of support, $\rho U D_s / \mu_{f,s}$
S	dimensionless term defined by eq. (B25)
T	static or free-stream air temperature
ΔT	temperature difference, $T_w - T_e$
T _a	air temperature
T _e	recovery or equilibrium wire temperature
T _t	total air temperature
T _w	length-average wire temperature
T _{w,∞}	length-average temperature of infinitely long wire, $T_{w,\infty} \equiv \sigma_1/\sigma$
t*	dimensionless ratio (eq. (B18))
t _w	local wire temperature at any point x

U	free-stream air velocity, ft/sec
v'	rms turbulent velocity, ft/sec
x	any position along length of wire, $x = 0$ at wire center
Y	dimensionless term defined by eq. (B18)
z	factor in end-loss correction procedure, defined by eq. (B19)
α	first-order coefficient of electrical resistance - temperature relation (eq. (12)), $^{\circ}\text{F}^{-1}$
β	second-order coefficient of electrical resistance - temperature relation (eq. (12)), $^{\circ}\text{F}^{-2}$
γ	ratio of specific heats, 1.4 for air
δ	perturbation component
η	recovery temperature ratio, $\eta \equiv T_e/T_t$
λ	mean free path of air, ft
μ	air viscosity, lb(M)/(ft)(sec)
ξ	nonlinear overheat coefficient (eq. (3))
ρ	air density, lb(M)/cu ft
σ	coefficient defined in eq. (B7)
σ_1	coefficient defined in eq. (B8)
τ	temperature ratio, $\tau \equiv (T_w - T_e)/T_t$
ψ	end-loss correction ratio, $\psi \equiv \text{Nu}/\text{Nu}'$
Ω_a	length-average wire resistance at air temperature T_a , ohms
Ω_e	length-average wire resistance at recovery air temperature T_e , ohms
Ω_w	length-average wire resistance at hot-wire temperature T_w , ohms
Ω_0	length-average wire resistance at 32° F , ohms
ω	wire resistance per unit length, ohms/ft

511

Subscripts:

- C convection
f film temperature, $T_f \equiv (T_s + T_e)/2$
K conduction
m measured
P production
R radiation
s support (except a_s)
t total air temperature T_t
w wire or cylinder
0 evaluated at 32° F (except h_0)

5111

CS-4 back

APPENDIX B

CORRECTIONS FOR CONDUCTION TO SUPPORTS

Linear Correction

The steady-state heat transfer from a hot wire having negligible radiant heat loss is treated by Lowell in reference 10, where equations for making precise corrections for finite wire length are presented. Except for a minor innovation, the following analysis is that of reference 10.

The energy-balance equation at any cross section x for this problem is simply

$$q_P = q_C + q_K \quad (B1)$$

The convection heat loss per unit length of wire at x can be expressed as

$$q_C = hD_w \pi(t_w - T_e) = \pi k_t N_u t (t_w - T_e) \quad (B2)$$

The expression for conduction of heat to the supports can be simplified if it is assumed that the heat flow through the wire is one-dimensional and that the wire thermal conductivity K_w is not affected by temperature:

$$q_K = - K_w A_w \frac{d^2 t_w}{dx^2} \quad (B3)$$

Neglecting the second-order term $\beta(t_w - 32)^2$, the resistance per unit length of wire can be written in terms of the local wire temperature:

$$\omega = \omega_0 [1 + \alpha(t_w - 32)] \quad (B4)$$

where ω_0 is the resistance per unit length in ohms per inch at 32° F. Substituting equations (B2) to (B4) into (B1),

$$J' I^2 \omega_0 [1 + \alpha(t_w - 32)] = \pi k_t N_u t (t_w - T_e) - K_w A_w \frac{d^2 t_w}{dx^2} \quad (B5)$$

Equation (B5) can be written more simply as

$$\frac{d^2 t_w}{dx^2} - \sigma t_w = -\sigma_1 \quad (B6)$$

where the constants are defined as follows:

$$\sigma = \frac{\pi k_t N u_t - J' I^2 \omega_0 \alpha}{K_w A_w} \quad (B7)$$

$$\sigma_1 = \frac{\pi k_t N u_t T_e + J' I^2 \omega_0 \alpha \left(\frac{1}{\alpha} - 32 \right)}{K_w A_w} \quad (B8)$$

The lengthwise variation of $k_t N u_t$ or its equivalent $h D_w$ is ignored; that is, h is assumed unaffected by t_w or T_e .

Equation (B6) is a second-order, ordinary differential equation with constant coefficients. The following boundary conditions are used to find the temperature distribution along the wire length:

(1) The wire is symmetrical; therefore, at the center of the wire (at $x = 0$), the temperature gradient must be zero: $\frac{dt_w}{dx} \Big|_{x=0} = 0$.

(2) The temperature at each support, $x = \pm l/2$, is $T_{w,s}$ (an as yet undetermined temperature, but physically it is known that $T_e \geq T_{w,s} \geq T_w$).

The solution of equation (B6) satisfying these conditions is

$$t_w = T_{w,\infty} - (T_{w,\infty} - T_{w,s}) \frac{\cosh \frac{\sigma^{1/2}}{2} x}{\cosh \frac{\sigma^{1/2}}{2} l} \quad (B9)$$

The measured mean resistance Ω_w is related to the length-average wire temperature ($\omega_0 l = \Omega_0$):

$$\Omega_w = \Omega_0 [1 + \alpha(T_w - 32)] \quad (B10)$$

Here, T_w is obtained from integration of (B9) over the wire length:

$$T_w = T_{w,\infty} - \frac{T_{w,\infty} - T_{w,s}}{\frac{\sigma^{1/2} l}{2}} \tanh \frac{\sigma^{1/2} l}{2} \quad (B11)$$

Having obtained the wire-temperature distribution, the next step is to write an energy balance on the entire wire. The power input is now written in terms of equation (B10), the convection loss in terms of (B11), and the conduction loss in terms of the derivative of (B9) evaluated at the point of attachment ($x = l/2$):

$$\begin{aligned} J' I^2 \omega_0 [1 + \alpha(T_w - 32)] \\ = \pi k_t N_u t (T_w - T_e) + \frac{2 K_w A_w \sigma^{1/2}}{l} (T_{w,\infty} - T_{w,s}) \tanh \frac{\sigma^{1/2} l}{2} \end{aligned} \quad (B12)$$

At this point, it is convenient to define a quantity C as the ratio of the heat lost by conduction to the supports to that lost directly to the airstream by convection:

$$C \equiv \frac{4 K_w A_w}{l^2} \frac{(T_{w,\infty} - T_{w,s}) \left(\frac{\sigma^{1/2} l}{2} \right) \tanh \frac{\sigma^{1/2} l}{2}}{\pi k_t N_u t (T_w - T_e)} \quad (B13)$$

Equation (B12) can be expressed in terms of C as follows:

$$J' I^2 \omega_0 [1 + \alpha(T_w - 32)] = \pi k_t N_u t (T_w - T_e) (1 + C) \quad (B14)$$

The only unknown in C (other than $N_u t$) is the temperature at the support $T_{w,s}$. An energy balance on the support is made to determine $T_{w,s}$. The problem is analogous to the wire treatment just outlined except that the heat input is the conduction from the wire, the output is convection from the support, and the electrical power input is assumed zero in the supports. Solving this energy balance for $T_{w,s}$ and approximating $\tanh(\sigma^{1/2} l/2)$ as 1.0 give the following:

$$T_{w,s} = \frac{2 N_u f^{1/2} s_f^{1/2} k_f^{1/2} D_s^{1/2} T_e + K_w D_w^2 \sigma^{1/2} T_{w,\infty}}{2 N_u f^{1/2} s_f^{1/2} k_f^{1/2} D_s^{1/2} + K_w D_w^2 \sigma^{1/2}} \quad (B15)$$

5111

Since the objective of the foregoing analysis of the heat transfer from the support was to determine $T_{w,s}$ in terms of known quantities (so that ultimately the end loss ratio C could be found), it appears that the introduction of $Nu_{f,s}$ in equation (B15) has simply replaced one unknown by another. Fortunately, the Nusselt number of the support can be adequately represented by the following empirical relation, because the support is large and in continuum flow:

$$Nu_{f,s} = B_1 + B_2 (Re_{f,s})^n \quad (B16)$$

where

$$Re_{f,s} = \frac{\rho U D_s}{\mu_{f,s}}$$

Equation (B16) neglects the small Mach number effect observed at $Re > 250$. Following are values of n , B_1 , and B_2 from reference 11 (p. 260, table 10-4):

$Re_{f,s}$ range	n	B_1	B_2
0.1 - 1000	0.52	0.32	0.43
1000 - 50,000	.60	0	.24

Equations (B13), (B15), and (B16) can be combined with equation (B14); the only unknown quantity is the corrected wire Nusselt number Nu_t^* . Lowell (ref. 10) has shown that the combination of essentially the equations just mentioned can be written as

$$C = \frac{1 - t^*(1 + C)}{B^* [(1 + C)^{-1} - t^*] + Y [(1 + C)^{-1} - t^*]^{1/2} - 1} \quad (B17)$$

where

$$\left. \begin{aligned} t^* &\equiv \frac{T_w - T_e}{\left(\frac{1}{\alpha} - 32\right) + T_w} \\ B^* &\equiv \frac{7k_t Nu_t''}{(B_1 + B_2 Re_{f,s}^n)^{1/2} K_s^{1/2} k_{f,s}^{1/2} D_s} \\ Y &\equiv \left(\frac{k_t}{K_w}\right)^{1/2} \frac{l}{D_w} (Nu_t'')^{1/2} \end{aligned} \right\} \quad (B18)$$

A more usable form of equation (B17) was derived by Lowell after reference 10 was published. Another form of the ratio of corrected to uncorrected Nusselt number was defined as follows:

$$\frac{Nu_f}{Nu_{f'}^m} = \frac{1}{1 + C} = (1 - t^*) \left(\frac{t^*}{1 - t^*} + z^2 \right) \quad (B19)$$

Then, by letting

$$\left. \begin{array}{l} e \equiv Y(1 - t^*)^{1/2} \\ G \equiv B^*(1 - t^*) \end{array} \right\} \quad (B20)$$

an algebraically simpler expression for equation (B19) is obtained:

$$Gz + e = \frac{1}{z - z} \quad (B21)$$

The procedure used to calculate Nu_t for table I was to solve (B21) for the root of z between $z = 0.5$ and $z = 1.0$. This solution is straightforward once the physical constants in both G and e are evaluated. The following values were used in the electronic digital computer data-reduction program:

Tungsten wire: $l = 0.077$ in.

$$D_w = 2.2 \times 10^{-4} \text{ in.}$$

$$\alpha = 2.24 \times 10^{-3} \text{ }^{\circ}\text{F}^{-1}$$

$$K_w = 3.43 \times 10^{-2} \text{ Btu}/(\text{sec})(\text{ft})(^{\circ}\text{F})$$

Inconel support: $D_s = 0.027$ in. (at point of attachment)

$$K_s = 2.19 \times 10^{-3} \text{ Btu}/(\text{sec})(\text{ft})(^{\circ}\text{F})$$

Air properties: $\mu_{f,s} \approx \mu_t$ $k_{f,s} \approx k_t$ $\left. \right\} \text{ (ref. 18)}$

Another method of making end-loss corrections on hot-wire data has been widely used by investigators at other laboratories. Essentially, it is a limiting case of the more general method just outlined. Kovásznay originally published the method (without derivation) in reference 7; reference 25 gives a more complete presentation.

The problem is identical to that treated by Lowell, except that Kovasznay uses the mathematically simpler boundary condition $T_{w,s} = T_e$. Since the recovery temperature T_e is immediately available, equations (B7) and (B12) can be solved without further ado for Nu_t . A further simplification can be gained if the reference temperature of the calibration of wire temperature and resistance is taken at T_e rather than at $32^\circ F$ as in the previous section. If these substitutions are made in equations (B13) and (B14), it can be shown that the following equation is the desired solution for ψ :

$$\frac{Nu_t}{Nu_t''} = \frac{\frac{\bar{a}_w}{\bar{a}_*} + \bar{a}_w}{1 + \bar{a}_w} \quad (B22)$$

where

$$\bar{a}_w = \frac{\Omega_w - \Omega_e}{\Omega_e} \quad (B23)$$

$$\frac{\bar{a}_w}{\bar{a}_*} = 1 - S \left(\frac{\bar{a}_*}{\bar{a}_w} \right)^{1/2} \tanh \frac{1}{S} \left(\frac{\bar{a}_w}{\bar{a}_*} \right)^{1/2} \quad (B24)$$

$$S = \frac{D_w(K_w)}{l(k_t)}^{1/2} Nu_t''^{-1/2} (1 + \bar{a}_w)^{1/2} \quad (B25)$$

This procedure was also used in the data-reduction program. The results of this end-loss correction agreed with those obtained using equation (B21) within a small fraction of 1 percent of Nu_t for all flow conditions of this research. Therefore, the probe supports did act effectively as an infinite sink. That is, the wire-support junction was effectively maintained at recovery temperature, $T_e = T_{w,s}$.

Nonlinear Correction

The linear correction procedures just outlined are rather elaborate. However, the methods differ only in the manner used to treat the temperature of the wire-support junction. Both procedures assume that the wire has no second-order temperature dependence ($\beta = 0$), that the heat-transfer coefficient is not dependent on wire temperature, and that the wire thermal conductivity is constant. Generally, none of these

assumptions are true. So, it is conceivable that the end-loss correction is incorrect and that this mistake causes the nonlinearity of N_{ut} with ΔT and T_t . An excellent discussion of this problem is published in reference 16. Mechanically integrated solutions of the nonlinear equation that includes β , ξ (eq. (3)), and $K_w = f(t_w)$ are compared with the linear solution, and it is concluded that the linear solution of Kovásznay differs by only 1/2 percent from the nonlinear solutions for any realistic probe design. Therefore, the procedure used to correct for finite wire length in this report is adequate.

APPENDIX C

DERIVATION OF HOT-WIRE-ANEMOMETER SENSITIVITY EQUATIONS

Assume that the general heat-loss characteristics of normal cylinders are known in terms of Nusselt number corrected for conduction loss to supports. Specifically, the Nusselt number is a function of the Mach and Knudsen (or Reynolds) numbers, and the effect of air temperature at constant wire temperature is assumed described by a single parameter τ :

$$Nu_t = f(M, Kn, \tau) \quad (C1)$$

$$\tau = \frac{T_w - T_e}{T_t} \quad (C2)$$

The subscript t on Nu and k will be dropped here and understood throughout appendix C. The recovery temperature ratio η will be assumed to be independent of Kn , as in figure 8; this is valid at least to $Kn = 0.10$:

$$\eta = \frac{T_e}{T_t} = f(M) \quad (C3)$$

The heat loss from a wire may be written as

$$J' I^2 \Omega_w = \pi l k (T_w - \eta T_t) Nu \quad (C4)$$

Equation (C4) assumes that Nu is corrected for finite wire length so that I^2 is the square of the measured wire current times the end-loss correction factor, ψI_m^2 . Naturally, if a calibration curve for a particular wire is being used, it is possible to set $\psi = 1$ and correlate data as Nu'' .

It will be assumed that the hot-wire resistance (and temperature) is maintained constant by a fluctuating feedback current:

$$2J' I \Omega_w dI = \frac{\partial}{\partial U} [\pi l k (T_w - \eta T_t) Nu] dU + \frac{\partial}{\partial \rho} [\pi l k (T_w - \eta T_t) Nu] d\rho + \frac{\partial}{\partial T_t} [2l k (T_w - \eta T_t) Nu] dT \quad (C5)$$

If the fluctuating current dI is set equal to i and small finite flow fluctuations are approximated by δ to replace the derivatives, equation (C5) can be written as

$$\begin{aligned}
 i = & \left[\frac{\pi l}{2J' I \Omega_w} k N u T_t \left(-\frac{\partial \eta}{\partial U} \right) + \frac{\pi l}{2J' I \Omega_w} k N u n \left(-\frac{\partial T_t}{\partial U} \right) + \frac{\pi l}{2J' I \Omega_w} k (T_w - \eta T_t) \frac{\partial N u}{\partial U} \right] \delta U \\
 & + \left[\frac{\pi l}{2J' I \Omega_w} k (T_w - \eta T_t) \frac{\partial N u}{\partial \rho} \right] \delta \rho \\
 & + \left[\frac{\pi l}{2J' I \Omega_w} (T_w - \eta T_t) N u \frac{\partial k}{\partial T_t} - \frac{\pi l}{2J' I \Omega_w} k N u \eta + \frac{\pi l}{2J' I \Omega_w} k (T_w - \eta T_t) \frac{\partial N u}{\partial T_t} \right] \delta T_t
 \end{aligned} \tag{C6}$$

It will be convenient to introduce the following dimensionless groups to generalize equation (C6) for numerical evaluation of the various sensitivity derivatives:

$$\frac{\partial}{\partial \rho} = \frac{\partial K_n}{\partial \rho} \frac{\partial}{\partial K_n} = - \frac{K_n}{\rho} \frac{\partial}{\partial K_n} \tag{C7}$$

$$\frac{\partial}{\partial U} = \frac{\partial M}{\partial U} \frac{\partial}{\partial M} = \frac{1 + \frac{\gamma - 1}{2} M^2}{a_s} \frac{\partial}{\partial M} \tag{C8}$$

$$\frac{\partial T_t}{\partial U} = \frac{U}{c_p g_c J} \tag{C9}$$

$$\frac{\partial}{\partial T_t} = \frac{\partial \tau}{\partial T_t} \frac{\partial}{\partial \tau} = - \frac{\tau + \eta}{T_t} \frac{\partial}{\partial \tau} \tag{C10}$$

Substituting (C7) to (C10) into equation (C6) and recalling that

$M = \frac{U}{a_s}$ and $\frac{I}{2N u} = \frac{\pi l}{2J I \Omega_w} k (T_w - \eta T_t)$, the following form may be written:

$$\begin{aligned}
 i = & \frac{I}{2} \left[- \left(1 + \frac{\gamma - 1}{2} M^2 \right) \frac{M}{\tau} \frac{\partial \eta}{\partial M} - \frac{\eta}{T_w - \eta T_t} \frac{U^2}{c_p g_c J} + \left(1 + \frac{\gamma - 1}{2} M^2 \right) \frac{M}{N u} \frac{\partial N u}{\partial M} \right] \frac{\delta U}{U} \\
 & + \frac{I}{2} \left(- \frac{K_n}{N u} \frac{\partial N u}{\partial K_n} \right) \frac{\delta \rho}{\rho} + \frac{I}{2} \left(\frac{T_t}{k} \frac{\partial k}{\partial T_t} - \frac{\eta T_t}{T_w - \eta T_t} - \frac{\tau + \eta}{N u} \frac{\partial N u}{\partial \tau} \right) \frac{\delta T_t}{T_t}
 \end{aligned} \tag{C11}$$

Replacing $\left(\frac{u}{v} \frac{\partial v}{\partial u}\right)$ by $\frac{\partial \log v}{\partial \log u}$ and using a familiar identity, the sensitivity equation can be written in its final form, which is given as equation (21) of the text.

REFERENCES

1. King, Louis Vessot: On the Convection of Heat from Small Cylinders in a Stream of Fluid. Proc. Roy. Soc. (London), ser. A, vol. 214, no. 14, Nov. 12, 1914, pp. 373-432.
2. Dryden, H. L., and Kuethe, A. M.: The Measurement of Fluctuations of Air Speed by the Hot-Wire Anemometer. NACA Rep. 320, 1929.
3. Corrsin, Stanley: Extended Applications of the Hot-Wire Anemometer. NACA TN 1864, 1949.
4. Carbon, M. W., Kutsch, H. J., and Hawkins, G. A.: The Response of Thermocouples to Rapid Gas-Temperature Changes. Trans. ASME, vol. 72, no. 5, July 1950, pp. 655-657.
5. Flock, Ernest: Ninth Monthly Report of Progress on the Development of Thermocouple Pyrometers for Gas Turbines. NBS, Sept. 6, 1946.
6. Glawe, George E., and Johnson, Robert C.: Experimental Study of Heat Transfer to Small Cylinders in a Subsonic, High-Temperature Gas Stream. NACA TN 3934, 1957.
7. Kovásznay, Leslie S. G., and Törmarck, Sven I. A.: Heat Loss of Hot-Wires in Supersonic Flow. Bumblebee Rep. No. 127, Dept. Aero., The Johns Hopkins Univ., Apr. 1950. (Contract NOrd 8036 with BuOrd., U. S. Navy.)
8. Laufer, J., and McClellan, R.: Measurement of Heat Transfer from Fine Wires in Supersonic Flows. Jour. Fluid Mech., vol. 1, pt. 3, Sept. 1956, pp. 276-289.
9. Laurence, James C., and Landes, L. Gene: Auxiliary Equipment and Techniques for Adapting the Constant-Temperature Hot-Wire Anemometer to Specific Problems in Air-Flow Measurements. NACA TN 2843, 1952.
10. Lowell, Herman H.: Design and Applications of Hot-Wire Anemometers for Steady-State Measurements at Transonic and Supersonic Airspeeds. NACA TN 2117, 1950.
11. McAdams, William H.: Heat Transmission. Third ed., ch. 10, McGraw-Hill Book Co., Inc., 1954.

12. Sandborn, Virgil A., and Laurence, James C.: Heat Loss from Yawed Hot Wires at Subsonic Mach Numbers. NACA TN 3563, 1955.
13. Scadron, Marvin D., and Warshawsky, Isidore: Experimental Determination of Time Constants and Nusselt Numbers for Bare-Wire Thermocouples in High-Velocity Air Streams and Analytic Approximation of Conduction and Radiation Errors. NACA TN 2599, 1952.
14. Spangenberg, W. G.: Heat-Loss Characteristics of Hot-Wire Anemometers at Various Densities in Transonic and Supersonic Flow. NACA TN 3381, 1955.
15. Stalder, Jackson R., Goodwin, Glen, and Creager, Marcus O.: Heat Transfer to Bodies in a High-Speed Rarefied-Gas Stream. NACA Rep. 1093, 1952. (Supersedes NACA TN 2438.)
16. Winovich, Warren, and Stine, Howard A.: Measurements of the Non-linear Variation with Temperature of Heat-Transfer Rate from Hot Wires in Transonic and Supersonic Flow. NACA TN 3965, 1957.
17. Mickelsen, William R., and Baldwin, Lionel V.: Aerodynamic Mixing Downstream from Line-Source of Heat in High-Intensity Sound Field. NACA TN 3760, 1956.
18. Hilsenrath, Joseph, et al.: Tables of Thermal Properties of Gases. Cir. 564, NBS, Nov. 1, 1955.
19. Van Der Hegge Zijnen, B. G.: Heat Transfer from Horizontal Cylinders to a Turbulent Air Flow. Appl. Sci. Res., sec. A, vol. 7, nos. 2-3, 1958, pp. 205-223.
20. Collis, D. C., and Williams, M. J.: Two-Dimensional Forced Convection from Cylinders at Low Reynolds Numbers. Rep. A. 105, Res. & Dev. Branch, Aero. Res. Labs. (Australia), Nov. 1957.
21. Kennard, Earle H.: Kinetic Theory of Gases. McGraw-Hill Book Co., Inc., 1938, pp. 312-315.
22. Morkovin, M. V.: Fluctuations and Hot-Wire Anemometry in Compressible Flows. AGARDograph 24, North Atlantic Treaty Organization, AGARD, Nov. 1956.
23. Sauer, F. M., and Drake, R. M., Jr.: Forced Convection Heat Transfer from Horizontal Cylinders in a Rarefied Gas. Jour. Aero. Sci., vol. 20, no. 3, Mar. 1953, pp. 175-180.

24. Stalder, Jackson R., Goodwin, Glen, and Creager, Marcus O.: A Comparison of Theory and Experiment for High-Speed Free-Molecule Flow. NACA Rep. 1032, 1951. (Supersedes NACA TN 2244.)
25. Kovasznay, L. S. G.: Turbulence Measurements. Vol. IX of Physical Measurements in Gas Dynamics and Combustion, sec. F, pt. 1, R. Ladenburg, ed., Princeton Univ. Press, 1954, pp. 213-285.

TABLE I. - RESULTS OF STUDY OF HEAT TRANSFER FROM CYLINDERS IN SUBSONIC SLIP FLOW

M	Kn	Re _t	T _t	T _w	Nu _t ^a	Nu _t	Run ^a	M	Kn	Re _t	T _t	T _w	Nu _t ^a	Nu _t	Run	
0.0488	0.0753	0.9763	12.8	35.8	1.054	0.7396	342	0.0503	0.0255	2.867	87.5	133.2	1.303	0.9931	133	
		.9814	11.5	86.6	.9479	.6534	343					183.6	1.525	1.022	134	
		9.9	183.6	.9212	.6402	344	283.2						1.299	1.013		
0.0490	0.0143	4.677	272.9	335.2	1.361	1.089	319	0.0506	0.0442	1.862	85.0	133.2	1.081	0.7928	108	
		4.679	272.7	333.9	1.402	1.133	320					183.6	1.086	0.8050	110	
		4.685	272.1	483.4	1.429	1.170	321						283.2	1.066	0.7994	
		4.689	271.8	583.8	1.450	1.199	322					385.9	1.051	0.7947	112	
		4.693	271.4	620.0	1.456	1.208	323						483.4	1.037	0.7891	
		0.0748	0.9973	8.5	33.6	1.058	0.7428	420					583.8	1.031	0.7883	114
		.9952	9.0	86.6	.9783	.6803	421	583.8					1.031	0.7883		
0.0492	0.0142	5.238	8.4	33.6	2.002	1.596	348	0.0507	0.0253	2.762	198.6	233.1	1.281	0.9981	223	
		5.222	9.3	86.6	1.797	1.424	349					194.4	1.236	0.9768	225	
		5.206	10.1	183.6	1.715	1.370	350						278.7	1.235	0.9858	
		5.190	10.9	383.9	1.698	1.384	351					192.1	1.237	0.9867	227	
		5.174	11.7	483.4	1.698	1.394	352						280.4	1.235	0.9974	
		5.158	12.5	583.4	1.700	1.407	353					191.0	1.235	0.9974	228	
		0.0551	1.308	71.5	133.2	1.021	0.7364	85					265.5	0.9844	0.7457	288
					183.6	1.003	.7278	86					264.2	1.244	0.9717	224
					283.2	.9908	.7280	87					1.721	0.9849	0.7514	289
					383.9	.9819	.7281	88					262.9	1.483	0.9945	284
					483.4	.9619	.7147	89					261.7	0.9845	0.7769	281
					583.8	.9504	.7061	90					260.4	1.255	0.9888	292
0.0495	0.0744	0.9724	72.5	132.0	0.9212	0.6468	1	0.0508	0.0403	1.711	265.5	333.2	0.8621	0.6558	283	
				183.0	.9094	.6426	2					1.716	0.9849	0.7514	289	
				234.5	.8082	.6471	3					262.4	1.236	0.9768	225	
				285.1	.9008	.6450	4					1.728	0.9844	0.7603	280	
				332.6	.8960	.6441	5					279.5	1.235	0.9851	281	
				386.5	.8871	.6390	6					277.6	1.237	0.9851	281	
				437.3	.8815	.6359	7					275.8	1.235	0.9851	282	
				488.0	.8712	.6275	8					269.2	1.235	0.9856	287	
				538.5	.8658	.6201	9					1.728	0.9845	0.6692	194	
				590.2	.8572	.6120	10					1.732	0.9845	0.6789	195	
0.0496	0.0570	1.331	3.5	33.6	1.101	0.7804	398					1.729	0.9845	0.6789	198	
		1.329	3.9	86.6	1.069	.7614	397					1.728	0.9845	0.6789	198	
		1.324	4.8	183.6	1.028	.7374	398					1.727	0.9845	0.6789	195	
		1.321	5.4	383.9	1.010	.7344	399					1.726	0.9845	0.6789	195	
		1.318	6.1	483.4	1.002	.7258	400					1.725	0.9845	0.6789	196	
		1.255	18.9	583.8	.9929	.7182	401					1.724	0.9845	0.6789	197	
		0.0498	0.0259	2.603	283.8	333.2	1.090	0.8420	309				1.723	0.9845	0.6789	198
		2.611	282.5	383.9	1.114	.8697	310	1.722	0.9845			0.6789	198			
0.0500	0.0143	2.618	281.3	483.4	1.141	.9045	311	0.0516	0.0582	1.723	265.5	333.2	0.8621	0.6558	283	
		2.626	280.0	583.8	1.151	.9224	312					188.0	1.235	0.9845	284	
		2.634	278.7	620.0	1.149	.9235	313					188.3	1.235	0.9845	284	
		5.6	133.2	1.607	1.270	145	188.6					1.235	0.9845	284		
		185.6	1.459	1.145	1.270	146	188.9					1.235	0.9845	284		
		283.2	1.598	1.289	1.270	147	189.0					1.235	0.9845	284		
		383.9	1.590	1.295	1.270	148	189.0					1.235	0.9845	284		
		483.4	1.594	1.310	1.270	149	189.0					1.235	0.9845	284		
		583.8	1.595	1.321	1.270	150	189.0					1.235	0.9845	284		
0.0501	0.0259	2.951	5.6	33.6	1.517	1.155	380	0.0516	0.0281	1.724	233.1	333.2	0.8621	0.6558	283	
		2.941	6.5	86.6	1.418	1.078	361					188.0	1.235	0.9845	284	
		2.929	7.5	183.6	1.374	1.056	352					188.3	1.235	0.9845	284	
		2.918	6.5	383.9	1.361	1.059	363					188.6	1.235	0.9845	284	
		2.907	9.5	483.4	1.362	1.078	364					188.9	1.235	0.9845	284	
		2.897	10.5	583.8	1.357	1.079	365					189.2	1.235	0.9845	284	
		1.706	184.9	233.1	1.065	0.8019	217					189.5	1.235	0.9845	284	
		1.708	184.5	283.2	1.053	.7974	218					189.8	1.235	0.9845	284	
		1.710	184.0	383.9	1.037	.7938	219					189.0	1.235	0.9845	284	
		1.712	183.6	483.4	1.031	.7970	220					189.3	1.235	0.9845	284	
0.0502	0.00922	7.896	89.0	133.2	1.903	1.541	151	0.0516	0.0740	2.028	133.2	1.239	0.9354	127		
				183.6	1.898	1.548	152					183.6	1.246	0.9501	128	
				283.2	1.875	1.545	153									

TABLE I. - Continued. RESULTS OF STUDY OF HEAT TRANSFER FROM CYLINDERS IN SUBSONIC SLIP FLOW

M	Kn	Ret	T _t	T _w	Nut [†]	Nut _t	Run	M	Kn	Ret	T _t	T _w	Nut [†]	Nut _t	Run	
0.0990	0.0259	5.199	277.5	533.2	1.279	1.014	514	0.1020	0.00916	16.91	2.0	33.6	2.653	2.194	984	
		5.208	276.7	533.9	1.351	1.086	315			16.90	2.1	86.6	2.555	2.121	985	
		5.217	276.0	463.4	1.391	1.155	316			2.2	183.6	2.505	2.101	986		
		5.226	275.3	583.8	1.406	1.158	317			16.89	2.3	383.9	2.507	2.143	987	
		5.235	274.5	620.0	1.407	1.162	318		0.00917	16.89	2.4	483.4	2.509	2.180	988	
				133.2	1.207	0.9042	91			16.88	2.5	583.8	2.509	2.172	989	
	0.0549	2.628	72.5	163.6	1.180	.8861	92		0.1024	0.0445	5.356	65.0	133.2	1.342	1.028	115
				283.2	1.152	.8764	93					183.6	1.294	.9951	116	
				363.9	1.131	.8669	94					283.2	1.274	.9896	117	
				463.4	1.113	.8579	95					583.9	1.251	.9798	118	
				583.8	1.098	.8486	96					483.4	1.229	.9682	119	
0.0995	0.0256	5.804	13.8	35.6	2.068	1.658	366	0.1024	0.0757	1.866	185.5	233.1	1.006	0.7488	163	
		5.802	13.9	88.6	1.780	1.409	567			1.873	185.3	283.2	.9663	.7188	164	
		5.800	14.0	183.6	1.684	1.342	568			1.879	185.1	383.9	.9621	.7252	165	
		5.798	14.1	383.9	1.645	1.336	569			1.886	184.9	483.4	.9455	.7178	166	
	0.0407	5.797	14.2	483.4	1.634	1.336	570			1.893	184.7	585.8	.9320	.7116	167	
		5.795	14.2	583.8	1.621	1.332	571			1.900	184.5	620.1	.9244	.7062	168	
		3.397	188.5	233.1	1.222	0.9438	211	0.1029	0.0415	3.360	290.4	333.2	1.119	0.8688	293	
		3.406	187.5	283.2	1.242	.9696	212			3.371	278.9	383.9	1.144	.8972	294	
0.1000	0.0569	3.415	186.5	583.9	1.234	.9744	213			3.383	277.5	483.4	1.160	.9216	295	
		3.424	185.6	483.4	1.227	.9784	214			3.394	276.0	583.8	1.164	.9340	296	
		3.433	184.6	583.8	1.221	.9811	215			3.406	274.5	620.0	1.166	.9383	297	
		3.442	183.6	620.1	1.216	.9787	216		0.1032	0.0776	1.776	281.9	333.2	0.9775	0.7403	247
		2.707	-4.0	33.6	1.252	0.8958	390			1.788	278.9	383.9	.9868	.7559	248	
0.1008	0.0255	2.692	-2.5	86.6	1.273	.9442	391			1.801	276.0	483.4	.9093	.6919	249	
		2.678	-1.0	183.6	1.224	.9159	392			1.816	272.3	583.8	.9002	.6904	250	
		2.661	-4.4	583.9	1.193	.9081	393			1.829	269.4	620.0	.8909	.6858	251	
		2.646	1.9	483.4	1.174	.8953	394		0.1039	0.0145	10.48	90.5	133.2	1.661	1.319	1035
		2.631	3.3	583.8	1.156	.8793	395					183.6	1.827	1.482	1036	
0.1006	0.0564	5.704	89.5	153.2	1.553	1.220	522					283.2	1.913	1.581	1037	
				183.6	1.548	1.226	523					383.9	1.936	1.617	1038	
				283.2	1.559	1.253	524					483.4	1.941	1.635	1039	
				383.9	1.556	1.264	525					583.8	1.952	1.657	1040	
				483.4	1.550	1.269	526		0.1069	0.0580	2.495	184.4	233.1	1.068	0.8042	181
	0.0250	2.440	259.8	333.2	0.9797	0.7410	273			2.498	185.9	283.2	1.083	.8243	182	
		2.445	259.5	383.9	1.016	.7797	274			2.501	185.3	383.9	1.072	.8259	183	
		2.445	259.1	483.4	1.022	.7942	275			2.504	183.0	483.4	1.061	.8248	184	
		2.447	258.7	583.8	1.021	.8015	276			2.507	182.5	583.8	1.052	.8230	185	
		2.449	258.3	620.0	1.020	.8024	277			2.510	182.1	620.1	1.047	.8214	186	
0.1009	0.0250	5.586	188.1	233.1	1.534	1.229	229	0.1069	0.0141	11.54	-2.0	33.6	2.202	1.778	935	
		5.602	187.1	283.2	1.528	1.232	230					86.6	2.180	1.774	936	
		5.618	186.0	383.9	1.523	1.241	251					183.6	2.128	1.750	937	
		5.634	185.0	483.4	1.515	1.243	252					383.9	2.117	1.776	938	
		5.650	185.9	583.8	1.511	1.251	233					483.4	2.110	1.782	939	
	0.0255	5.666	182.8	620.1	1.507	1.250	234		0.1614	0.0613	3.948	6.0	33.6	1.543	1.179	324
				183.6	2.278	1.920	1067			3.954	6.9	86.6	1.437	1.095	325	
				383.9	2.310	1.968	1068			3.919	7.9	183.6	1.355	1.038	326	
				483.4	2.329	2.000	1069			3.904	8.9	583.9	1.285	.9957	327	
				583.8	2.357	2.020	1070			3.890	9.9	483.4	1.258	.9788	328	
0.1010	0.00917	15.92	90.0	153.2	1.996	1.825	1065	0.1614	0.0139	3.875	10.9	583.8	2.103	1.786	940	
				183.6	2.194	1.821	1066			3.948	14.0	2.919	2.441	1.923	923	
				283.2	2.278	1.920	1067			3.954	14.6	2.790	2.339	1.924	924	
				383.9	2.310	1.968	1068			3.919	15.2	183.6	2.880	2.264	925	
				483.4	2.329	2.000	1069			3.904	15.8	583.9	2.611	2.241	926	
	0.0749	1.960	79.5	132.0	1.127	0.8328	13		0.1956	0.0139	21.29	-2.0	33.6	2.153	1.733	917
				185.5	1.064	.7836	14			3.919	16.6	86.6	1.375	1.039	331	
				234.5	1.050	.7776	15			3.880	16.4	183.6	1.290	.9792	332	
				285.1	1.023	.7585	16			3.866	14.3	383.9	1.213	.9514	333	
				332.6	1.016	.7585	17			3.852	15.3	483.4	1.186	.9121	334	
0.1012	0.0411	3.368	269.4	333.2	1.076	0.8283	299	0.1957	0.0746	3.838	11.4	33.6	1.574	1.207	330	
		3.367	269.5	383.9	1.133	.8864	300			3.844	12.4	86.6	1.375	1.039	331	
		3.365	269.8	483.4	1.161	.9218	301			3.820	13.4	183.6	1.290	.9792	332	
		3.364	270.0	583.8	1.169	.9386	302			3.806	14.3	383.9	1.213	.9514	333	
		3.363	270.1	620.0	1.172	.9441	303			3.858	16.3	583.8	1.164	.9838	335	
0.1019	0.0255	5.780	87.0	153.2	1.592	1.256	139	0.1972	0.0735	3.619	259.0	333.2	1.087	0.8386	252	
				185.5	1.623	1.295	140			3.622	258.6	383.9	1.091	.8479	253	
				285.1	1.590	1.281	141			3.625	258.3	483.4	1.079	.8465	254	
				383.9	1.566	1.273	142			3.628	257.9	583.1	1.070	.8457	255	
				483.4	1.556	1.274	143			3.632	257.5	620.0	1.066	.8444	256	
0.1010	0.0766	1.928	85.0	153.2	1.112	0.8202	37	0.1986	0.00908	33.03	-5.5	33.6	3.458	2.942	947	
				185.6	1.057	.7782	38			0.00909	33.00	-3.2	86.6	3.334	2.846	948

TABLE I. - Continued. RESULTS OF STUDY OF HEAT TRANSFER FROM CYLINDERS IN SUBSONIC SLIP FLOW

M	Kn	Re _t	T _t	T _w	Nu ^u _t	Nu _t	Run	M	Kn	Re _t	T _t	T _w	Nu ^u _t	Nu _t	Run		
0.1987	0.0400	6.708	267.9	333.2	1.358	1.086	304	0.2050	0.0407	7.195	91.8	133.2	1.702	1.357	262		
		6.720	287.1	363.9	1.409	1.159	305			7.185	92.5	183.6	1.652	1.322	263		
		6.732	266.4	483.4	1.425	1.185	306			7.174	92.7	283.2	1.616	1.306	264		
		6.743	265.6	583.8	1.417	1.168	307			7.164	93.2	383.9	1.587	1.293	265		
		6.755	264.9	620.0	1.419	1.173	308			7.153	93.7	483.4	1.562	1.281	266		
0.1989	0.00918	31.09	90.0	133.2	2.496	2.088	1053	0.2068	0.0789	3.856	88.0	132.0	1.465	1.140	25		
				183.6	2.798	2.393	1054				185.0	1.321	1.018	28			
				283.2	2.904	2.506	1055				234.5	1.262	0.9719	27			
				383.9	2.935	2.554	1056				285.1	1.229	0.9485	28			
				483.4	2.942	2.580	1057				332.6	1.197	0.9248	29			
0.1996	0.0559	5.147	79.0	133.2	1.484	1.138	97	0.2068	0.0789			386.5	1.168	0.9036	30		
				183.8	1.359	1.052	98				437.3	1.147	0.8879	31			
				283.2	1.374	1.081	99				488.0	1.130	0.8761	32			
				383.9	1.355	1.057	100				538.5	1.124	0.8735	33			
				483.4	1.302	1.036	101				590.2	1.119	0.8724	34			
0.1997	0.0745	3.840	90.0	133.2	1.412	1.093	48	0.2072	0.0570	4.949	183.5	233.1	1.382	1.089	187		
				183.6	1.250	0.9540	50			4.960	182.7	285.2	1.273	0.9971	188		
				233.1	1.221	0.9351	51			4.970	182.0	383.9	1.313	1.047	189		
				283.2	1.201	0.9231	52			4.980	181.2	483.4	1.283	1.029	190		
				333.2	1.185	0.9145	53			4.990	180.5	583.8	1.263	1.020	191		
0.1998	0.0254	10.79	192.0	620.1	1.792	1.518	748	0.2072	0.0570	5.000	179.7	620.1	1.251	1.011	192		
				533.0	1.140	0.8826	55			5.795	179.0	233.1	1.128	0.8584	157		
				483.4	1.125	0.8700	56			5.801	178.7	285.2	1.182	0.8961	158		
				533.0	1.112	0.8634	57			5.809	178.4	383.9	1.135	0.8808	159		
				583.8	1.110	0.8639	58			5.817	178.1	483.4	1.113	0.8715	160		
0.1998	0.0255	10.74	194.4	383.9	1.635	1.530	745	0.2072	0.0570	5.825	177.8	583.8	1.091	0.8591	161		
		10.76	193.6	483.4	1.617	1.527	746			5.833	177.5	620.1	1.079	0.8498	162		
		10.77	192.8	583.8	1.798	1.520	747										
0.1999	0.0256	10.71	196.0	235.1	1.556	1.249	743	0.2072	0.0570								
		7.503	-2.0	33.6	1.776	1.388	657										
		7.499	-1.8	66.6	1.742	1.371	658										
0.1999	0.0402	7.484	-1.6	183.6	1.675	1.351	659	0.2072	0.0570	15.22	284.0	333.2	1.675	1.378	727		
		7.490	-1.4	383.9	1.628	1.318	660			15.22	284.2	383.9	1.618	1.328	728		
		7.488	-1.2	483.4	1.605	1.305	861			15.21	284.5	483.4	1.907	1.615	729		
0.2004	0.0143	20.08	90.5	133.2	2.120	1.740	1029	0.2072	0.0570	15.20	284.8	583.8	1.946	1.665	730		
				183.6	2.334	1.951	1030			15.20	285.0	620.0	1.962	1.682	731		
				233.2	2.412	2.045	1031			5.474	20.4	35.6	4.287	3.725	402		
				383.9	2.451	2.082	1032			5.557	16.4	88.6	1.918	1.534	403		
				483.4	2.433	2.098	1033			5.643	12.4	183.6	1.528	1.198	404		
0.2008	0.0251	10.64	287.0	483.4	1.744	1.463	724	0.2072	0.0570	5.731	6.5	383.9	1.364	1.071	405		
		10.65	286.5	583.8	1.753	1.482	725			5.821	4.3	483.4	1.314	1.030	406		
		10.65	286.0	620.0	1.757	1.489	726			5.914	0.2	583.8	1.282	1.003	407		
	0.0252	10.62	288.0	333.2	1.484	1.202	722										
		10.63	287.5	383.9	1.679	1.390	725										
0.2019	0.0257	11.24	90.0	133.2	1.908	1.546	528	0.2072	0.0570	10.11	184.5	233.1	1.533	1.228	611		
				183.6	1.940	1.587	529			10.11	184.6	283.2	1.649	1.343	612		
				233.2	1.931	1.597	530			10.10	184.7	383.9	1.633	1.344	613		
				383.9	1.918	1.601	531			10.10	184.9	583.8	1.589	1.354	615		
				483.4	1.892	1.589	532			10.10	185.0	620.1	1.586	1.325	616		
0.2025	0.0411	6.715	194.1	233.1	1.547	1.240	205	0.2072	0.0570	0.2959	0.00911	48.30	-2.0	583.8	3.584	3.195	983
		6.727	193.3	283.2	1.545	1.247	206			0.2959	48.26	-1.7	483.4	3.585	3.181	982	
		6.740	192.5	383.9	1.512	1.250	207			0.00912	48.22	-1.4	583.9	3.598	3.175	981	
		6.754	191.8	483.4	1.488	1.220	208			0.00913	48.18	-1.1	183.6	3.675	3.199	980	
		6.768	191.0	585.8	1.485	1.208	209			0.00914	48.14	-0.8	86.6	3.788	3.275	978	
0.2032	0.0567	4.803	271.6	333.2	1.217	0.9572	268	0.2072	0.0570	0.2964	0.0402	10.96	-3.0	35.6	1.982	1.577	839
		4.819	270.1	583.9	1.224	0.9701	269			0.2964	10.95	-2.9	66.6	1.913	1.529	840	
		4.836	268.6	483.4	1.213	0.9701	270			0.0403	10.95	-2.7	583.9	1.816	1.493	842	
		4.853	267.2	583.8	1.205	0.9710	271			0.0403	10.94	-2.6	483.4	1.771	1.462	843	
		4.870	265.7	620.0	1.206	0.9746	272			0.2972	0.00901	49.08	-4.0	33.6	4.055	3.481	955
0.2034	0.0582	5.237	7.8	33.6	1.665	1.290	384	0.2072	0.0570	0.00902	49.05	-3.8	86.6	3.807	3.290	954	
		5.222	8.6	86.6	1.540	1.189	385			0.00902	49.02	-3.8	183.6	3.703	3.225	955	
		5.209	9.2	183.6	1.454	1.129	386			0.00903	48.99	-3.4	383.9	3.651	3.206	956	
		5.193	10.0	583.9	1.384	1.091	387			0.00903	48.97	-3.2	483.4	3.605	3.200	957	
		5.179	10.7	483.4	1.350	1.067	388			0.00903	48.94	-3.0	583.8	3.611	3.221	958	
0.2048	0.0761	4.052	-0.7	33.6	1.458	1.100	408	0.2072	0.0570								
		4.037	.3	86.6	1.366	1.050	409										
		4.021	1.3	183.6	1.287	0.9748	410										
		4.006	2.3	383.9	1.218	0.9320	411										
		3.991	3.2	483.4	1.192	0.9127	412										
		3.976	4.2	583.8	1.161	0.8847											

TABLE I. - Continued. RESULTS OF STUDY OF HEAT TRANSFER FROM CYLINDERS IN SUBSONIC SLIP FLOW

M	Kn	Re _t	T _t	T _w	Nu _t ^h	Nu _t	Run	M	Kn	Re _t	T _t	T _w	Nu _t ^h	Nu _t	Run
0.2975	0.0752	5.172	282.7	333.2 383.9 483.4 583.8 620.0	1.234 1.214 1.178 1.159 1.155	0.9750 .9614 .9387 .9293 .9271	257 258 259 260 261	0.3088	0.0750	5.536 5.542 5.548 5.554 5.559 5.565	181.0 180.8 180.6 180.4 180.2 180.0	233.1 283.2 383.9 483.4 583.8 620.1	1.295 1.270 1.250 1.218 1.188 1.178	1.010 .9949 .9888 .9898 .9501 .9430	175 176 177 178 179 180
0.2979	0.0550	7.674	82.5	135.2 183.6 283.2 383.9 483.4 583.8	1.617 1.581 1.526 1.479 1.437 1.405	1.278 1.256 1.222 1.191 1.183 1.141	103 104 105 106 107 108	0.3183	0.0444	10.09	88.5	135.2 183.6 283.2 383.9 483.4	1.763 1.790 1.753 1.730 1.704	1.413 1.448 1.432 1.426 1.414	486 487 488 489 490
0.2980	0.0142	29.57	89.0	133.2 183.6 283.2 383.9 483.4 583.8	2.434 2.674 2.715 2.762 2.758 2.758	2.031 2.268 2.329 2.393 2.405 2.419	1023 1024 1025 1026 1027 1028	0.3948	0.00919	59.46	88.0	135.2 183.6 283.2 383.9 483.4 583.8	3.334 3.549 3.644 3.672 3.683 3.659	2.871 3.089 3.206 3.254 3.284 3.278	1071 1072 1073 1074 1075 1076
0.2983	0.0142	31.23 31.25 31.27 31.29 31.30 31.32	-5.0	33.6 86.6 183.6 383.9 483.4 583.8	3.172 3.151 2.605 2.598 2.582 2.582	2.675 2.576 2.605 2.598 2.582 2.582	929 930 931 932 933 934	0.3961	0.0242	23.94 23.95 23.96 23.97 23.98	-8.0 -8.1 -8.2 -8.3 -8.4	35.6 86.6 183.6 383.9 483.4 583.8	2.699 2.684 2.586 2.488 2.406	2.237 2.240 2.177 2.172 2.073	881 882 883 884 885 886
	0.0253	15.91 15.92	194.4 194.0	583.8 620.1	2.059 2.039	1.766 1.751	741 742	0.3977	0.0410	14.15 14.14 14.13	-6.0 -5.9 -5.8 -5.7	35.6 86.6 183.6 383.9	2.174 2.097 2.005 1.926	1.753 1.698 1.656 1.596	833 834 835 836
	0.0254	15.86 15.89 15.90	196.0 195.2 194.8	233.1 383.8 483.4	1.776 2.062 2.067	1.452 1.742 1.761	737 739 740	0.3982	0.0776	14.15 14.13	-6.0 -5.6 -5.5	35.6 483.4 583.8	2.174 1.498 1.369 1.352 1.295	1.753 1.672 1.633 1.552 1.032	833 834 835 836 837
0.2987	0.00922	45.74	89.0	133.2 183.6 283.2 383.9 483.4 583.8	2.911 3.236 3.314 3.359 3.359 3.356	2.475 2.794 2.893 2.938 2.938 2.988	1058 1060 1061 1062 1063 1064	0.4111	0.0411	14.15 14.13	-6.0 -5.6 -5.5	35.6 483.4 583.8	2.174 1.881 1.842	1.753 1.565 1.538	833 834 835
0.2990	0.0739	5.714	80.4	135.2 163.6 233.1 283.2 333.2 383.9 483.4 583.8	1.437 1.561 1.330 1.311 1.298 1.268 1.245 1.226 1.210 1.194	1.115 1.055 1.035 1.025 1.019 1.007 1.024 1.026 1.053 1.048	61 62 63 64 65 66 67 68 69 70	0.3986	0.00911 .00912 .00913 .00914 .00915	63.76 63.67 63.58 63.49 63.40	-4.0 -3.5 -3.0 -2.5 -2.0	483.4 583.9 183.6 86.6 33.6	3.919 3.915 4.017 4.166 4.459	3.500 3.477 3.523 3.528 3.881	994 995 992 991 990
	0.3987	0.0766	7.556	0.5	35.6	1.713	1.332	767	0.0767	7.554 7.550 7.547 7.545	0.6 -7 -8 -9 -1.0	86.6 183.6 383.9 483.4 583.8	1.583 1.491 1.389 1.351 1.320	1.237 1.163 1.094 1.066 1.041	768 769 770 771 772
0.2994	0.0399	9.843 9.851 9.859	284.0 283.5 283.0	483.4 583.8 620.0	1.557 1.565 1.558	1.288 1.507 1.504	699 700 701	0.3991	0.0141	41.31	-6.0	33.6 86.6 183.6 383.9 483.4 583.8	3.559 3.421 3.273 3.226 3.196 5.172	3.037 2.929 2.821 2.822 2.811 2.803	941 942 943 944 945 946
	0.0400	9.827 9.835	285.0 284.5	333.2 383.9	1.442 1.513	1.163 1.236	697 698	0.3992	0.0254	20.81	180.0	620.1	2.189	1.892	754
0.3005	0.0254	16.67	89.5	135.2 183.6 283.2 383.9 483.4 583.8	2.184 2.190 2.183 2.159 2.142 2.132	1.800 1.818 1.832 1.827 1.824 1.827	554 535 536 537 538 539	0.4000	0.0407	13.60	87.8	135.2 183.6 383.9 483.4 583.8	2.689 1.914 2.017 1.880 1.794	2.268 1.553 1.523 1.550 1.509	1041 942 943 944 945
0.3012	0.0253	17.63 17.64 17.65	0.4 .2 0	383.9 483.4 583.8	2.247 2.222 2.205	1.898 1.890 1.884	890 891 892	0.4003	0.0255	20.71 20.76	192.4 191.2	583.8	2.209	1.895	752
	0.0254	17.60 17.61 17.62	1.0 .8 .6	35.6 86.6 183.6	2.428 2.352 2.287	1.986 1.984 1.899	887 888 889	0.4003	0.0256	20.67	175.6	383.9	2.209	1.880	751
0.3019	0.0591	7.574 7.570	0	33.6 86.6	1.739 1.640	1.356 1.279	815 816	0.4003	0.0257	20.57	196.0	233.1	1.869	1.538	749
	0.0592	7.555 7.551 7.557 7.552	0.4 .6 .8 1.0	183.6 383.9 483.4 583.8	1.567 1.487 1.451 1.421	1.252 1.185 1.181 1.158	817 818 819 820	0.4003	0.0407	13.60	87.8	135.2 183.6 383.9 483.4 583.8	2.689 1.914 1.851 1.816 1.794	2.268 1.553 1.538 1.519 1.509	1041 942 943 944 945
0.3021	0.0564 .0565 .0566	7.057 7.019 7.002	282.0 283.5 285.0	333.2 383.9 483.4	1.141 1.271 1.305	0.8888 1.013 1.056	671 672 673	0.4003	0.0574	9.645	88.0	135.2 183.6 283.2 383.9 483.4 583.8	2.689 2.925 2.993 2.999 2.994 2.984	2.268 2.591 2.617 2.629 2.634 2.634	1041 1043 1044 1045 1046 1046
	0.0567	6.997 6.991	285.5 286.0	583.8 620.0	1.306 1.312	1.056 1.074	674 675	0.4004	0.0574	9.645	89.5	133.2 183.6 283.2 383.9 483.4 583.8	1.712 1.646 1.593 1.561 1.492 1.225	1.366 1.316 1.285 1.269 1.262 1.225	444 445 446 447 448 449
0.3040	0.0565	7.232 7.236 7.241 7.245 7.250 7.254	186.0 185.9 185.6 185.4 185.2 184.9	233.1 283.2 383.9 483.4 583.8 620.1	1.479 1.472 1.439 1.396 1.372 1.365	1.178 1.179 1.164 1.135 1.122 1.118	199 200 201 202 203 204								

TABLE I. - Continued. RESULTS OF STUDY OF HEAT TRANSFER FROM CYLINDERS IN SUBSONIC SLIP FLOW

M	Kn	Ret	T _t	T _w	Nut ^u	Nut _t	Run	M	Kn	Ret	T _t	T _w	Nut ^u	Nut _t	Run
0.4007	0.0565	9.116	281.5	333.1 383.9 483.4 583.8 620.0	1.241 1.349 1.398 1.398 1.386	0.9801 1.085 1.143 1.151 1.144	666 667 668 669 670	0.4931	0.00910	77.03	-5.0	33.6 133.2 183.6 283.2 383.9 483.4 583.8	4.587 2.898 5.044 5.145 5.158 5.149 3.136	4.002 2.277 2.615 2.735 2.768 2.777 2.780	996 1047 1048 1049 1050 1051 1052
0.4008	0.0408	12.99	192.2 192.0	583.8 620.1	1.720 1.712	1.447 1.444	621 622	0.4951	0.0143	46.77	87.0	133.2 183.6 283.2 383.9 483.4 583.8	2.898 5.044 5.145 5.158 5.149 3.136	2.277 2.615 2.735 2.768 2.777 2.780	1047 1048 1049 1050 1051 1052
0.4009	0.0409	12.97	193.0 192.8	233.1 283.2	1.647 1.705	1.333 1.395	617 618	0.4965	0.0143	49.35	-3.0	33.6 86.6 183.6 383.9 483.4 583.8	3.605 3.520 3.469 3.384 3.357 3.315	3.081 3.023 3.007 2.973 2.966 2.940	859 860 861 862 863 864
		12.98	192.6 192.4	383.9 483.4	1.739 1.732	1.442 1.444	619 620					86.6 183.6 383.9 483.4 583.8	2.788 2.702 2.578 2.525 2.484	2.339 2.286 2.211 2.175 2.148	894 895 896 897 898
0.4010	0.0256	21.64	89.0	133.2 183.6 283.2 383.9 483.4 583.8	2.355 2.384 2.359 2.339 2.309 2.269	1.953 1.998 1.996 1.996 1.982 1.976	540 541 542 543 544 545	0.4968	0.0249	28.31	-6.0	33.6 86.6 183.6 383.9 483.4 583.8	2.871 2.788 2.702 2.578 2.525 2.484	2.397 2.339 2.286 2.211 2.175 2.148	893 894 895 896 897 898
0.4013	0.0402	12.84	282.0	333.2 583.9 483.4 583.8	1.350 1.568 1.652 1.678	1.080 1.287 1.377 1.412	702 703 704 705 706	0.4974	0.0398	17.80	-8.0	33.6 17.79 17.78 17.77 17.76 17.75	2.270 86.6 183.6 383.9 483.4 583.8	1.842 2.217 2.146 2.050 2.011 1.986	845 846 847 848 849 850
0.4024	0.0749	6.911	283.0	333.2	1.027	0.7852	646	0.4981	0.0255	26.34	-6.0	33.6 17.79 17.78 17.77 17.76 17.75	2.577 2.467 2.464 2.445 2.418 2.387	1.980 2.077 2.095 2.086 2.086 2.068	546 547 548 549 550 551
		6.908	283.2	383.9	1.141	.8950	647					183.6 283.2 383.9 483.4 583.8	2.457 2.454 2.445 2.418 2.387	2.077 2.095 2.086 2.086 2.068	546 547 548 549 550
0.4028	0.0750	6.899	284.0	620.0	1.185	0.9571	650	0.4986	0.0403	16.70	-6.0	133.2 185.6 283.2 383.9 483.4 583.8	1.936 1.971 1.967 1.885 1.907 1.877	1.572 1.616 1.632 1.571 1.604 1.587	498 499 500 501 502 503
		7.503	91.3	133.2 183.6 233.1 283.2 333.2 383.9	1.494 1.458 1.437 1.405 1.377 1.258	1.167 1.144 1.134 1.111 1.092 .9878	73 74 75 76 77 78					185.6 283.2 383.9 483.4 583.8	1.572 1.616 1.632 1.571 1.604 1.587	498 499 500 501 502 503	
0.4032	0.0250	20.74	282.0	333.2	1.958	1.641	732	0.4992	0.0388	18.49	-24.0	33.6 18.46 18.44 18.42	2.295 86.6 183.6 283.2 383.9	1.863 1.860 1.862 1.868	869 870 871 872
		20.89	283.5	383.9	2.064	1.747	733					185.6 283.2 383.9 483.4 583.8	2.274 2.132 2.132 2.027	1.860 1.862 1.868	869 870 871 872
0.4032	0.0251	20.68	283.7	483.4	2.071	1.768	734	0.4998	0.0573	11.26	-6.0	133.2 180.0	1.936 1.936	1.572 1.616	498 499
		20.88	283.8	583.8	2.113	1.820	735					185.6 283.2 383.9 483.4 583.8	1.967 1.967 1.967 1.967 1.967	1.632 1.632 1.632 1.632 1.632	500 501 502 503 504
0.4056	0.0141	20.57	284.0	620.0	2.120	1.831	736	0.5005	0.0254	25.45	-6.0	233.1 283.2 383.9 483.4 583.8	1.285 1.476 1.499 1.482 1.476	1.001 1.185 1.220 1.225 1.223	541 542 543 544 546
		38.02	184.5	233.1	2.215	1.857	1113					283.2 383.9 483.4 583.8	1.285 1.476 1.499 1.482	1.001 1.185 1.220 1.223	541 542 543 544 546
0.4056	0.0142	37.99	184.9	283.2	2.583	2.211	1114	0.5006	0.0255	25.37	-6.0	233.1 189.6 25.33 25.29 25.26	1.285 86.6 183.6 181.2 192.0	1.001 1.185 1.220 1.225 1.223	541 542 543 544 546
		37.98	185.3	383.9	2.848	2.490	1115					283.2 383.9 483.4 583.8	1.285 1.476 1.499 1.482	1.001 1.185 1.220 1.223	541 542 543 544 546
0.4072	0.0585	37.93	185.7	483.4	2.862	2.510	1116	0.5010	0.0401	15.62	-6.0	233.1 189.6 25.33 25.29 25.26	1.285 86.6 183.6 181.2 192.0	1.001 1.185 1.220 1.225 1.223	541 542 543 544 546
		37.90	186.1	583.8	2.855	2.518	1117					283.2 383.9 483.4 583.8	1.285 1.476 1.499 1.482	1.001 1.185 1.220 1.223	541 542 543 544 546
0.4072	0.0586	37.87	186.5	620.1	2.860	2.527	1118	0.5010	0.0565	11.11	-6.0	233.1 180.0	1.285 1.285	1.001 1.001	541 542
		10.10	-2.0	33.6	1.843	1.451	809					283.2 383.9 483.4 583.8	1.285 1.476 1.499 1.482	1.001 1.185 1.220 1.223	541 542
0.4074	0.0577	10.10	-1.8	88.6	1.777	1.405	810	0.5016	0.0761	9.316	-6.0	233.1 189.6 25.33 25.29 25.26	1.285 86.6 183.6 181.2 192.0	1.001 1.185 1.220 1.225 1.223	541 542 543 544 546
		10.09	-1.6	183.6	1.699	1.354	811					283.2 383.9 483.4 583.8	1.285 1.476 1.499 1.482	1.001 1.185 1.220 1.223	541 542 543 544 546
0.4074	0.0577	10.08	-1.4	383.9	1.602	1.293	812	0.5016	0.0761	9.316	-6.0	233.1 189.6 25.33 25.29 25.26	1.285 86.6 183.6 181.2 192.0	1.001 1.185 1.220 1.225 1.223	541 542 543 544 546
		10.07	-1.2	483.4	1.558	1.262	813					283.2 383.9 483.4 583.8	1.285 1.476 1.499 1.482	1.001 1.185 1.220 1.223	541 542 543 544 546
0.4415	0.0570	10.13	194.5	233.1	1.158	0.8870	552	0.5048	0.0411	15.80	-6.0	233.1 189.6 25.33 25.29 25.26	1.285 86.6 183.6 181.2 192.0	1.001 1.185 1.220 1.225 1.223	541 542 543 544 546
		10.17	192.4	283.2	1.290	1.014	553					283.2 383.9 483.4 583.8	1.285 86.6 183.6 181.2 192.0	1.001 1.185 1.220 1.225 1.223	541 542 543 544 546
0.4415	0.0570	10.21	190.3	383.9	1.301	1.057	554	0.5048	0.0412	15.75	-6.0	233.1 189.6 25.33 25.29 25.26	1.285 86.6 183.6 181.2 192.0	1.001 1.185 1.220 1.225 1.223	541 542 543 544 546
		10.25	188.2	483.4	1.275	1.023	555					283.2 383.9 483.4 583.8	1.285 86.6 183.6 181.2 192.0	1.001 1.185 1.220 1.225 1.223	541 542 543 544 546
0.4415	0.0570	10.30	186.1	583.8	1.260	1.018	556	0.5048	0.0412	15.70	-6.0	233.1 189.6 25.33 25.29 25.26	1.285 86.6 183.6 181.2 192.0	1.001 1.185 1.220 1.225 1.223	541 542 543 544 546
		10.34	184.0	620.1	1.248	1.009	557					283.2 383.9 483.4 583.8	1.285 86.6 183.6 181.2 192.0	1.001 1.185 1.220 1.225 1.223	541 542 543 544 546
0.4717	0.0647	9.212	280.0	620.0	1.228	0.9970	645	0.5048	0.0413	15.74	-6.0	233.1 189.6 25.33 25.29 25.26	1.285 86.6 183.6 181.2 192.0	1.001 1.185 1.220 1.225 1.223	541 542 543 544 546
		9.200	280.8	583.8	1.241	1.006	644					283.2 383.9 483.4 583.8	1.285 86.6 183.6 181.2 192.0	1.001 1.185 1.220 1.225 1.223	541 542 543 544 546
0.4717	0.0648	9.190	281.5	483.4	1.249	1.004	643	0.5048	0.0412	15.75	-6.0	233.1 189.6 25.33 25.29 25.26	1.285 86.6 183.6 181.2 192.0	1.001 1.185 1.220 1.225 1.223	541 542 543 544 546
		9.179	282.2	383.9	1.250	0.9761	642					283.2 383.9 483.4 583.8	1.285 86.6 183.6 181.2 192.0	1.001 1.185 1.220 1.225 1.223	541 542 543 544 546
0.4717	0.0649	9.179	282.2	383.9	1.250	0.9761	642	0.5048	0.0413	15.74	-6.0	233.1 18			

TABLE I. - Continued. RESULTS OF STUDY OF HEAT TRANSFER FROM CYLINDERS IN SUBSONIC SLIP FLOW

M	Kn	Re _t	T _t	T _w	Nu [*] _t	Nu _t	Run	M	Kn	Re _t	T _t	T _w	Nu [*] _t	Nu _t	Run
0.5051	0.0578	11.73	89.5	133.2	1.767	1.418	450	0.5977	0.0143	57.24	-3.8	86.6	3.677	3.171	966
				183.6	1.751	1.395	451			57.29	-4.1	183.6	3.605	3.156	967
				283.2	1.860	1.347	452			57.34	-4.4	583.9	3.518	3.102	968
				383.9	1.608	1.314	453			57.39	-4.7	483.4	3.475	3.078	970
				483.4	1.566	1.286	454			57.44	-5.0	583.8	3.429	3.051	971
	0.0570	12.55	-4.0	33.6	2.068	1.657	803		0.0144	57.19	-3.5	33.6	3.758	3.226	965
				86.6	1.917	1.554	804			57.29	-4.1	183.6	3.605	3.156	967
				183.6	1.764	1.414	805			57.34	-4.4	583.9	3.518	3.102	968
				383.9	1.676	1.363	806			57.39	-4.7	483.4	3.475	3.078	970
				483.4	1.622	1.322	807			57.44	-5.0	583.8	3.429	3.051	971
0.5061	0.0141	46.30	182.0	233.1	2.392	2.023	1119	0.5996	0.0144	54.48	84.0	133.2	2.880	2.448	1083
				46.25	182.6	2.316	2.356			54.53	84.0	183.6	3.148	2.714	1084
				46.20	183.2	2.385	2.970			54.58	84.0	283.2	3.278	2.861	1085
				46.14	185.8	483.4	3.012			54.63	84.0	383.9	3.320	2.922	1086
	0.0142	46.14	185.8	483.4	3.012	2.653	1122			54.68	84.0	483.4	3.302	2.923	1087
				46.09	184.4	583.8	3.024			54.73	84.0	583.8	3.297	2.834	1088
				46.04	185.0	620.1	3.013			54.78	84.0	620.1	3.292	2.834	1089
				46.00	186.0	620.1	3.013			54.83	84.0	620.1	3.292	2.834	1090
0.5087	0.0556	11.79	184.0	620.1	1.265	1.025	563	0.6001	0.0569	14.51	-6.0	33.6	2.100	1.687	797
				0.5557	11.77	185.2	583.8			14.56	-6.0	86.6	1.981	1.593	798
				0.5558	11.74	186.4	483.4			14.61	-6.0	183.6	1.871	1.514	799
				0.5559	11.71	187.6	383.9			14.66	-6.0	383.9	1.754	1.457	800
				0.5560	11.69	188.8	283.2			14.71	-6.0	483.4	1.697	1.393	801
	0.0561	11.66	190.0	233.1	1.237	0.9583	558			14.76	-6.0	583.8	1.657	1.363	802
				233.2	1.237	0.9583	558			14.81	-6.0	620.1	1.657	1.363	803
				233.3	1.237	0.9583	558			14.86	-6.0	620.2	1.657	1.363	804
				233.4	1.237	0.9583	558			14.91	-6.0	620.3	1.657	1.363	805
				233.5	1.237	0.9583	558			14.96	-6.0	620.4	1.657	1.363	806
0.5195	0.00924	75.32	86.0	133.2	3.480	3.009	1077	0.6005	0.0775	10.10	89.5	133.2	1.611	1.275	438
				183.6	3.692	3.225	1078			10.15	89.5	183.6	1.517	1.199	439
				283.2	3.892	3.442	1079			10.20	89.5	283.2	1.441	1.146	440
				383.9	3.914	3.486	1080			10.25	89.5	383.9	1.394	1.115	441
	0.0775	9.012	89.0	483.4	3.919	3.510	1081			10.30	89.5	483.4	1.345	1.079	442
				583.8	3.919	3.510	1081			10.35	89.5	583.8	1.305	1.050	443
				620.1	3.919	3.510	1081			10.40	89.5	620.1	1.305	1.050	444
				620.2	3.919	3.510	1081			10.45	89.5	620.2	1.305	1.050	445
0.5214	0.0775	9.012	89.0	133.2	1.626	1.289	432	0.6011	0.0406	18.49	189.0	233.1	1.711	1.393	630
				183.6	1.510	1.192	433			18.54	189.0	283.2	1.902	1.578	631
				283.2	1.431	1.136	434			18.59	189.0	383.9	1.880	1.574	632
				383.9	1.398	1.118	435			18.64	189.0	483.4	1.851	1.560	633
	0.0408	13.96	-4.5	483.4	1.354	1.087	436			18.69	189.0	583.8	1.818	1.541	634A
				583.8	1.307	1.051	437			18.74	189.0	620.1	1.801	1.528	634B
				620.1	1.307	1.051	437			18.79	189.0	620.2	1.801	1.528	635
				620.2	1.307	1.051	437			18.84	189.0	620.3	1.801	1.528	636
0.5651	0.0563	13.96	-4.5	33.6	2.136	1.720	791	0.6017	0.0742	11.15	-5.0	33.6	1.819	1.431	761
				86.6	1.993	1.604	792			11.20	-4.8	86.6	1.703	1.338	762
				183.6	1.872	1.515	793			11.25	-4.6	183.6	1.612	1.275	763
				383.9	1.755	1.437	794			11.30	-4.4	383.9	1.489	1.188	764
				483.4	1.715	1.410	795			11.35	-4.2	483.4	1.444	1.154	765
	0.0744	17.91	282.0	133.2	1.237	0.9583	796			11.40	-4.0	583.8	1.406	1.124	766
				183.6	1.237	0.9583	796			11.45	-3.9	620.1	1.406	1.124	767
				283.2	1.237	0.9583	796			11.50	-3.8	383.9	1.341	1.073	681
				383.9	1.237	0.9583	796			11.55	-3.7	483.4	1.450	1.179	682
				483.4	1.237	0.9583	796			11.60	-3.6	583.8	1.469	1.209	683
0.5906	0.0398	18.09	276.0	333.2	1.555	1.269	712	0.6030	0.0565	12.94	280.0	333.2	1.341	1.073	681
				383.9	1.697	1.407	713			12.99	280.0	383.9	1.450	1.179	682
				483.4	1.765	1.483	714			13.04	280.0	483.4	1.469	1.209	683
				583.8	1.768	1.488	715			13.09	280.0	583.8	1.465	1.215	684
	0.0400	17.99	279.0	483.4	1.765	1.483	716			13.14	280.0	620.0	1.465	1.218	685
				583.8	1.768	1.488	716			13.19	280.0	620.1	1.465	1.218	686
				620.1	1.768	1.488	716			13.24	280.0	620.2	1.465	1.218	687
				620.2	1.768	1.488	716			13.29	280.0	620.3	1.465	1.218	688
0.5915	0.0250	29.73	180.0	233.1	1.935	1.599	1095	0.6049	0.0400	20.79	-10.0	383.9	2.095	1.756	854
				29.68	1.935	1.599	1096			20.84	-9.9	483.4	2.048	1.724	855
				29.66	1.935	1.599	1096			20.89	-9.8	583.8	2.006	1.694	856
				29.64	1.935	1.599	1096			20.94	-9.7	620.0	1.996	1.668	857
				29.62	1.935	1.599	1096			21.00	-9.6	620.1	1.996	1.668	858
	0.0247	33.07	-8.8	483.4	2.596	2.242	903			21.05	-9.5	133.2	1.983	1.616	504

TABLE I. - Concluded. RESULTS OF STUDY OF HEAT TRANSFER FROM CYLINDERS IN SUBSONIC SLIP FLOW

M	Kn	Re _t	T _t	T _w	Nu ⁿ _t	Nu _t	Run	M	Kn	Re _t	T _t	T _w	Nu ⁿ _t	Nu _t	Run
0.6832	0.0557	15.05	186.0	233.1	1.502	1.202	593	0.7635	0.0559	15.59	275.2	583.8	1.465	1.216	695
				283.2	1.542	1.247	594			275.0	620.0	1.491	1.243	696	
				383.9	1.524	1.245	595		0.0560	15.57	276.0	333.2	1.430	1.155	692
				483.4	1.515	1.245	596			275.8	383.9	1.467	1.196	693	
				583.8	1.493	1.236	597			275.5	483.4	1.474	1.214	694	
	0.7008	20.73	184.0	620.1	1.823	1.550	640		0.0759	11.57	276.0	333.2	1.173	0.9194	681
				583.8	1.841	1.562	639			275.9	583.9	1.238	0.9850	682	
				483.4	1.874	1.582	638			275.6	483.4	1.241	0.9982	683	
		20.55	188.5	383.9	1.876	1.571	637			11.58	275.6	583.8	1.233	1.000	684
				233.1	1.735	1.415	635			275.5	620.0	1.224	0.9948	685	
	0.0412	20.49	190.0	283.2	1.808	1.492	636	0.7799	0.0570	15.99	183.0	233.1	1.430	1.136	605
	15.42	81.3	153.2	1.671	1.330	474	183.2			283.2	1.493	1.202	606		
			183.6	1.705	1.372	475	183.4			383.9	1.525	1.246	607		
			283.2	1.685	1.371	476	183.6			483.4	1.511	1.244	608		
			383.9	1.647	1.351	477	15.96			184.0	620.1	1.488	1.235	610	
			483.4	1.607	1.325	478	183.8			583.8	1.506	1.248	609		
	0.7012	0.0573	15.42	583.8	1.572	1.300	479		0.0570	15.99	183.0	233.1	1.430	1.136	605
				183.6	1.572	1.330	474			183.2	283.2	1.493	1.202	606	
				183.6	1.572	1.330	475			183.4	383.9	1.525	1.246	607	
				183.6	1.572	1.330	476			183.6	483.4	1.511	1.244	608	
				183.6	1.572	1.330	477			15.96	184.0	620.1	1.488	1.235	610
0.7019	0.0761	12.19	-3.7	183.6	1.568	1.235	781	0.7827	0.0772	11.85	185.0	233.1	1.254	0.9575	575
			-3.8	383.9	1.454	1.158	782			185.4	283.2	1.131	.8710	576	
			-3.9	483.4	1.407	1.120	783			185.8	383.9	1.293	1.031	577	
	0.0762	12.20	-4.0	583.8	1.368	1.088	784		0.0773	11.80	186.2	483.4	1.254	1.005	578
			-3.5	33.6	1.748	1.365	779			186.6	583.8	1.233	0.9944	579	
		12.18	-3.6	88.6	1.670	1.309	780		0.0774	11.78	187.0	620.1	1.222	0.9872	580
0.7035	0.0400	20.55	274.0	353.2	1.616	1.326	717		0.0386	26.32	-27.2	86.6	2.368	1.949	876
			20.50	275.5	383.9	1.748	1.455	718		26.34	-27.4	183.6	2.285	1.897	877
	0.0402	20.44	277.0	483.4	1.787	1.504	719	26.36		-27.6	383.9	2.154	1.809	878	
			20.39	278.3	583.8	1.793	1.522	720		26.37	-27.8	483.4	2.073	1.745	879
			20.34	280.0	620.0	1.792	1.524	721		26.39	-28.0	583.8	2.014	1.699	880
0.7060	0.0402	23.26	-11.0	33.6	2.350	1.898	863	0.7844	0.0408	22.47	176.5	233.1	1.599	1.290	1089
		23.28	-11.2	86.6	2.322	1.908	864			176.6	283.2	1.850	1.512	1080	
		23.29	-11.4	183.6	2.222	1.840	865			176.7	383.9	1.871	1.566	1081	
		23.30	-11.6	383.9	2.117	1.777	866		0.0408	22.45	176.8	483.4	1.860	1.570	1092
		23.32	-11.8	483.4	2.060	1.735	867			176.9	583.8	1.844	1.565	1093	
0.7077	0.0563	14.67	276.0	353.2	1.291	1.027	687	0.7857	0.0254	36.12	176.0	233.1	2.018	1.678	1107
		14.68	275.8	383.9	1.396	1.130	688			176.2	283.2	2.290	1.940	1108	
		14.69	275.5	483.4	1.466	1.207	689			176.4	383.9	2.394	2.055	1109	
		14.70	275.0	620.0	1.479	1.232	691		0.0255	36.06	176.8	583.8	2.400	2.089	1111
		10.99	276.5	353.2	1.153	0.9013	656			176.0	233.2	2.386	2.081	1112	
0.7091	0.0753	11.00	276.4	383.9	1.252	0.9792	657	0.7865	0.0249	40.63	-12.5	33.6	2.896	2.423	911
			276.2	483.4	1.248	1.004	658			176.6	283.2	2.290	1.940	912	
			276.1	583.8	1.238	1.004	659			176.8	383.9	2.394	2.055	913	
	0.0753	11.00	276.0	620.0	1.228	0.9981	660		0.0255	36.06	176.8	583.8	2.400	2.089	1111
			276.2	620.1	1.228	0.9981	660			177.0	233.2	2.386	2.081	1112	
0.7127	0.0237	37.88	80.3	153.2	2.293	1.908	1017	0.7870	0.0570	17.70	-11.0	33.6	1.988	1.585	827
		11.35	183.6	2.582	2.185	2.018	1018			-11.1	86.6	1.945	1.561	828	
			283.2	3.611	2.234	1.019	1019			17.71	-11.2	183.6	1.859	1.504	829
			583.9	2.808	2.250	1.020	1020		0.0570	17.72	-11.3	383.9	1.729	1.413	830
			483.4	2.899	2.542	1.021	1021			-11.4	483.4	1.669	1.587	831	
0.7158	0.0408	21.99	82.0	135.2	1.967	1.621	510	0.7888	0.0733	13.09	78.5	153.2	1.454	1.133	462
		11.35	183.6	2.145	1.778	511	183.6			1.498	1.182	463			
			283.2	2.036	1.698	512	285.2			1.466	1.168	464			
			583.9	1.997	1.677	513	0.0557	17.23	80.0	133.2	1.426	1.144	465		
			483.4	1.957	1.652	514			183.6	1.426	1.144	466			
0.7240	0.0582	16.22	-8.5	583.8	1.599	1.308	826	0.7899	0.0557	16.23	80.0	133.2	1.672	1.531	480
		16.20	-8.1	483.4	1.646	1.345	825			183.6	1.740	1.405	481		
	0.0583	16.19	-7.7	383.9	1.702	1.388	824		0.0557	17.23	80.0	133.2	1.740	1.405	482
		16.17	-7.5	183.6	1.818	1.465	823			183.6	2.080	1.739	518		
		16.15	-6.9	86.6	1.907	1.526	822			383.9	2.023	1.701	519		
0.7240	0.0762	11.35	-6.5	53.6	1.999	1.595	821	0.7928	0.0401	24.00	81.0	133.2	2.033	1.669	516
		11.35	-6.5	184.6	1.246	1.006	568			183.6	2.111	1.748	517		
	0.0763	11.35	185.0	620.1	1.242	1.005	569		0.0401	24.00	81.0	133.2	2.033	1.669	516
		583.8	1.372	1.112	461	183.6	2.111			1.748	517				
		483.4	1.366	1.098	460	283.2	2.080			1.739	518				
0.7373	0.0754	12.17	77.0	133.2	1.470	1.147	456	0.7944	0.0734	13.78	-6.0	33.6</			

TABLE II. - ORGANIZATION OF RESULTS FOR NOMINAL VALUES OF PARAMETERS

Nominal Knudsen number, Kn	Nominal Mach number, M								
	0.05	0.10	0.20	0.30	0.40	0.50	0.60	0.70	0.80
Run numbers ^a for $T_t = 0^{\circ}$ F									
0.0770	342 420	336 414	330 408	402	767	773	761	779	785
0.0555	396	390	324 384	815	809	791 803	797	821	827
0.0416	378	372	857	839	833	845 869	851	863	875
0.0256	354 360	366	917	887	881	893	899 905	---	911
0.0143	348	935	923	929	941	959	965	---	972
0.00916	---	984	947	953	990	995	---	---	---
Run numbers ^a for $T_t = 80^{\circ}$ F									
0.0770	1 37	13 49	25	61	73 426	432	438	456	462
0.0555	85	91	97	103	444	450	468	474	480
0.0416	109 127	115 262	121	486	492	498	504	510	516
0.0256	133 522	139 522	528	534	540	546	1005 1011 1017	---	---
0.0143	145	1035	1029	1023	1041	1047	1083	----	----
0.00916	151	1065	1053	1059	1071	1077	----	----	----
Run numbers ^a for $T_t = 180^{\circ}$ F									
0.0770	169	163	157	175	---	---	---	567	575
0.0555	193	181	187	199	552 599	558 581	587	593	605
0.0416	217	211	205	611	617	623	630	635	1089
0.0256	223	229	743	737	749	755	1095	1101	1107
0.0143	235	---	---	---	1113	1119	----	----	----
Run numbers ^a for $T_t = 280^{\circ}$ F									
0.0770	278	247	252	257	646	---	651	656	661
0.0555	283	273	268	671	666	641 676	681	687	692
0.0416	288	293 299	304	697	702	707	712	717	---
0.0256	309	314	722	727	732	----	----	----	----
0.0143	319	---	---	---	---	---	---	---	---

^aEach run number is the first of a group of runs in table I at the indicated nominal values of M, Kn, and T_t .

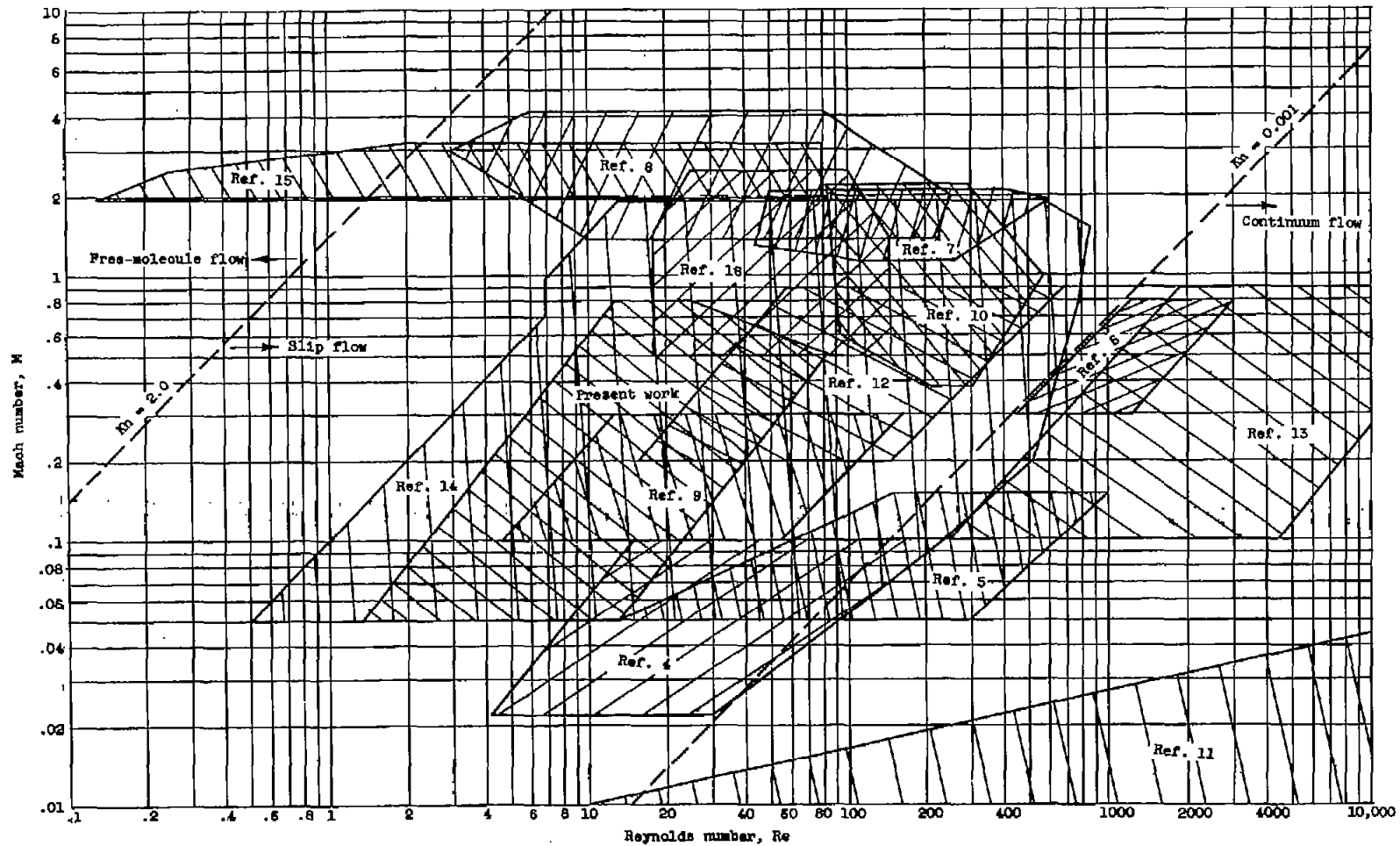
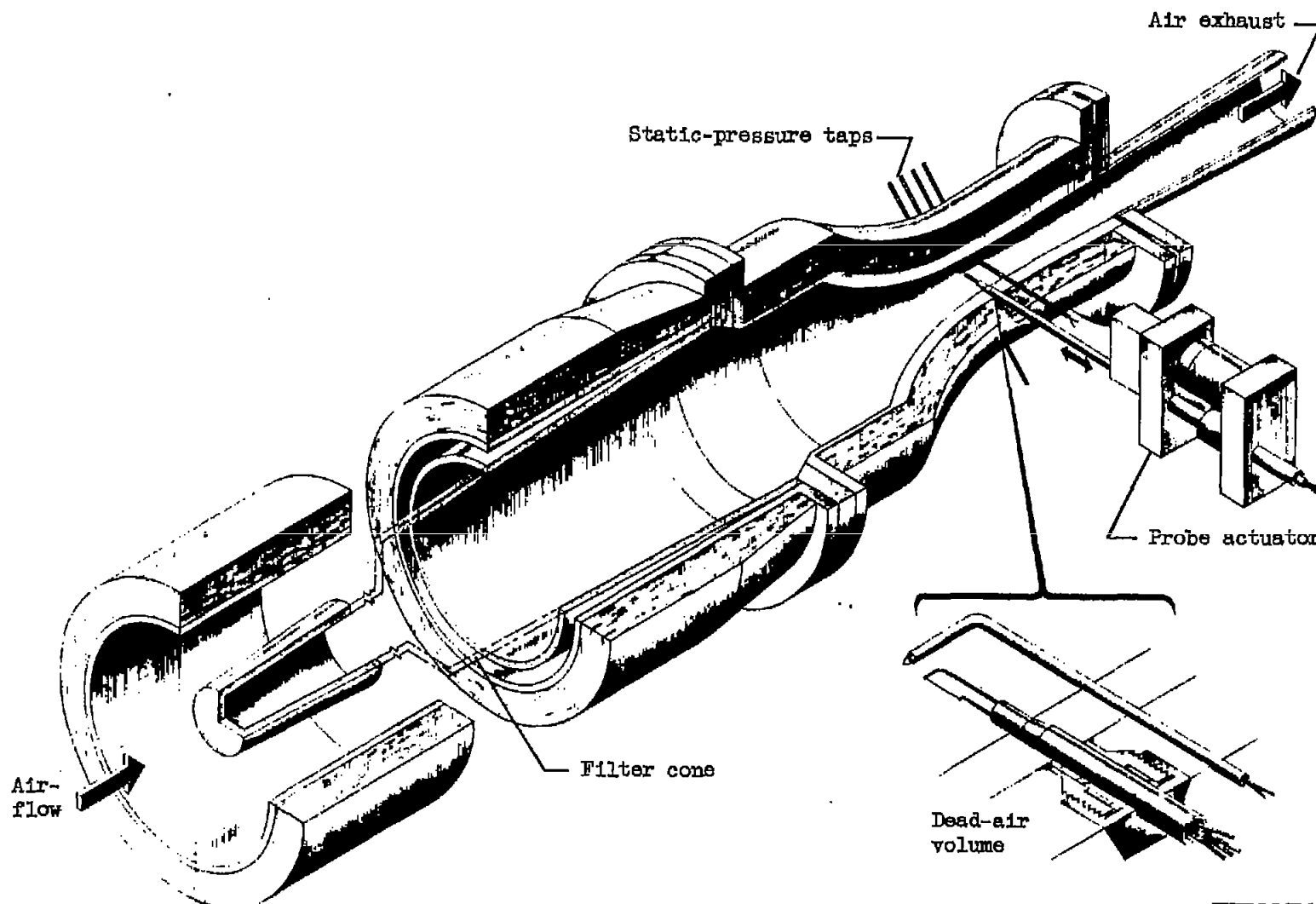


Figure 1. - Comparison of Mach and Reynolds number ranges of heat-transfer experiments with normal cylinders. Flow regions after reference 15.



/CD-6238

Figure 2. - Variable-density subsonic tunnel.

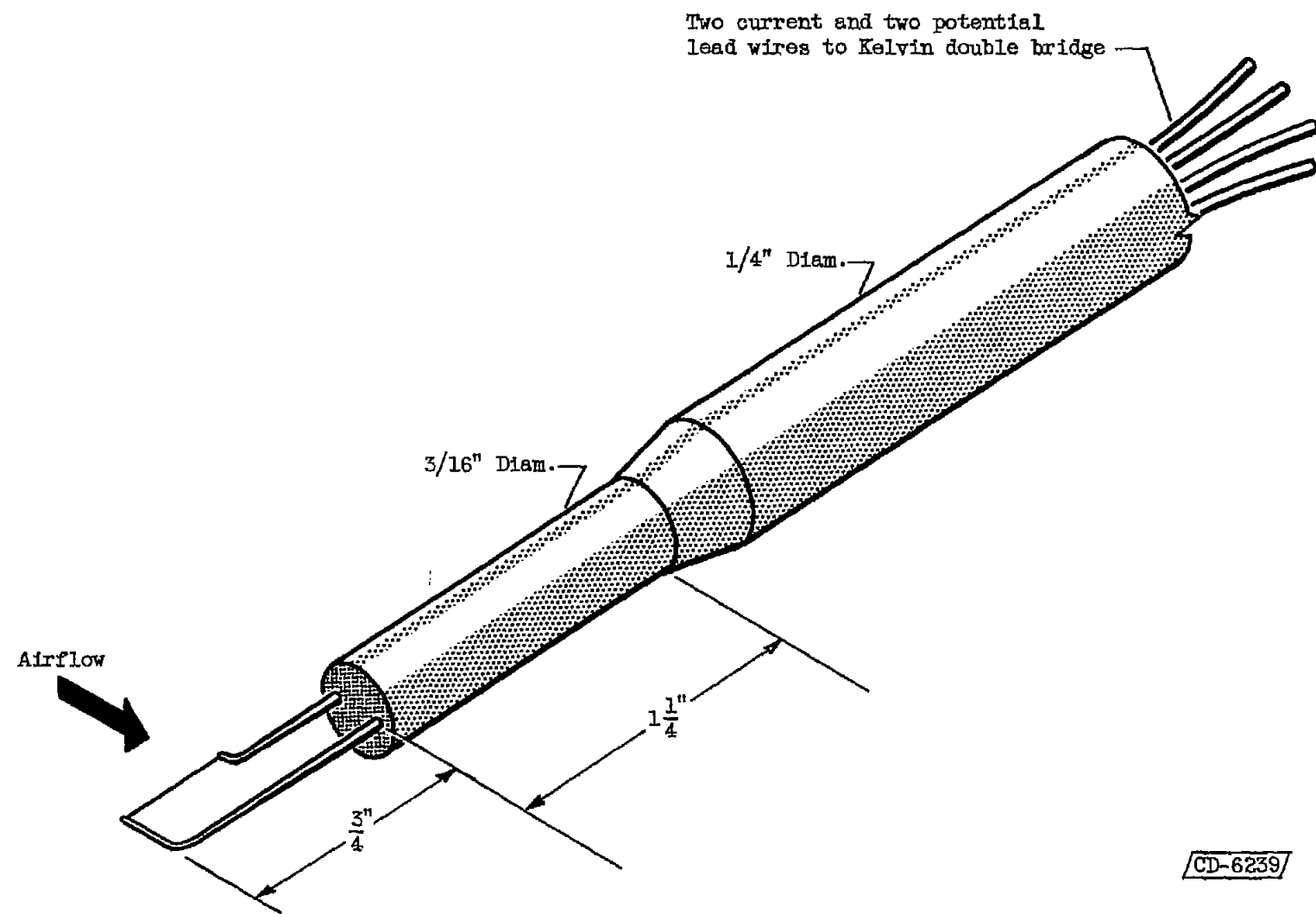
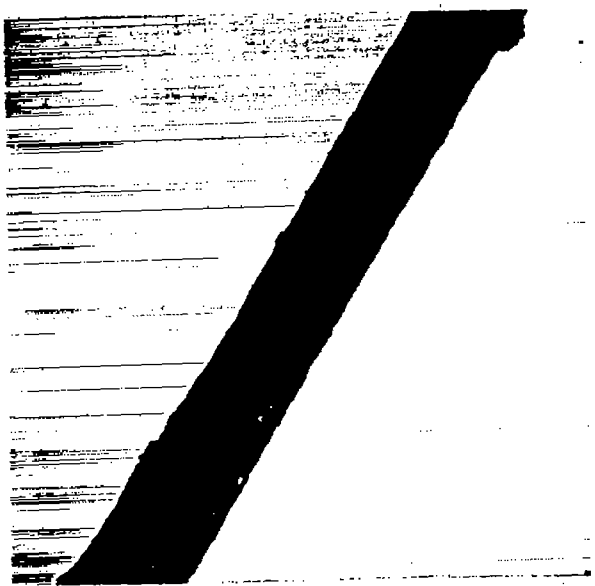


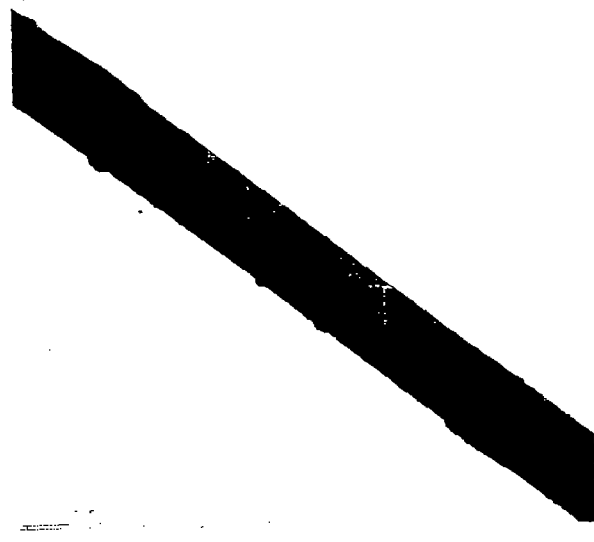
Figure 3. - Tungsten-wire supporting probe.

5111

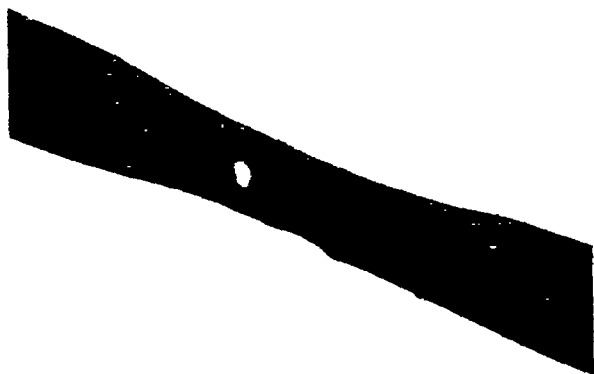
CS-7 back



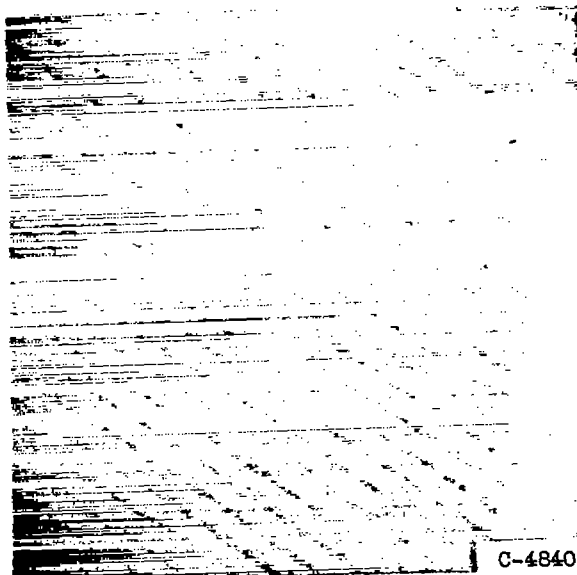
Sample A



Sample B



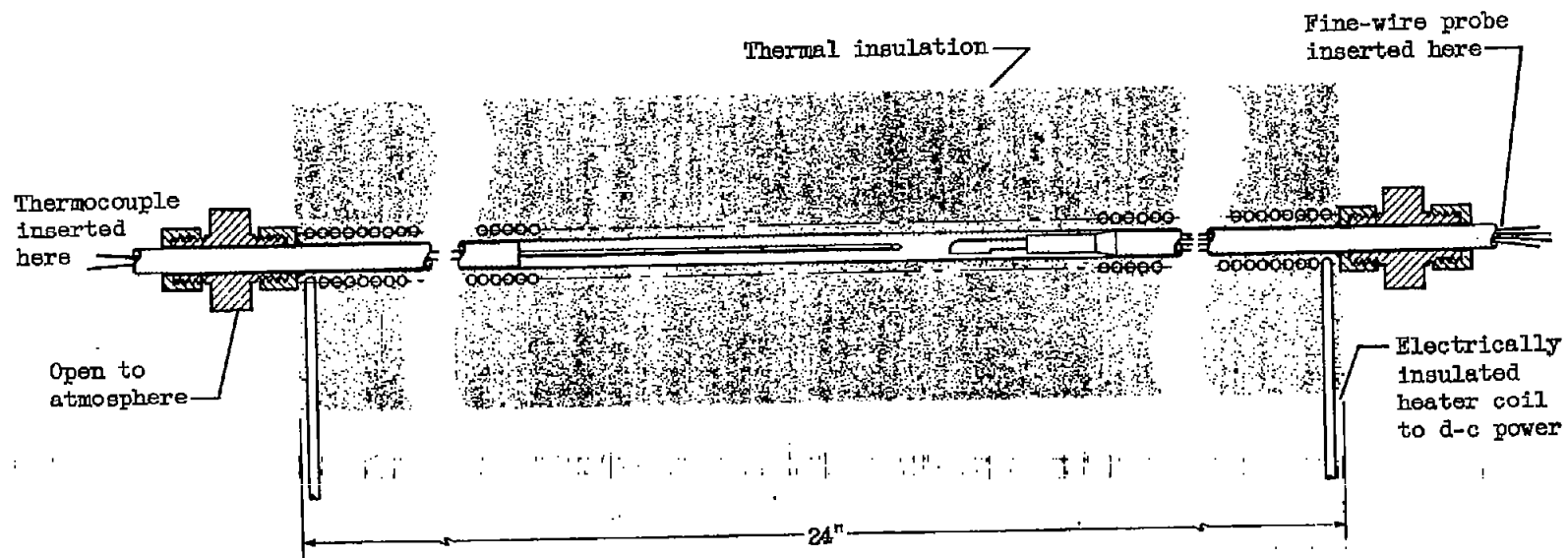
Sample C



C-48409

Scale factor; 600 grates = 1 millimeter

Figure 4. - Electron photomicrographs of tungsten wire.



CD-6240

Figure 5. - Resistance-temperature calibration tank.

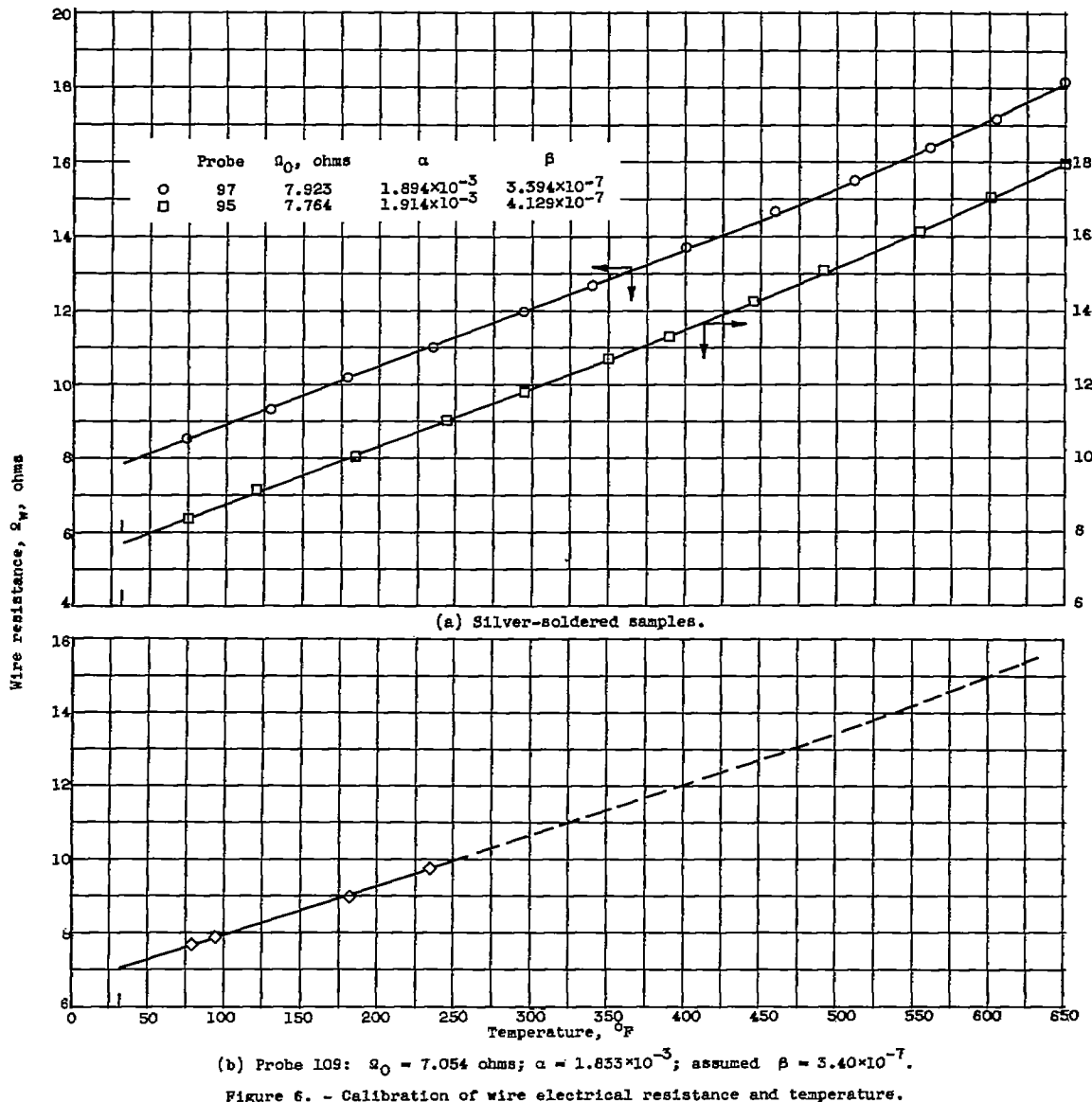
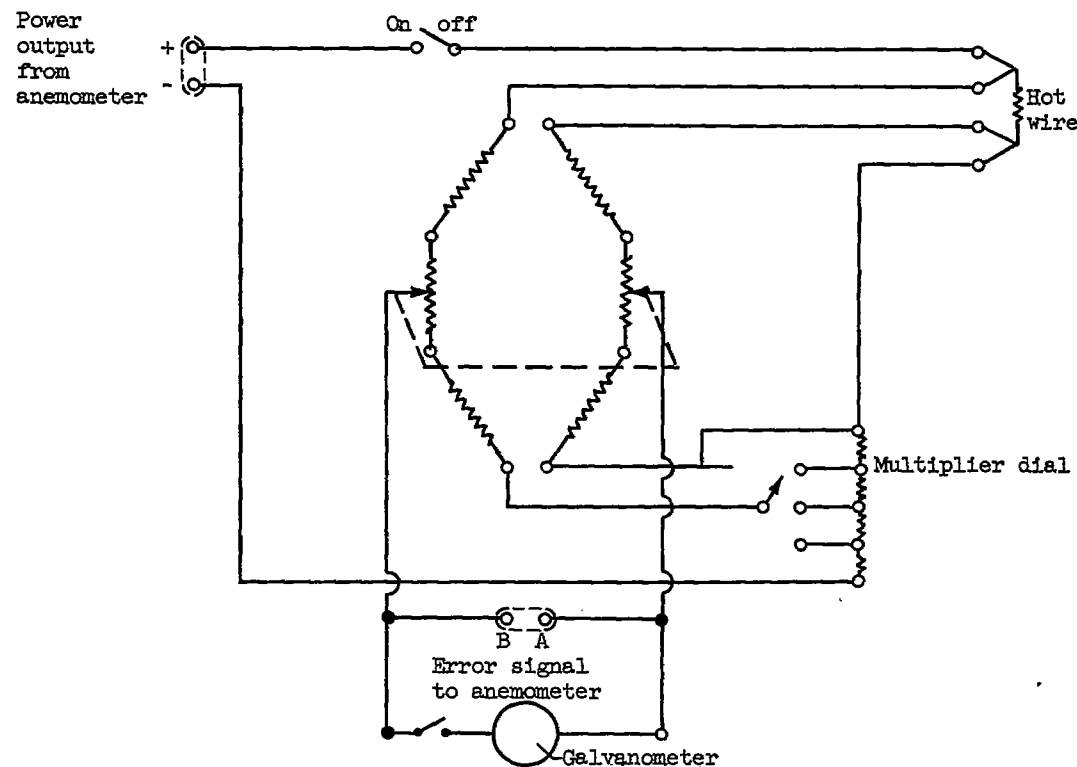
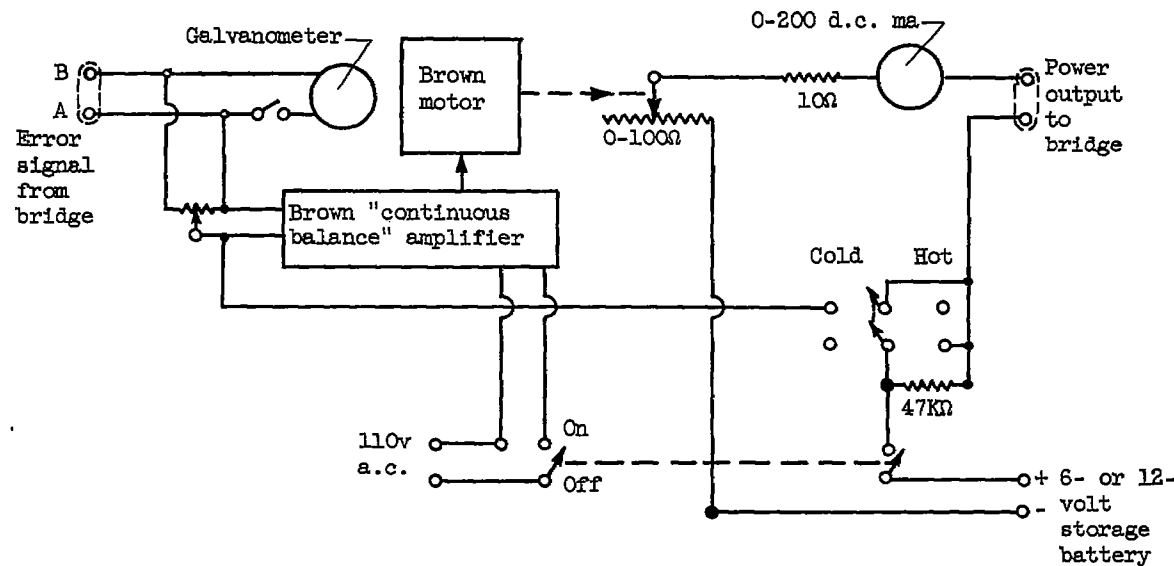


Figure 6. - Calibration of wire electrical resistance and temperature.



(a) Kelvin bridge ohmmeter.



(b) Constant-average-temperature anemometer.

Figure 7. - Anemometer electrical equipment.

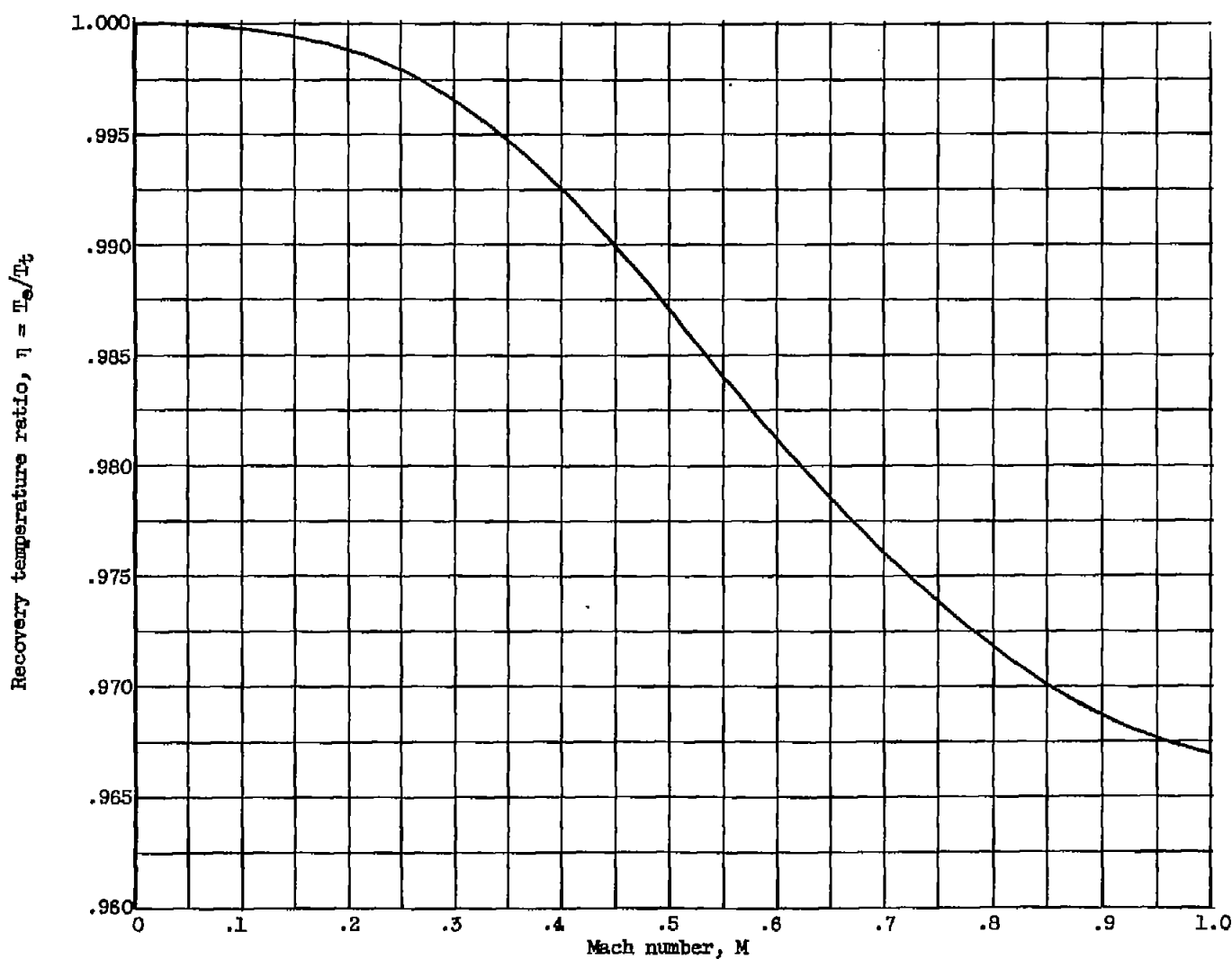


Figure 8. - Recovery temperature ratio as function of Mach number.

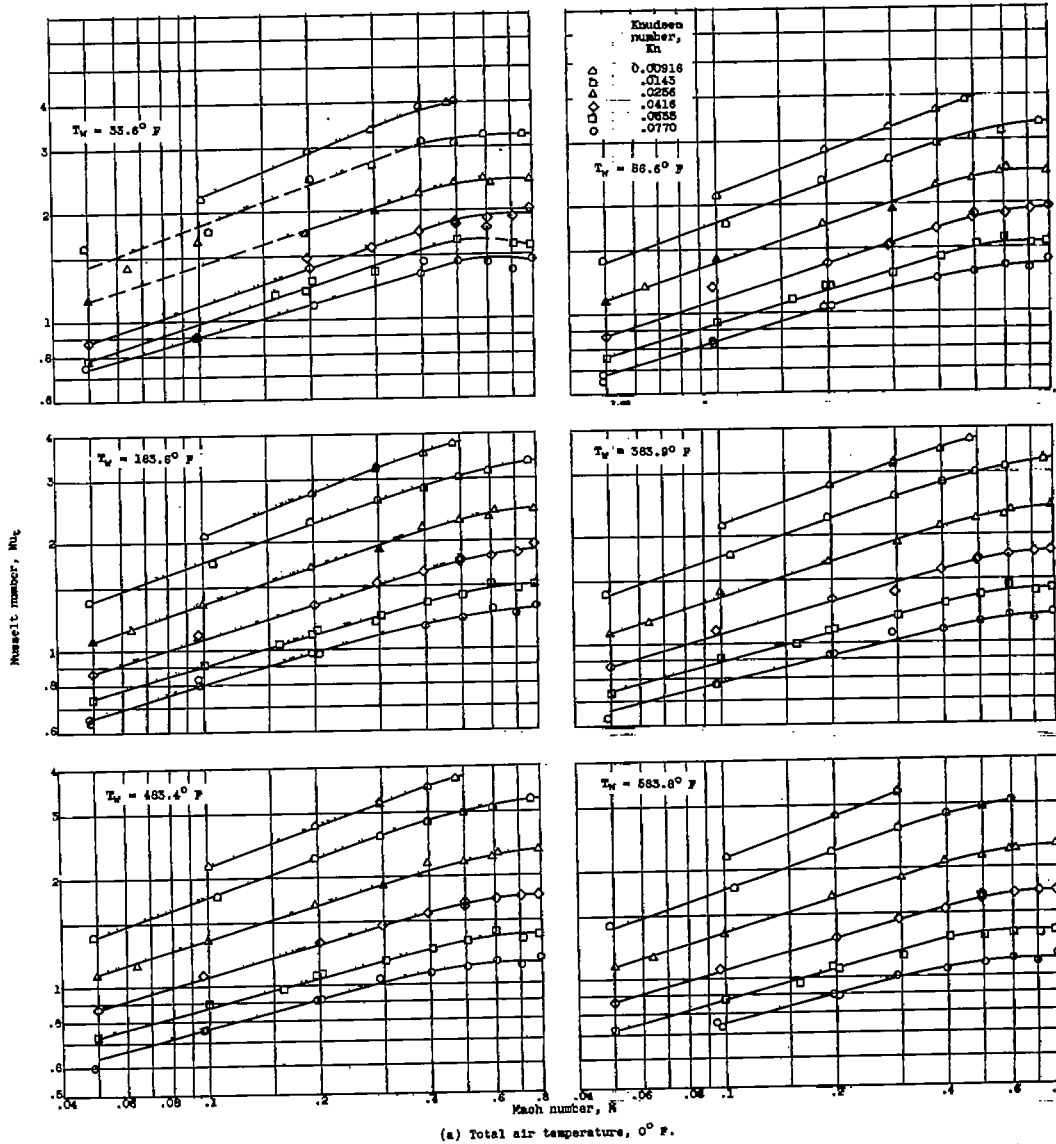


Figure 9. - Variation of Nusselt number with Mach number for constant Knudsen number and constant total air and cylinder temperatures.

UDC 511.1

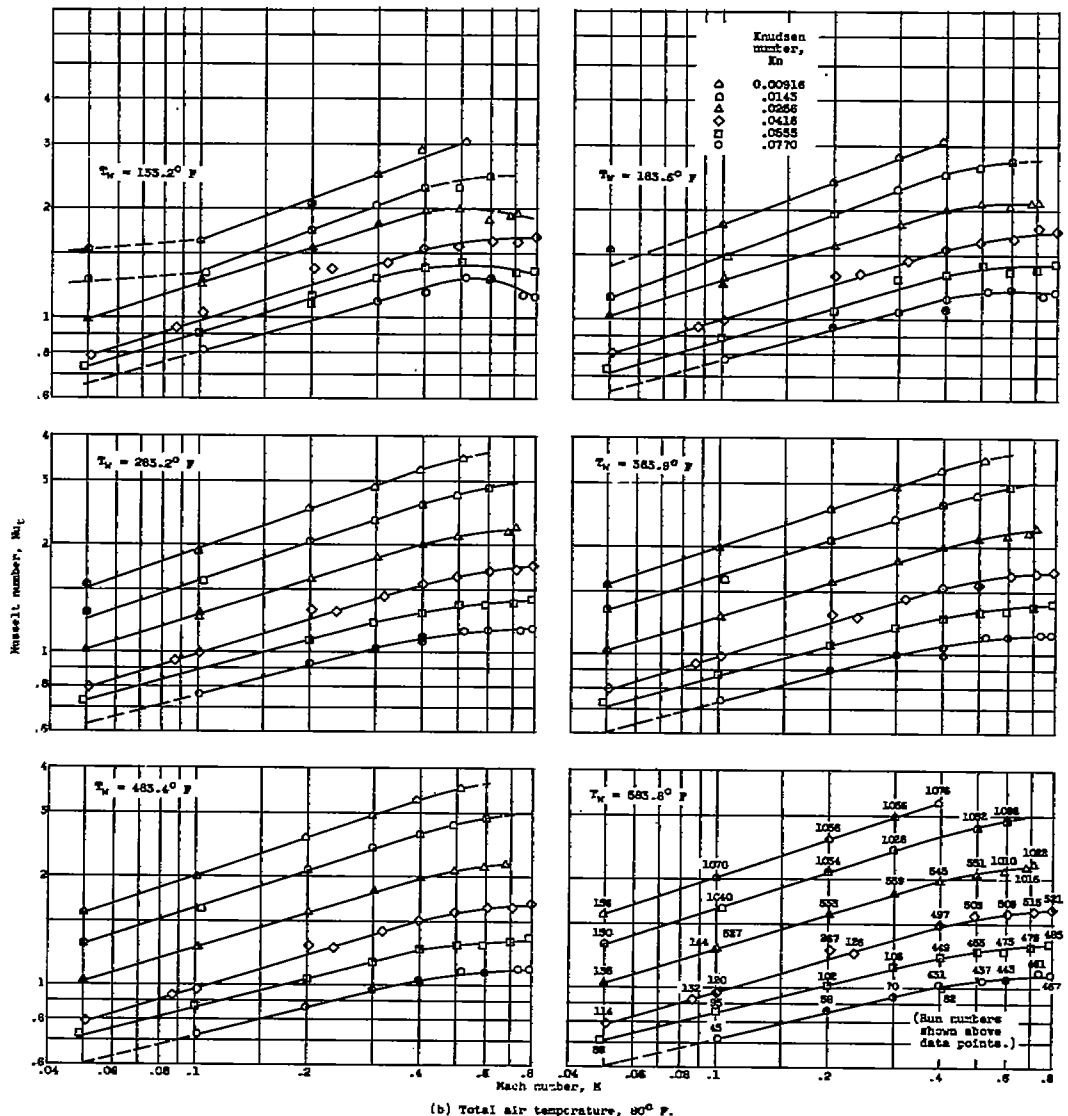
(b) Total air temperature, $^{\circ}$ F.

Figure 9. - Continued. Variation of Muszett number with Mach number for constant Knudsen number and constant total air and cylinder temperatures.

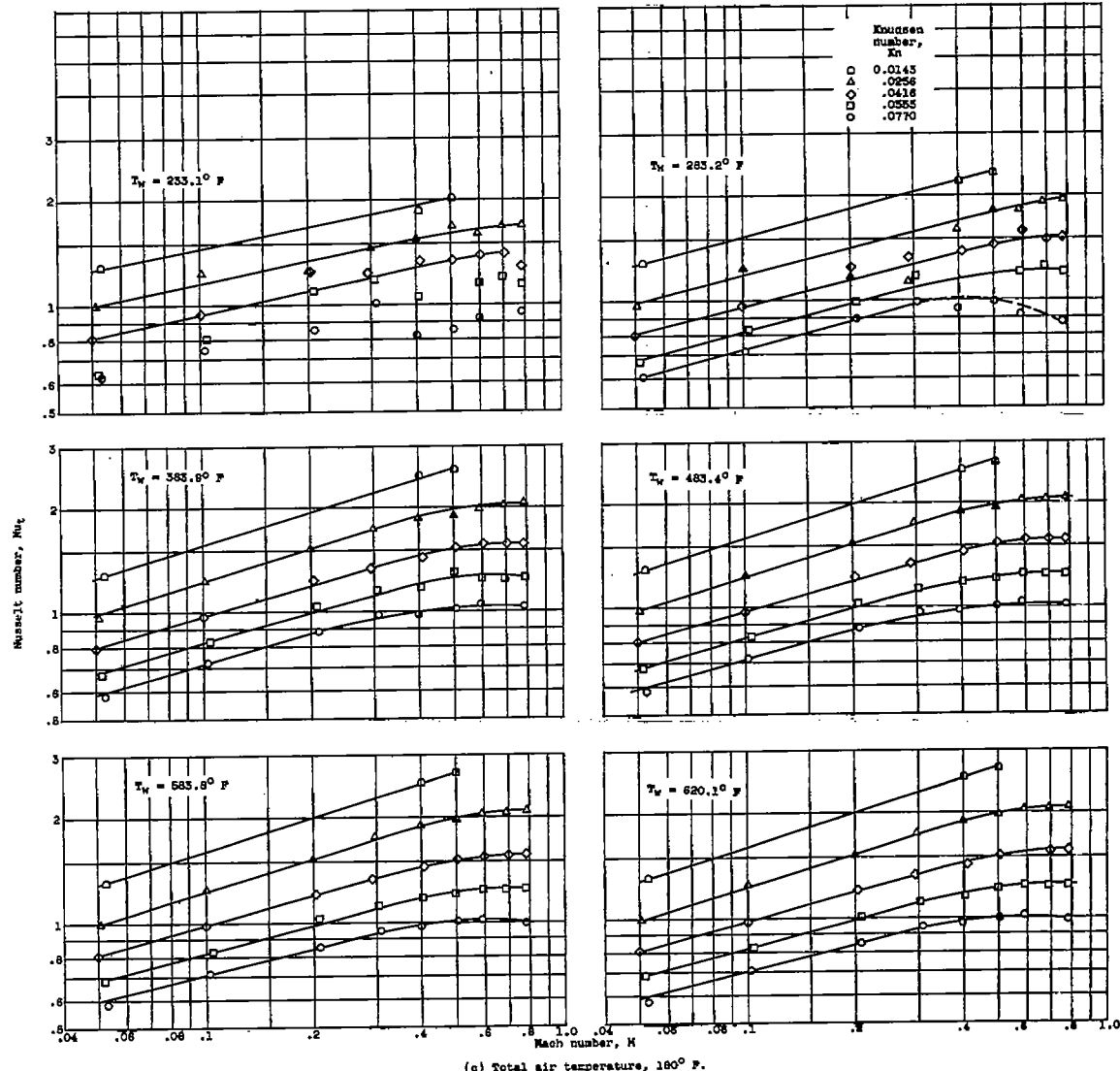


Figure 9. - Continued. Variation of Nusselt number with Mach number for constant Knudsen number and constant total air and cylinder temperatures.

CS-8 back 5111

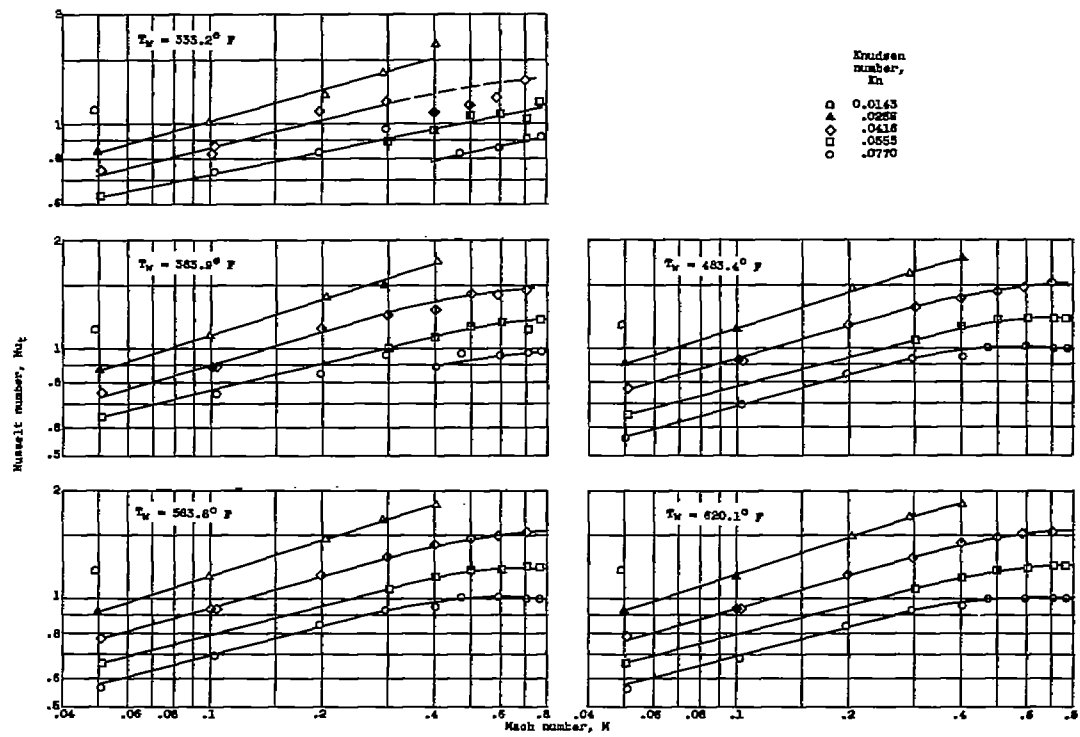


Figure S. — Concluded. Variation of Nusselt number with Mach number for constant Knudsen number and constant total air and cylinder temperatures.

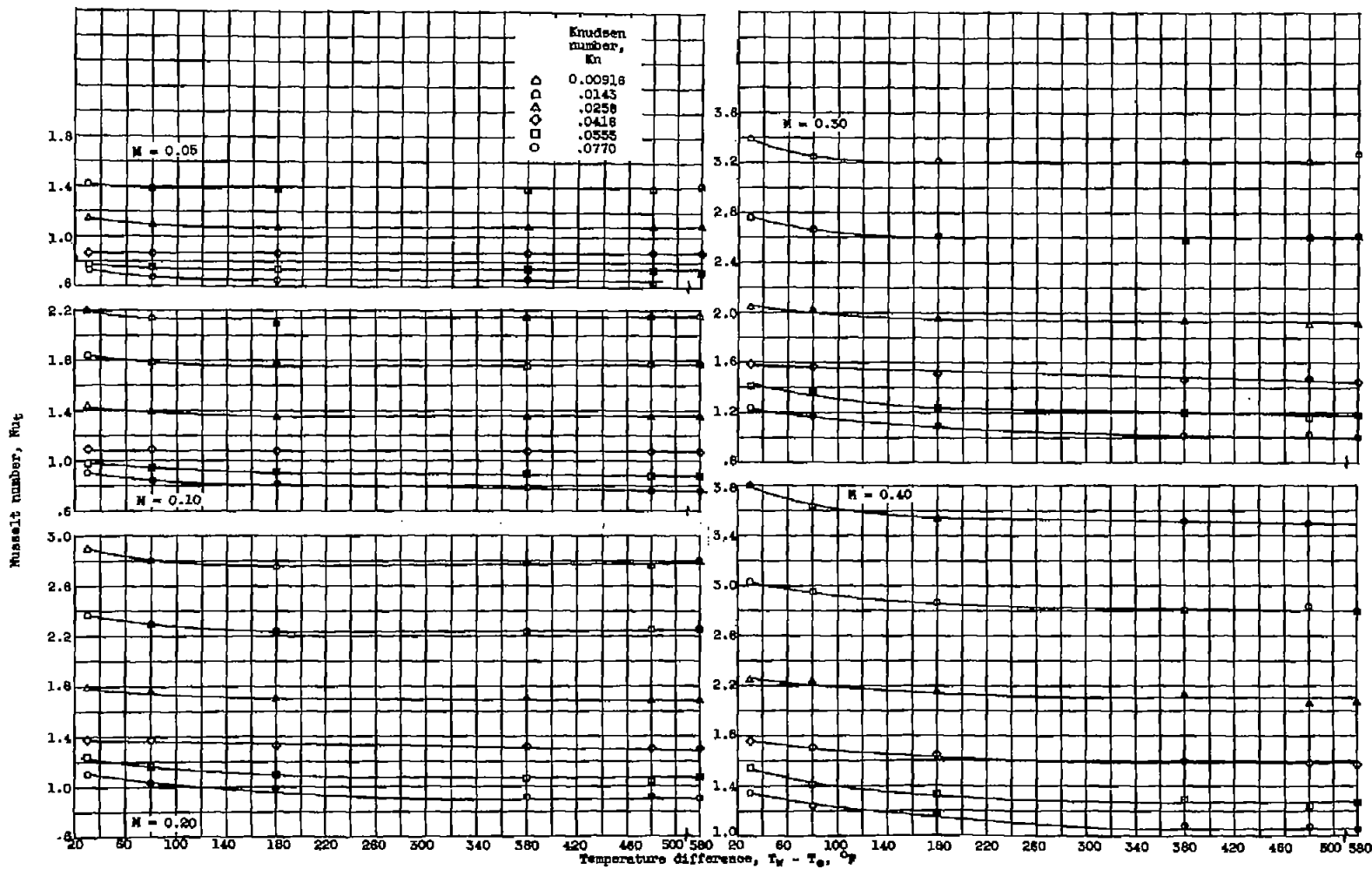
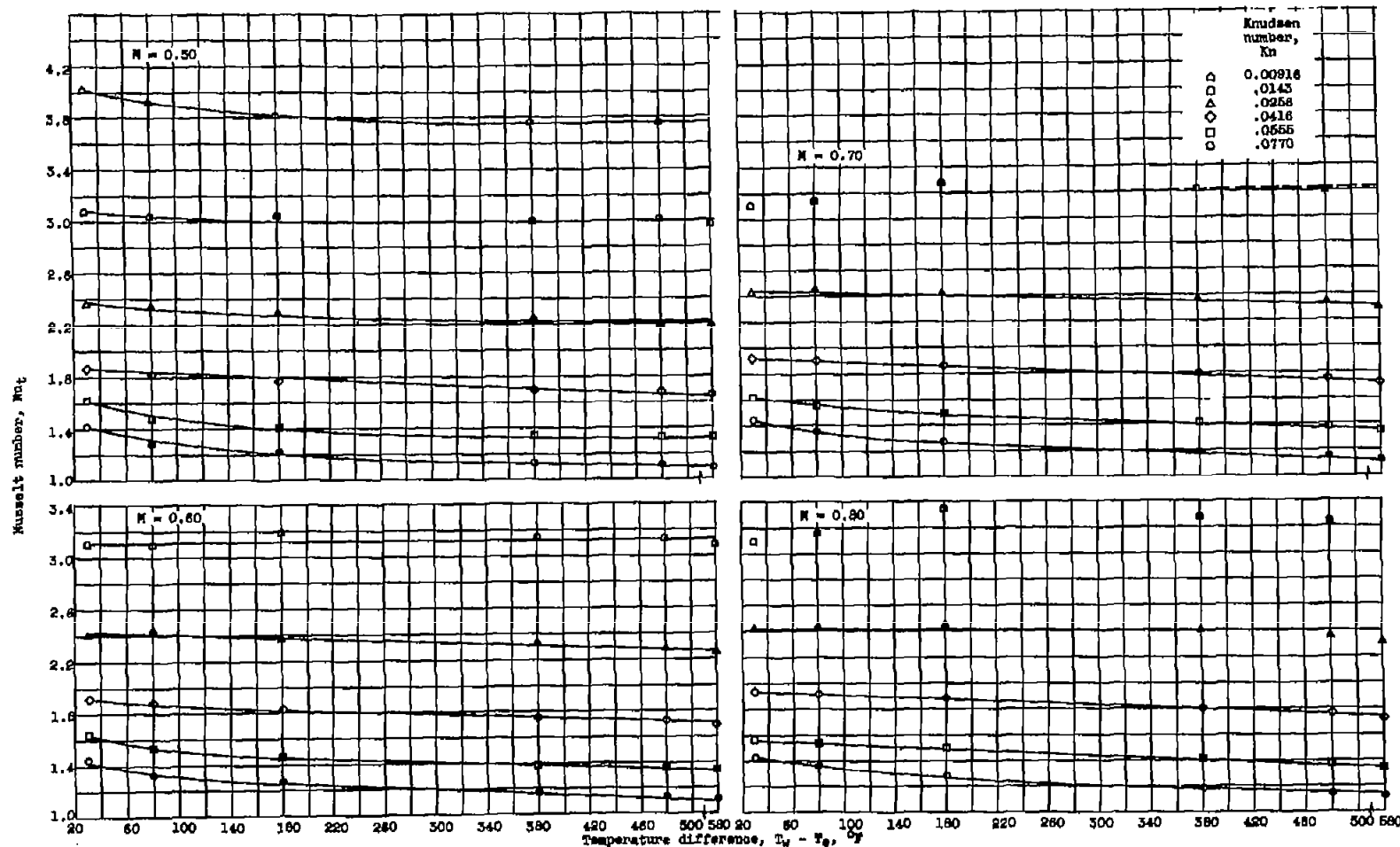


Figure 10. — Crossplots of figure 9 showing Nusselt number variation with cylinder temperature.



(a) Concluded. Total air temperature, 0° F (fig. 9(a)).

Figure 10. - Continued. Crossplots of figure 9 showing Nusselt number variation with cylinder temperature.

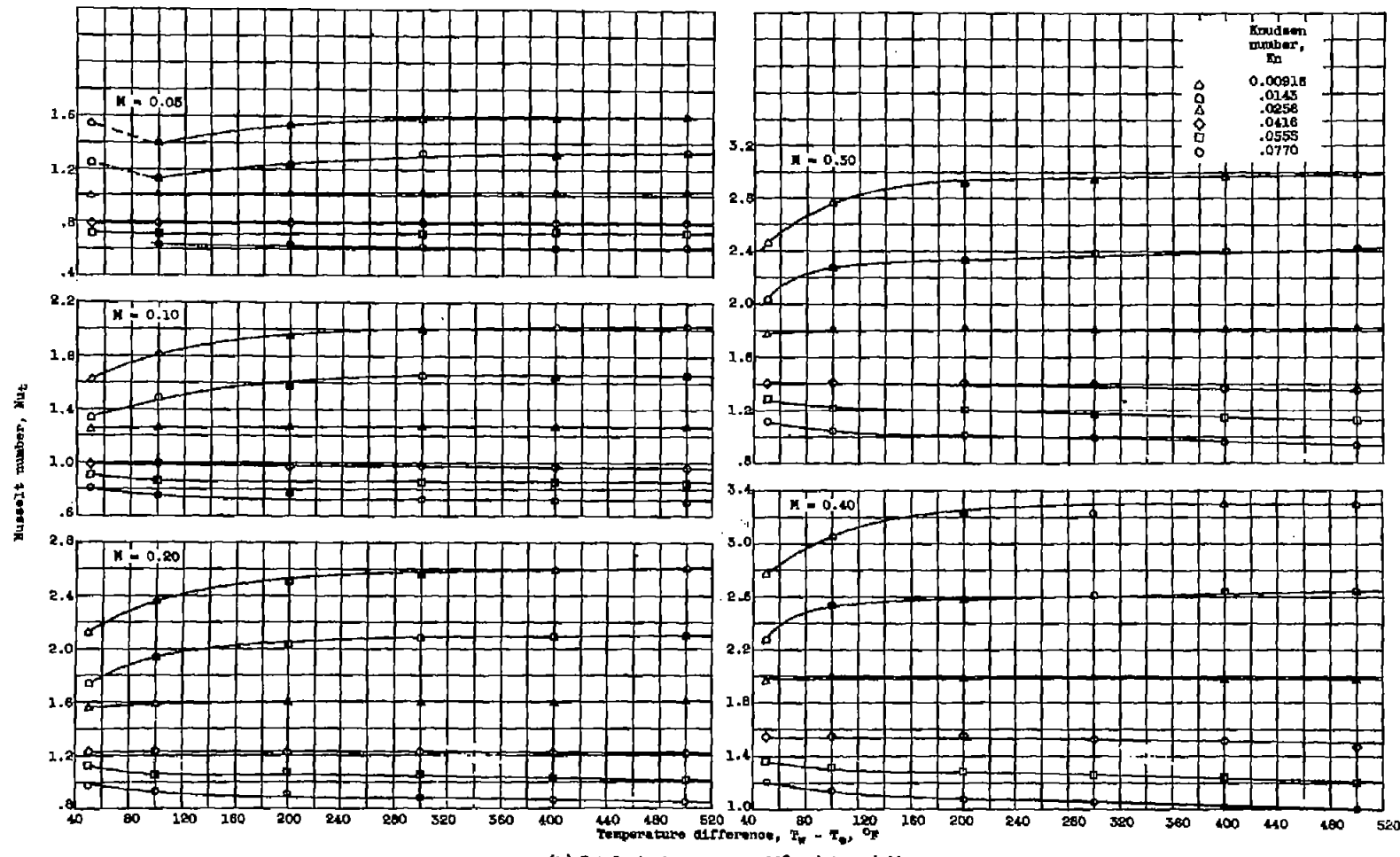
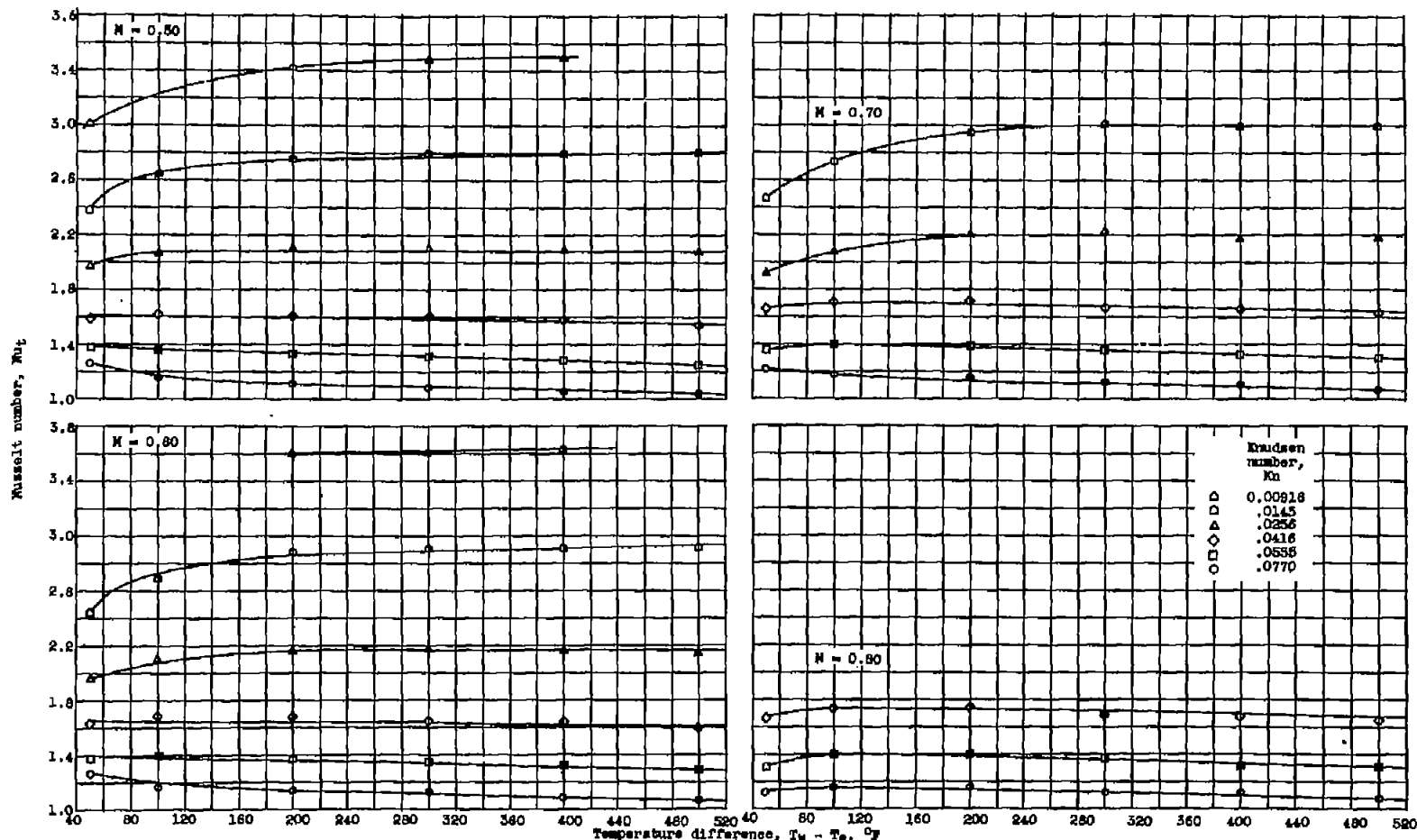


Figure 10. - Continued. Crossplots of figure 9 showing Nusselt number variation with cylinder temperature.



(b) Concluded. Total air temperature, 60° F (fig. 9(b)).

Figure 10. - Continued. Crossplots of figure 9 showing Nusselt number variation with cylinder temperature.

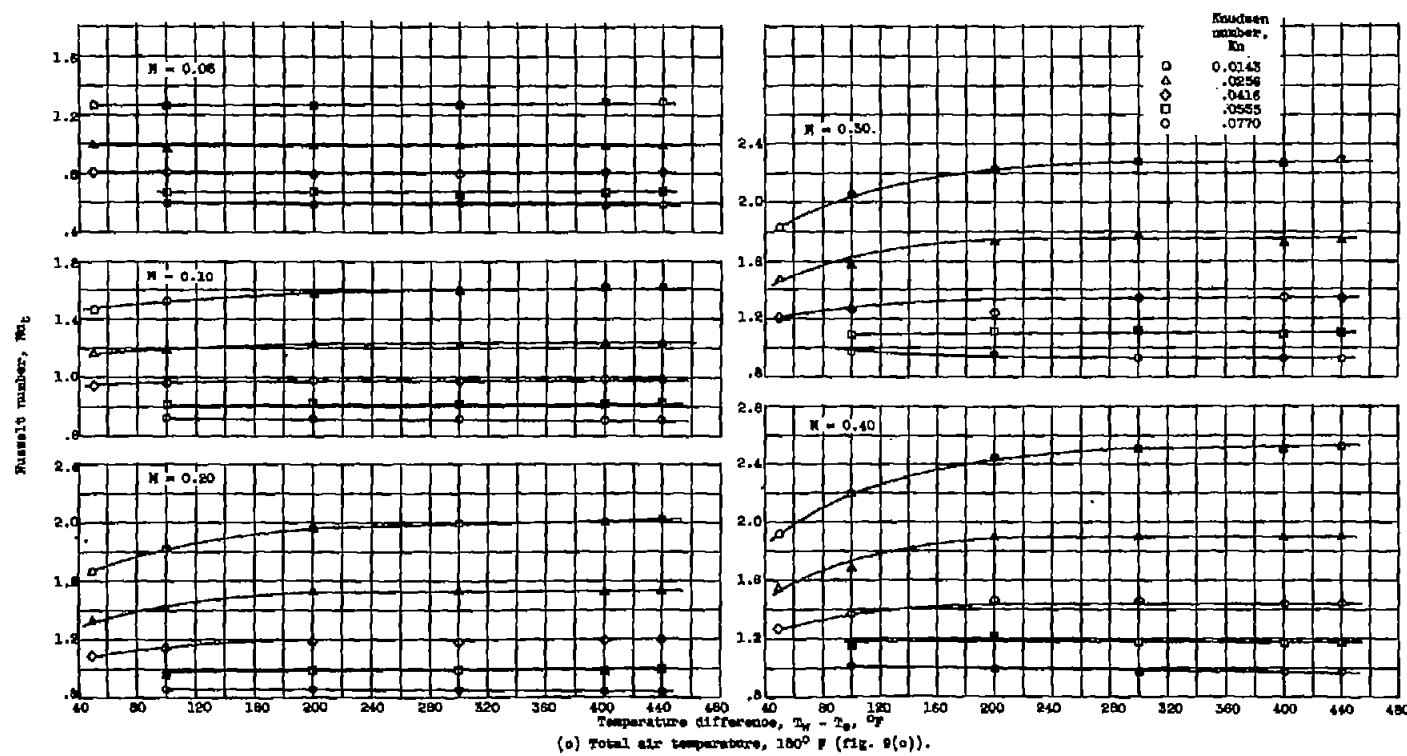
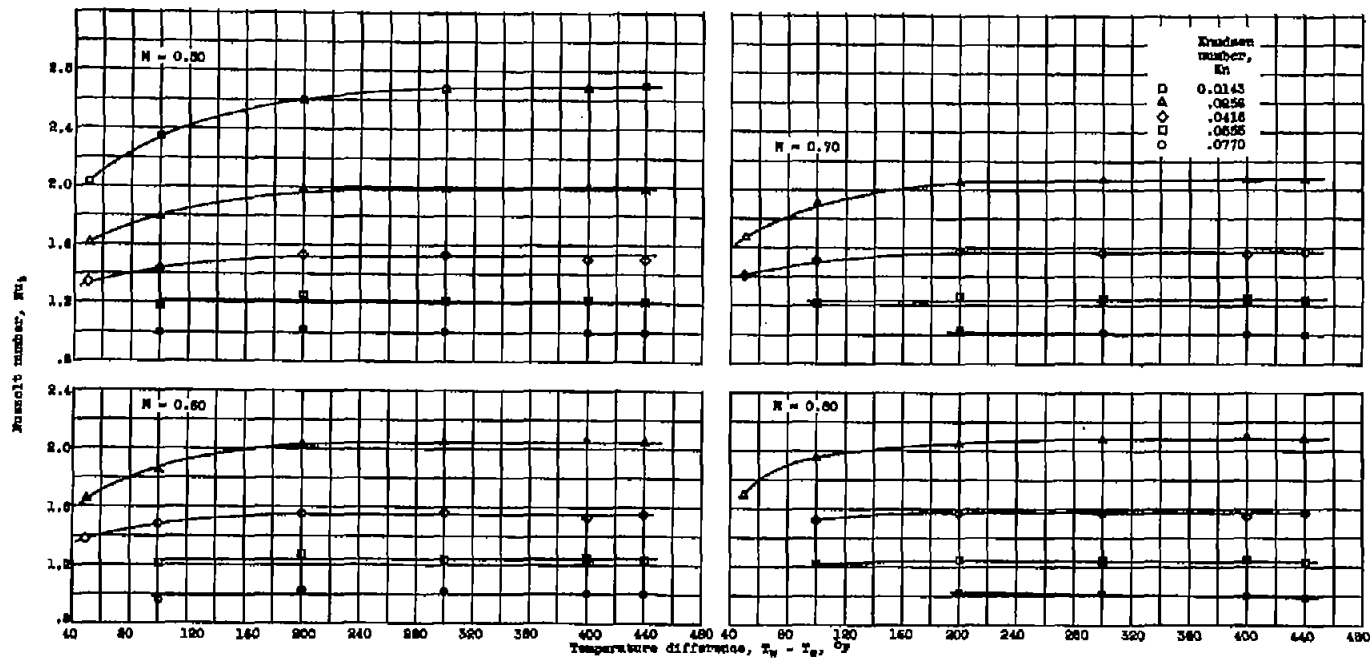


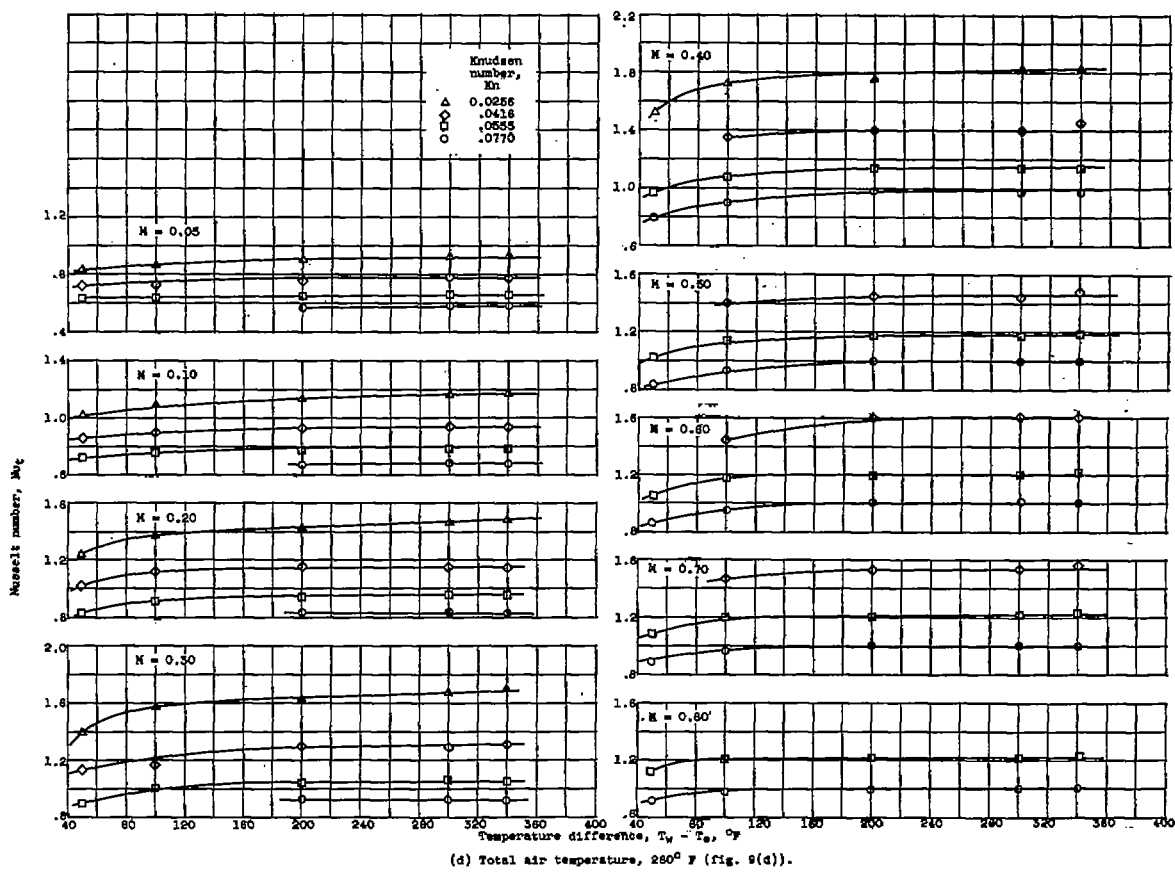
Figure 10. - Continued. Crossplots of figure 9 showing Nusselt number variation with cylinder temperature.



(a) Concluded. Total air temperature, 180° F (fig. 9(a)).

Figure 10. - Continued. Graphs of figure 9 showing Nusselt number variation with cylinder temperature.

5111



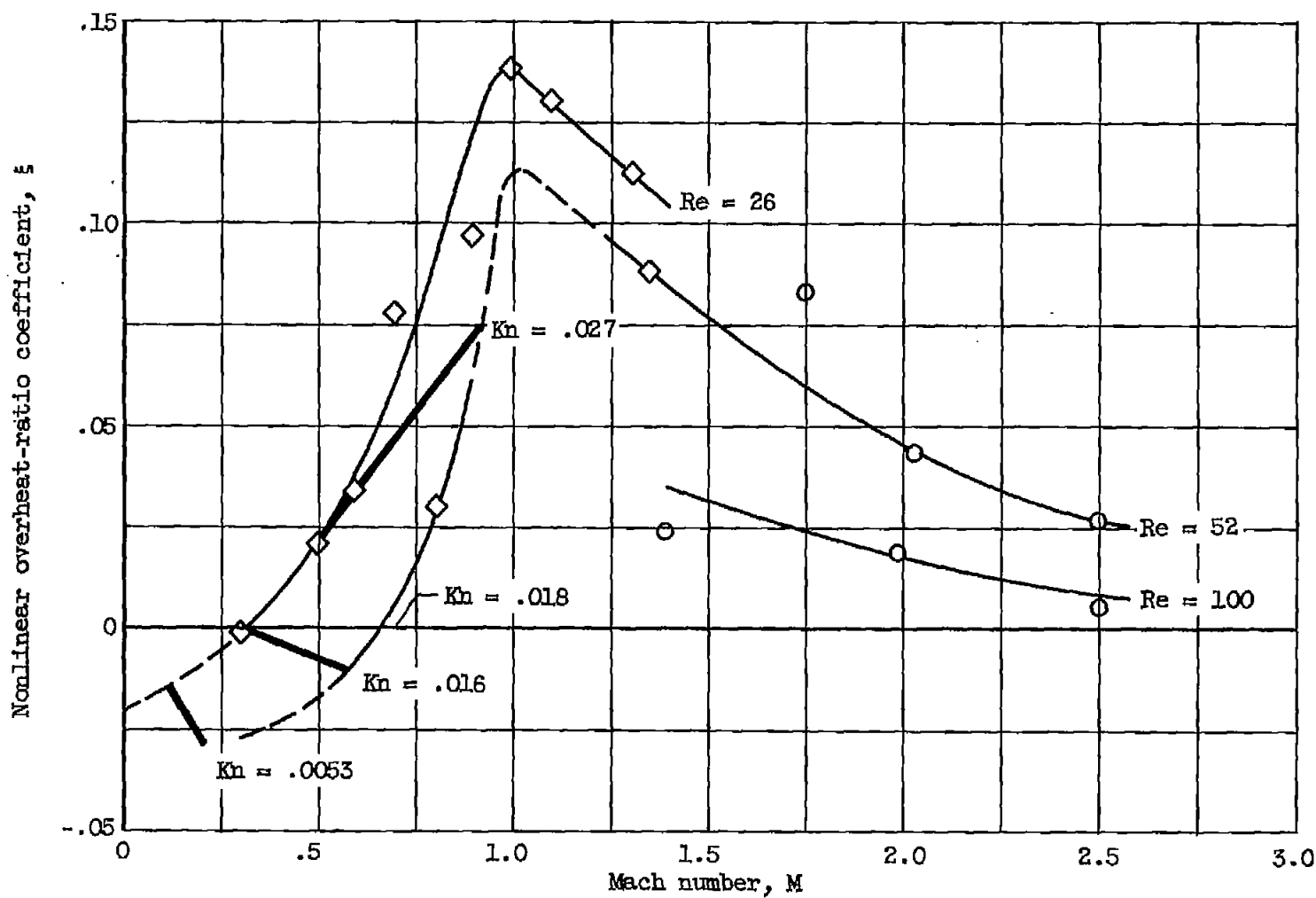


Figure 11. - Nonlinear overheat-ratio coefficient of reference 16 as function of Reynolds and Mach numbers with constant Knudsen number lines superimposed; $h = h_0(1 - \xi a_w)$. Data points of reference 16.

511

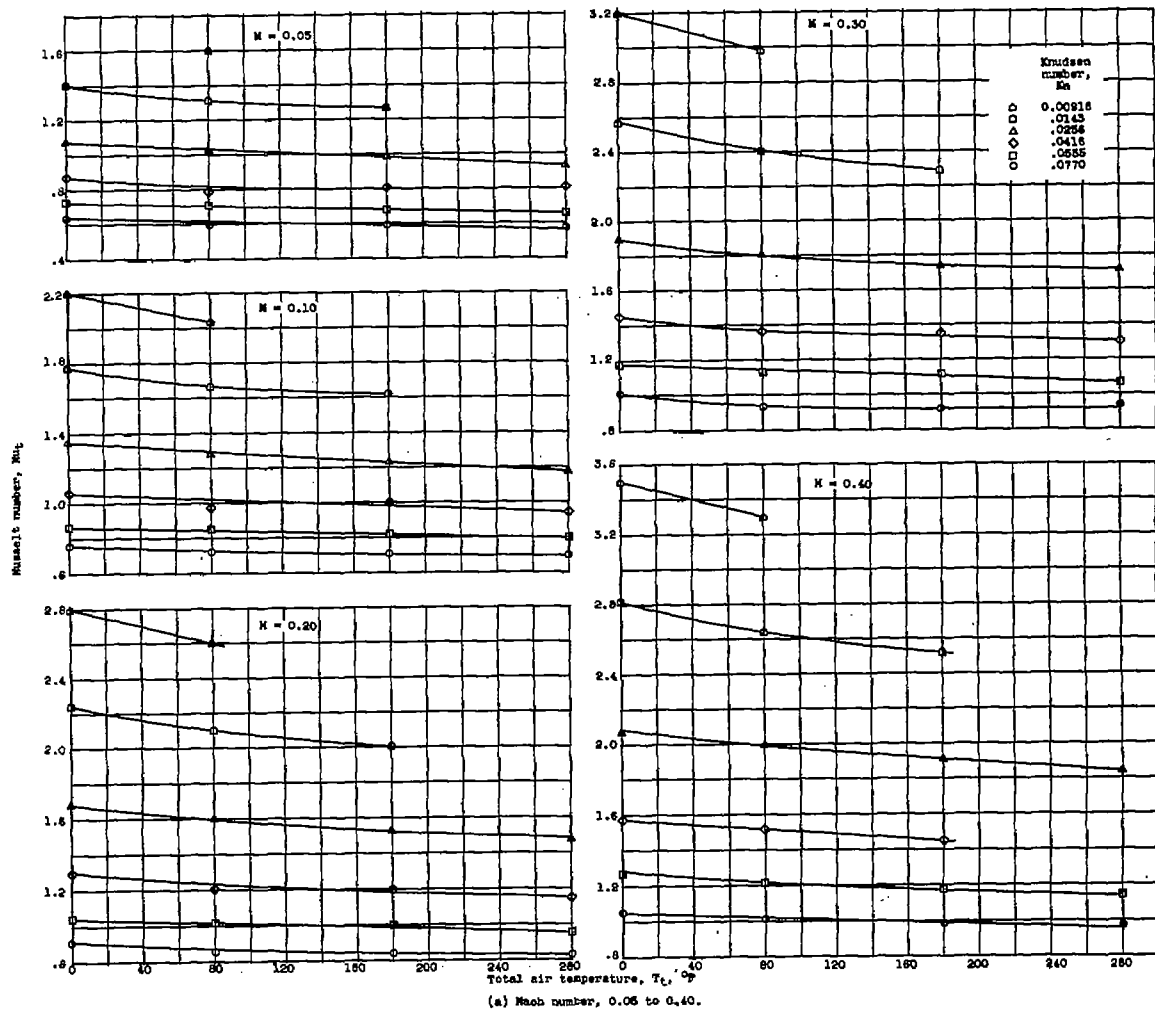


Figure 12. - Variation of Nusselt number with total air temperature. Crossplots of figure 10 showing asymptotic Nusselt number at $\Delta T > 200^{\circ}$ F.

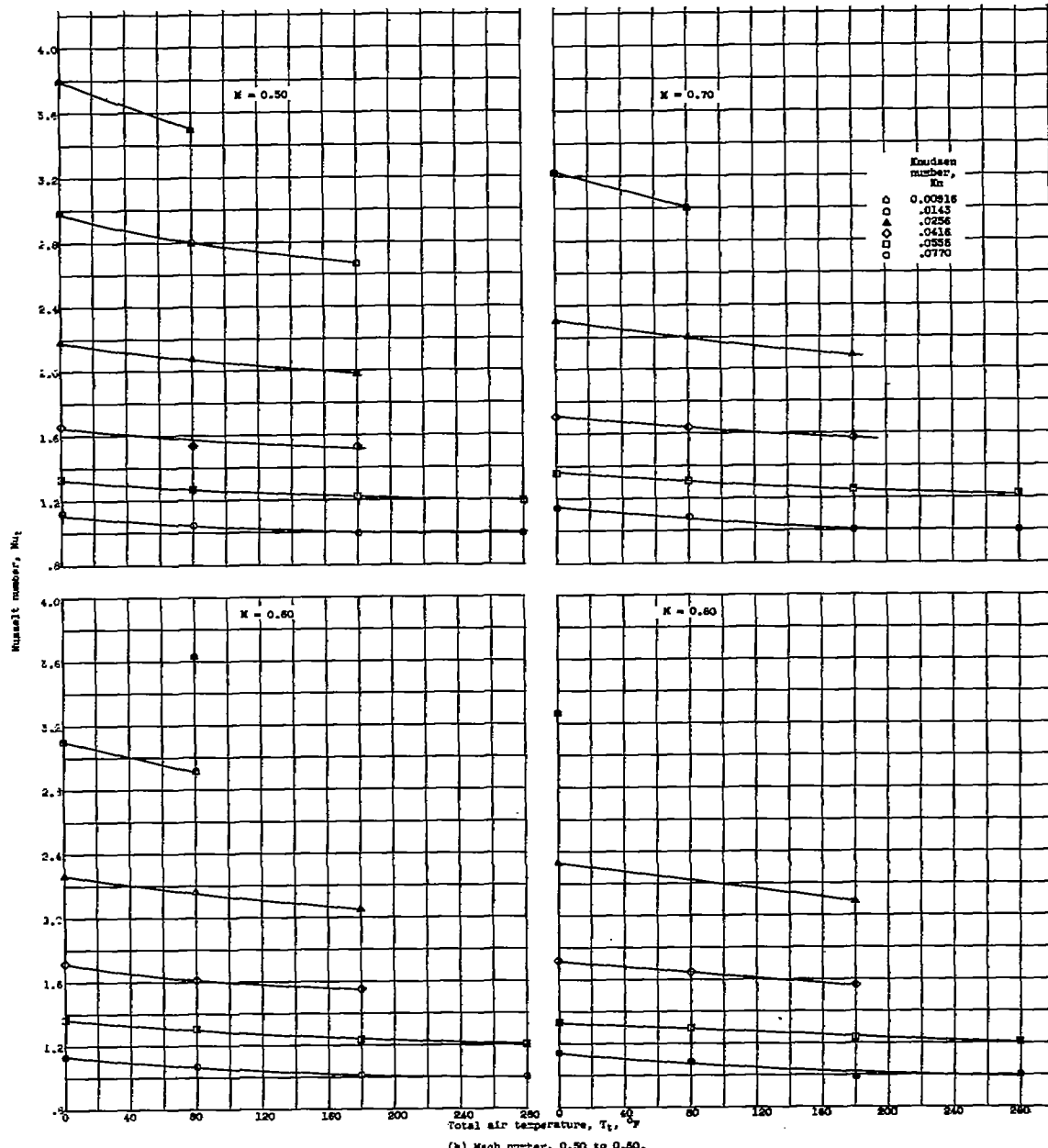


Figure 12c.—Concluded. Variation of Russell number with total air temperature. Chronoplots of figure 10 showing asymptotic Russell number at $\Delta T > 200^{\circ}\text{ F}$.

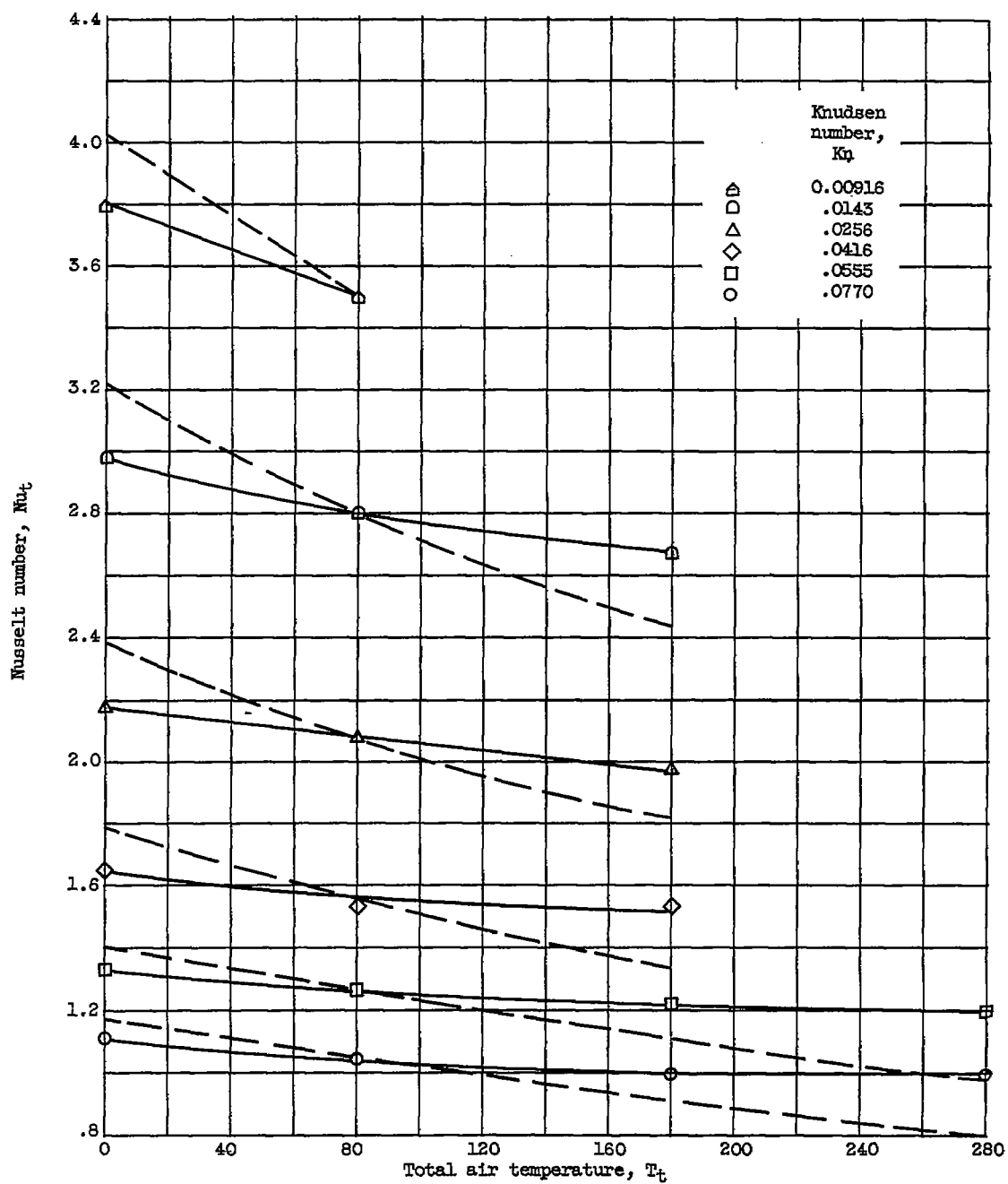


Figure 13. - Variation of Nusselt number with total air temperature. Curves of constant heat-transfer coefficient h_{800F} superimposed on figure 12(b) for $M = 0.50$.

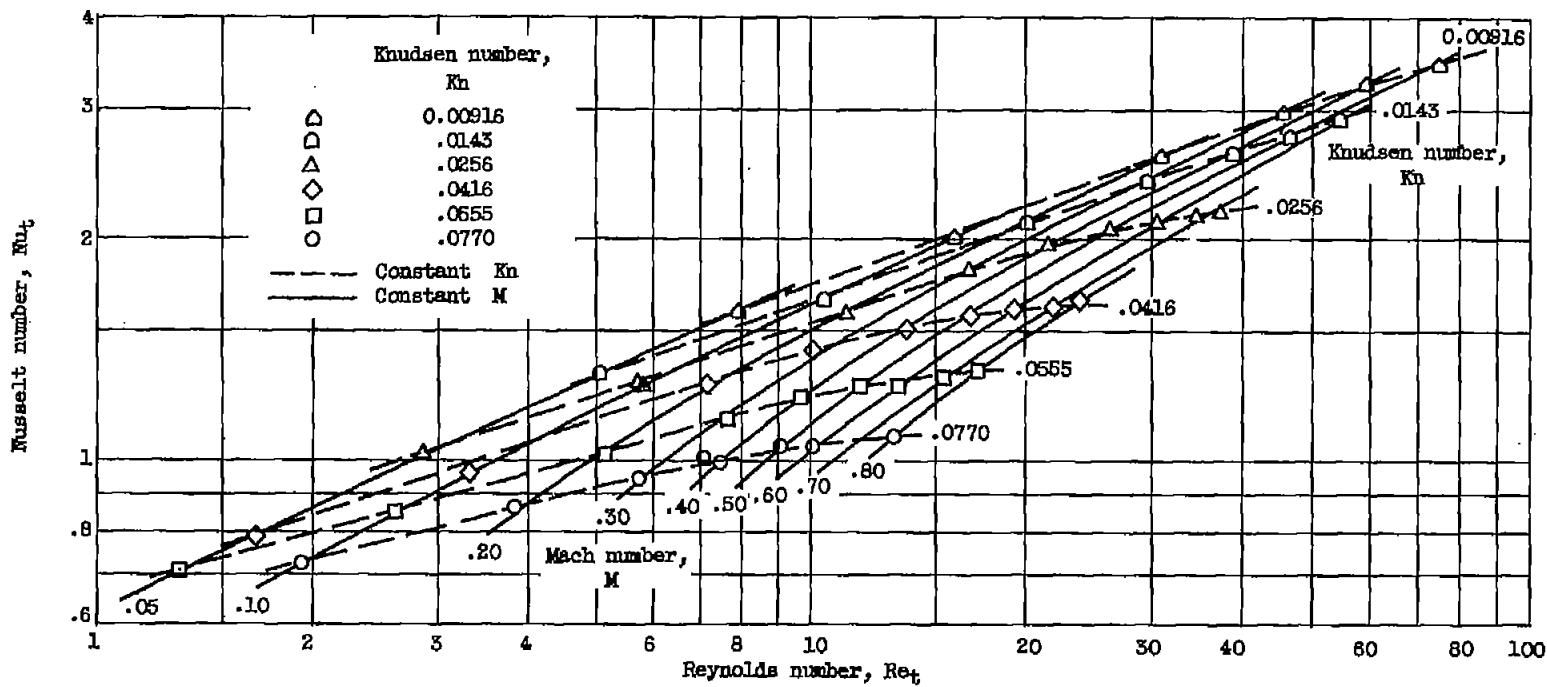


Figure 14. - Nusselt number correlation for cylinders in subsonic slip flow. Total air temperature, 80° F; length-average wire temperature, 584° F.

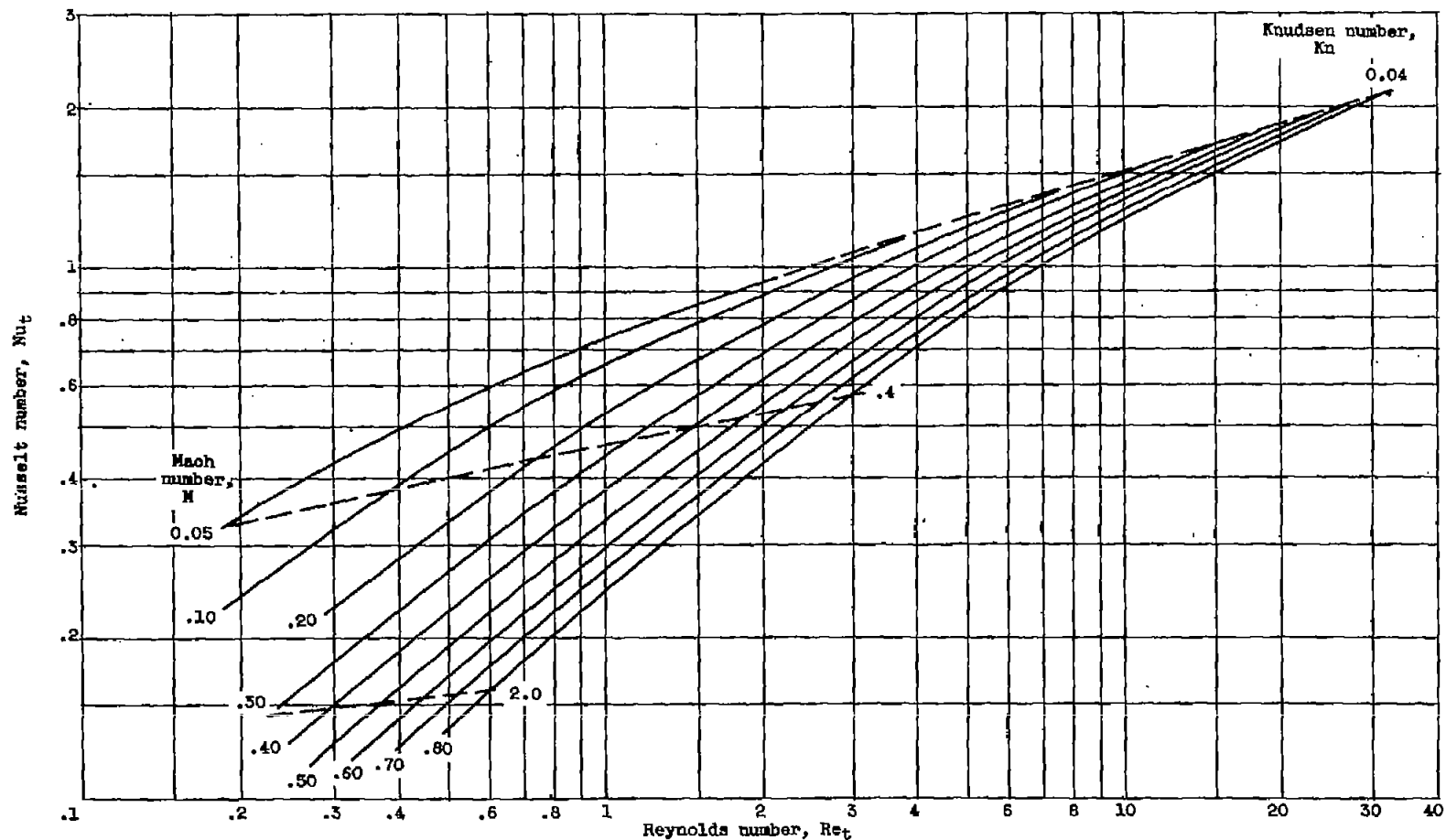


Figure 15. - Predicted Nusselt number correlation from approximate slip-flow theory (after ref. 23).

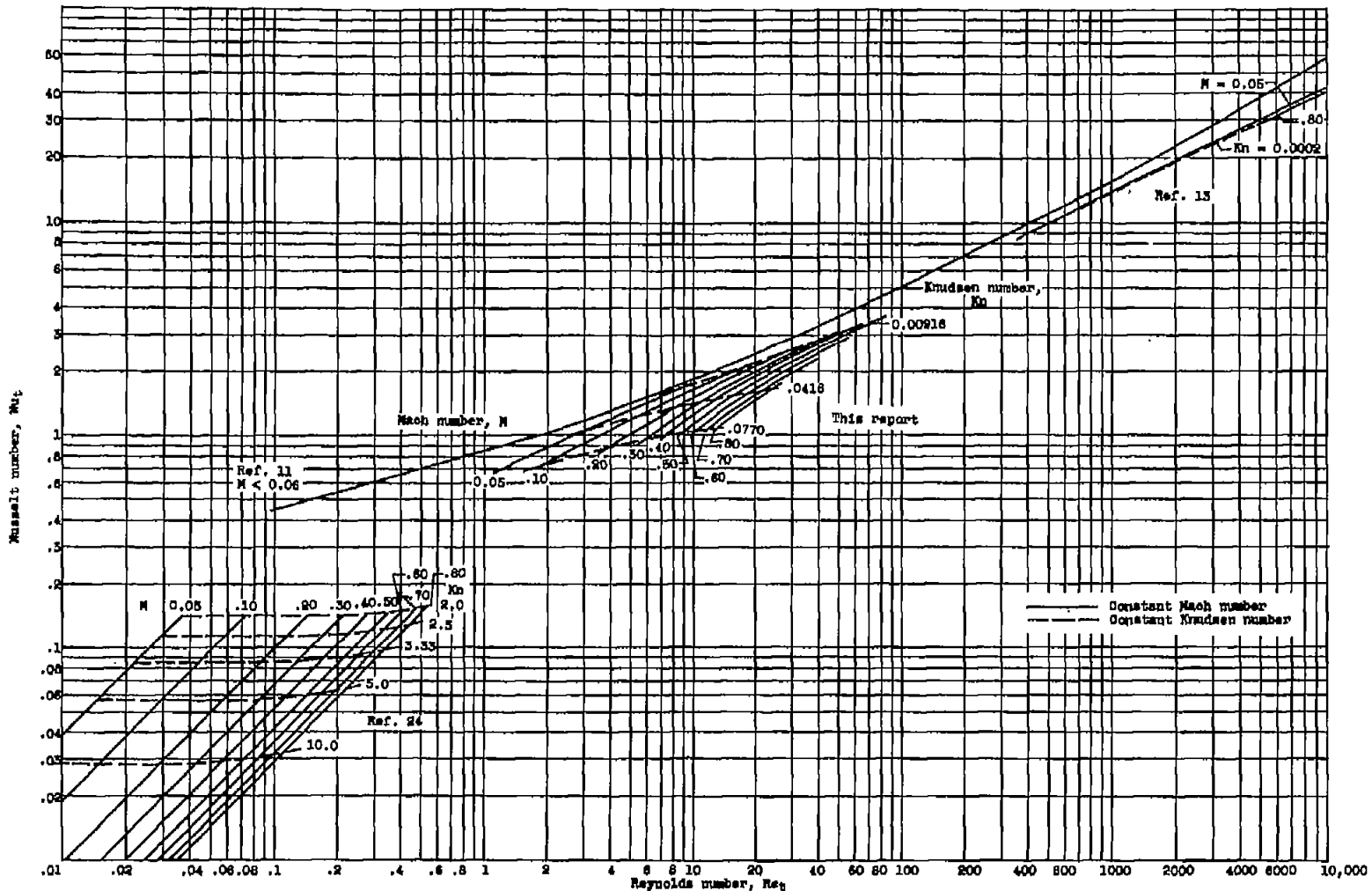


Figure 16. - Attempted Nusselt number correlation for cylinders in subsonic continuum, slip, and free-molecule flows.

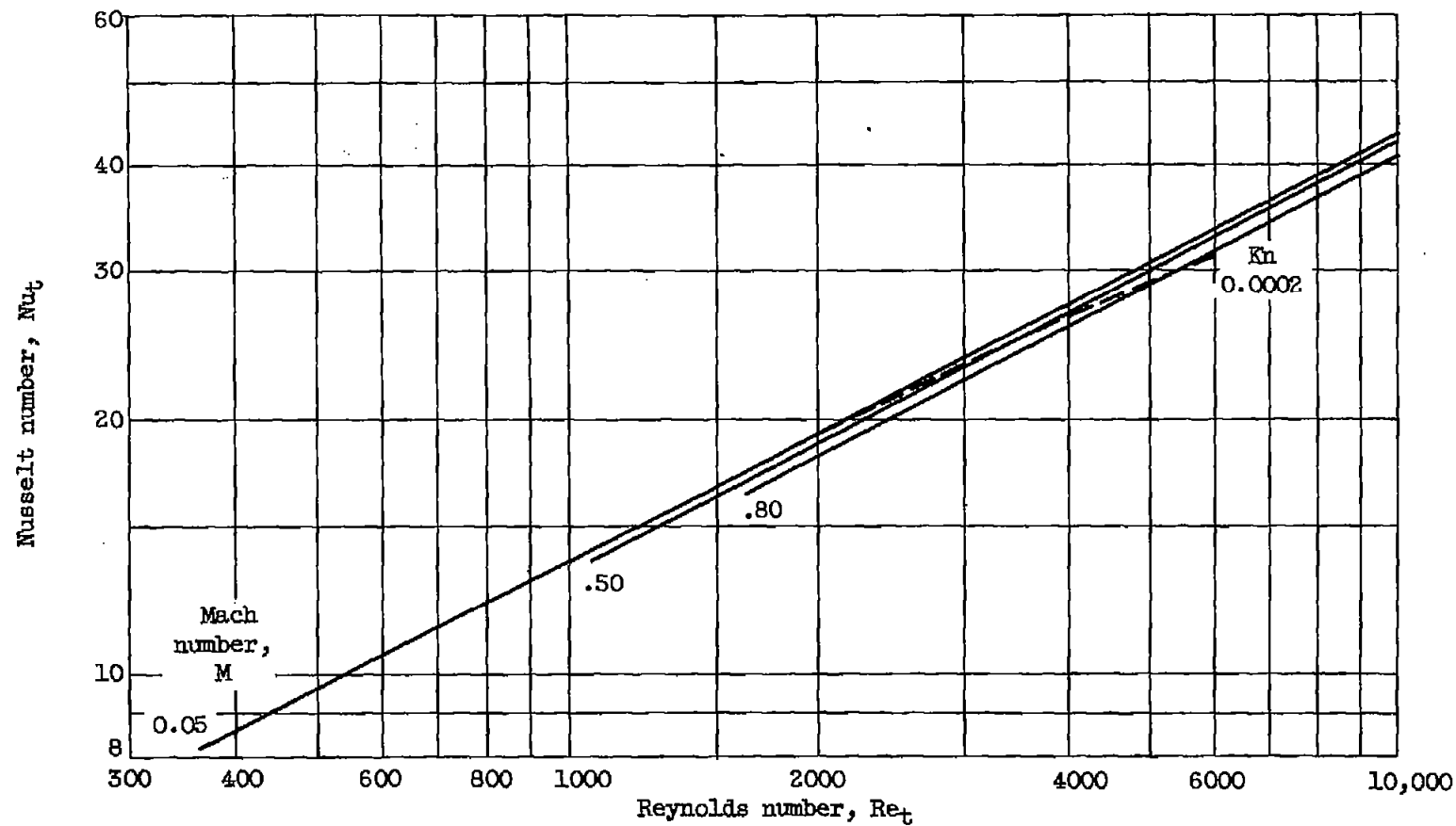
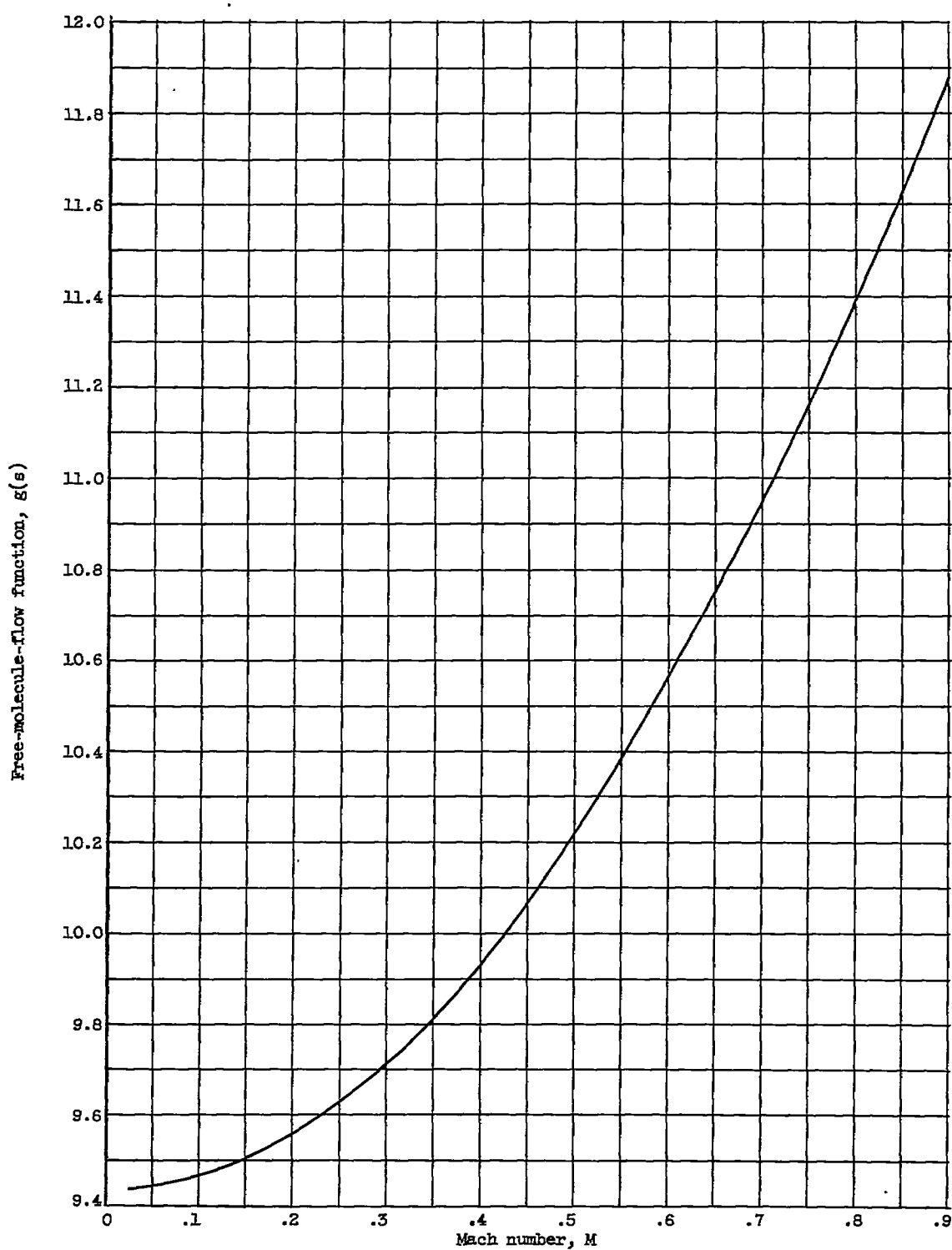


Figure 17. - Continuum-flow experimental Nusselt number correlation (after ref. 13).

Figure 18. - Free-molecule-flow function $g(s)$ as function of Mach number.

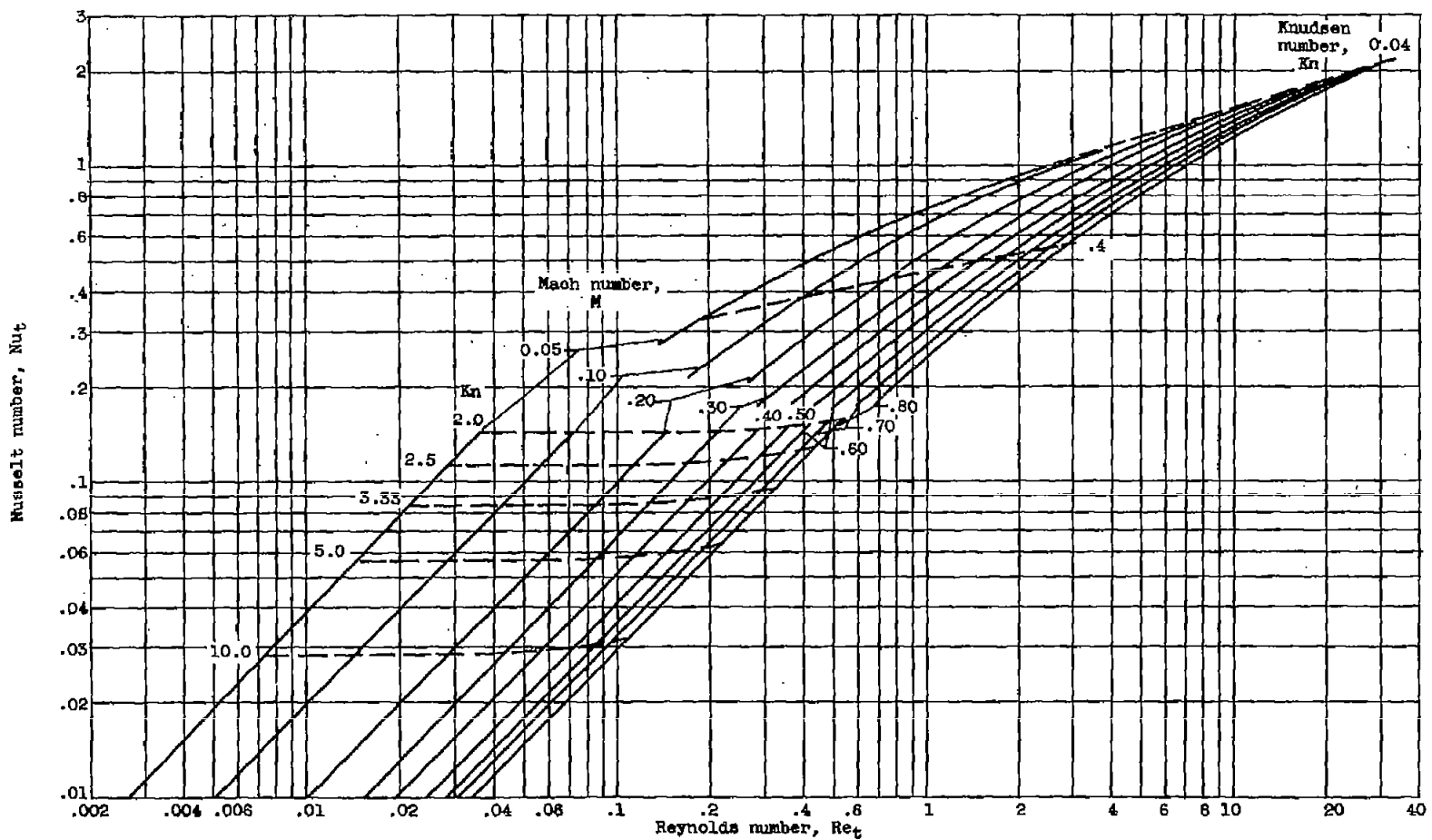
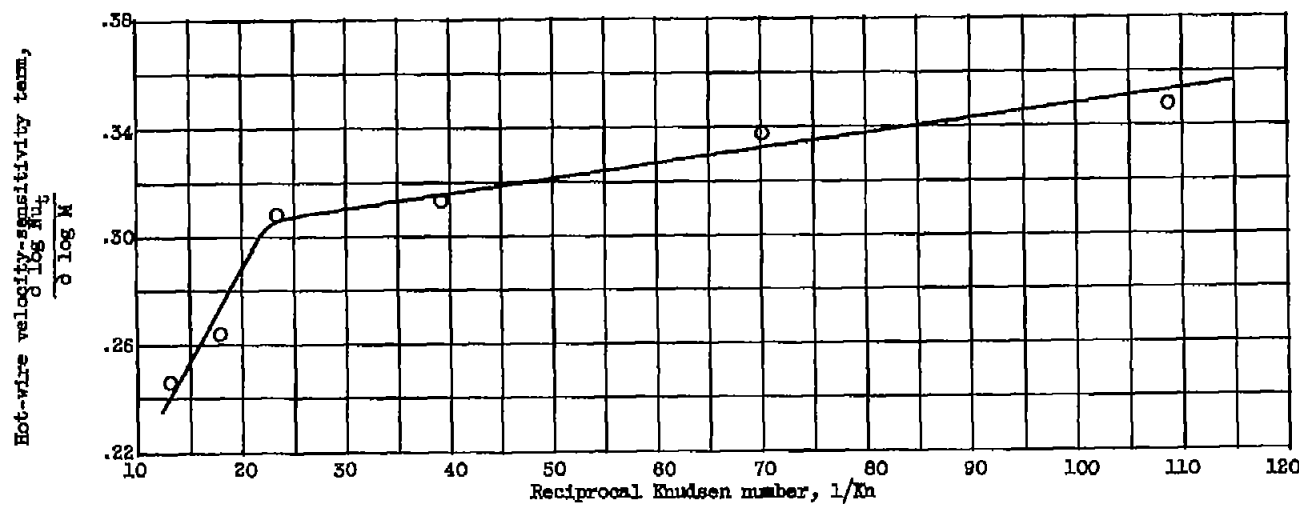
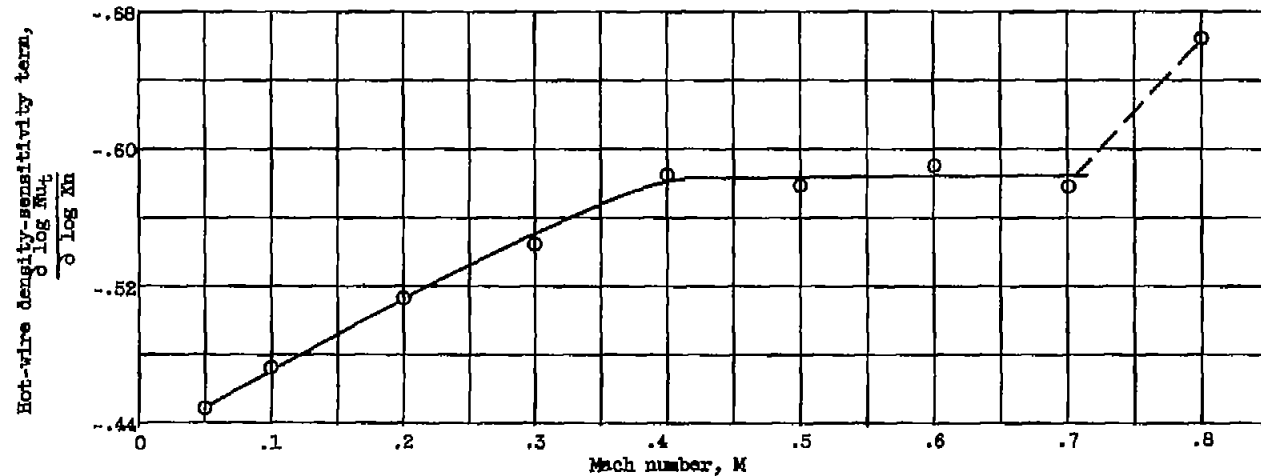


Figure 19. - Comparison of approximate slip-flow theory with free-molecule-flow prediction.

NACA - Langley Field, Va.

(a) Velocity sensitivity: $0.05 < M < 0.40$.(b) Density sensitivity: $0.009 < \lambda n < 0.077$.Figure 20. - Hot-wire sensitivity terms. Restrictions: $T_t = 80^{\circ} \text{ F}$; $T_w - T_e > 200^{\circ} \text{ F}$.